Activities of Daily Living and Their Impact on Total Knee Replacement Wear

BY

DIEGO ALEJANDRO OROZCO VILLASEÑOR
B.S. University of Colima, Col. Mexico, 2002
M.S. University of Illinois at Chicago, Chicago, 2006

THESIS

Submitted as partial fulfillment of the requirements
for the degree of Doctor of Philosophy in Bioengineering
in the Graduate College of the
University of Illinois at Chicago, 2013

Chicago, Illinois

Defense Committee:

Thomas Royston, Chair
Markus Wimmer, Advisor
Mark Grabiner, Kinesiology
Ahmed Shabana, Mechanical and Industrial Engineering
John Medley, University of Waterloo

This thesis is dedicated

to my wife, Danielle

ACKNOWLEDGMENTS

I would first like to thank my thesis supervisor, Markus Wimmer Ph.D., for his advice and mentorship throughout my PhD. I would also like to thank my committee members, Thomas Royston Ph.D., Mark Grabiner Ph.D., Ahmed Shabana Ph.D. and John Medley Ph.D. for their insights and assistance. I dedicate special acknowledgements to Aaron Rosenberg M.D., for his clinical guidance and support. In addition, I would like to thank Tobias Uth M.S., Valentina Ngai Ph.D., and Thorsten Schwenke Ph.D. for their valuable contributions throughout the many stages of the thesis. Finally, I would like to thank all the past and present graduate students at Rush and UIC who, in one way or another, made a helpful contribution to this thesis.

TABLE OF CONTENTS

LIST OF TABLES

LIST OF FIGURES

SUMMARY

There are multiple factors affecting the wear performance of total knee replacement (TKR) polyethylene tibial components. The prosthesis (materials and design), the patient (height, weight, joint loading during daily activities and their frequency) and the surgeon (implant alignment and soft tissue balancing) all influence the wear performance. While many of these factors have been investigated, the contributions of patient factors, such as daily physical activities and activity level, are not fully understood.

This thesis investigated the effect of various daily physical activities on wear of TKR tibial components. In order to compare the contact damage patterns of *in vivo* and *in vitro* worn components, a neural network model has been developed with the aim of investigating how closely current ISO standards simulating level walking recreate *in vivo* damage patterns. It was hypothesized that various daily physical activities contribute considerably to the overall wear scar features of the tibial liner, and therefore, components tested under ISO conditions will not be fully representative. This was confirmed using a neural network model, which grouped the simulator wear scars with wear scars from retrieved components. Simulator tested components were clustered together, non-centrally into the periphery of the feature map.

To gain more knowledge about frequencies and durations of daily physical activities and their transitions, a sample TKR population was followed throughout the day. External knee moments and internal knee motions were estimated for the most frequent physical activities. The knee moments and motions were used to calculate knee contact forces using a parametric modeling approach. Two previously proposed wear models, based on sliding distance or cross-shear motion, were used to assess the wear impact of different physical activities. An *in vitro* methodology to accelerate the creation and assessment of wear scars generated by different physical activities was also developed. This method was used to compare the wear scar characteristics of each physical activity with wear scars generated *in vivo*.

Among the various physical activities conducted throughout the day, those related to chair and stair were the most frequent and were therefore further investigated. In comparison to ISO walking, the loads and motions generated during chair and stair maneuvers were larger and applied for a longer period of time. Results from the sliding distance and cross-shear wear models indicated that the wear impact of chair and stair activities was substantial; going from 13% of the daily physical activity contribution to 29%, thus indicating that standardized preclinical wear evaluation may, in the worst case, only account for about 70% of the wear generated *in vivo*. Implementing stair ascent/descent and chair sitting/rising into the simulator protocol generated wear scars that were placed more centrally on the feature map when feeding the wear scar images into the neural network. The wear scar features produced by chair and stair activities shared more similarities with *in vivo* worn components than with those components tested according to ISO.

In conclusion, the results of this thesis suggest that daily physical activities, such as those related to chair and stair, should be included in standardized wear testing protocols for the pre-clinical wear evaluation of TKR prosthesis. Such a multi-activity wear testing protocol may generate wear conditions that better recreate those occurring *in vivo*.

Keywords: total knee replacement (TKR), polyethylene wear, daily physical activities, knee kinetics and kinematics, wear modeling.

1. INTRODUCTION

Total knee replacement (TKR) is a surgical procedure that patients with joint disease or trauma undergo to alleviate pain and increase functional mobility. Over the past decade, there have been several improvements in the materials and designs of TKR [1, 2]. However, even with these improvements, wear of the polyethylene tibial insert has remained as one of the leading causes of TKR long-term failure [3-7].

Wear of the TKR polyethylene tibial liner is multifactorial. The prosthesis (materials and designs), the patient (height, weight, joint loading during daily activities, and activity level) and the surgeon (alignment and soft tissue balancing) all influence the wear performance. While many of these factors have been investigated, the contributions of patient factors such as daily physical activities and activity level are not fully understood. Although walking is the most frequent physical activity during the day [8], human life incorporates a greater variety of daily physical activities, with even more complex combinations and transitions. These activities may produce high wear rates due to the high stresses generated. Additionally, daily physical activities may produce knee internal-external rotations and anterior-posterior translations (which are secondary motions of the knee joint) that could coincide with high contact forces. This effect may produce cross-shear motion which, when occurring under load, has been shown to drastically increase the wear rate in conventional polyethylene-based joint replacement devices [9-11].

Evaluation of wear performance of the polyethylene component *in vivo* has proven to be a rather difficult task. Currently, analysis of revision and postmortem explants is the only possibility to evaluate the *in vivo* wear behavior of TKR components. This type of analysis, however, is limited in that the observed tibiofemoral wear scar and the wear appearances cannot be related to the motions and loads that created them as these are unknown in the individual patient [12]. Furthermore, retrieval analysis is limited in that only the end-stage characteristics of the worn tibial component can be analyzed.

In order to address the wear performance of TKR components pre-clinically, *in vitro* wear testing has been established for the evaluation of new materials and designs. These *in vitro* tests are conducted on mechanical simulators that are meant to mimic the motions and forces of the knee joint during level walking. Retrieval analysis, however, has shown considerable differences in the shape and location of tibial wear scars between *in vivo* and *in vitro* tested components of the same design [12-15]. <u>One possible explanation for this finding is that the *in vivo* wear scaring process is the result of a complex combination of daily physical activities that level walking alone does not fully recreate.</u>

<u>Overall hypothesis:</u> **Daily physical activities contribute considerably to the overall wear of the prosthesis. Furthermore, the inclusion of daily physical activities in TKR wear testing will generate wear scar patterns comparable to those observed on retrieved tibial components of the same design.**

Four aims were formulated to investigate the overall hypothesis (<u>Figure 1-1</u>).

THE IMPACT OF CHAIR AND STAIR ACTIVITIES ON TOTAL KNEE REPLACEMENT WEAR

↓

Specific Aim I
To determine the need for an expanded TKR wear testing protocol.

↓

Specific Aim II
To determined what the relevant activities of daily live for a TKR patient are

Sub-aims:
2.1 – To select and validate an activity monitoring device
2.2 – To obtain physical activity frequency and duration parameters from a TKR patient population
2.3 – To obtain TKR joint kinematic and kinetic parameters from a TKR patient population

↓

Specific Aim III
To assess the impact of various physical activities in TKR wear testing

Sub-aims:
3.1 – To develop and validate a rapid wear scar identification method
3.2 – To generate and compare wear scars from various physical activities with wear scars from ISO walking and retrieved polyethylene components
3.3 – To compare the wear impact of various physical activities through available analytical wear models

Figure 1-1: Dissertation structure. Aim I and III are hypothesis driven, while aim II is descriptive.

2. SPECIFIC AIMS

Specific Aim 1: ***To investigate and establish whether the in vivo wear scar patterning is closely reproduced in vitro by wear testing according to ISO 14243-3***

A self-organizing feature map (SOFM) neural network model was used to create groups of tibial liners with similar wear scar characteristics. The SOFM model compared and clustered the wear scar images from walking-only simulator-tested components with wear scars from retrieved components of the same design type.

It was hypothesized that 1) despite using tibial liners of the same design that have been successfully implanted *in vivo* throughout the life of their hosts, there will be sufficient differences that clearly distinguishes components from each other by cluster generation, 2) using tibial liners that have been worn on simulators under ISO conditions [16, 17] will all end up in one cluster because only one activity is represented, and 3) the different ISO tests [16, 17] will be clustered in different groups since the two ISO tests were found generate different wear scar geometries [9].

Specific Aim 2: ***To assess the frequency and duration of daily physical activities and their potential impact on TKR polyethylene wear***

Specific Aim 2.1: ***To identify and* v*alidate a monitoring device for the acquisition of physical activity parameters***

In this Aim, an activity-monitoring device will be selected and compared with a real time controlled treadmill and an optical tracking system ("gold standards"). The accuracy of the activity monitor to identify and measure daily physical activities and their transitions as well as the accuracy to measure gait parameters will be evaluated. Under or over monitor estimations will be corrected based on the study results.

Specific Aim 2.2: ***To measure the frequency and duration of daily physical activities of relevance to TKR wear***

In order to develop a realistic TKR wear testing protocol, ratios of daily physical activities and their transitions over the entire daily routine are needed. In this aim, occurrences of daily physical activities and their transitions will be obtained from a sample TKR population. In addition, time-distance parameters during gait will be measured in order to assess their deviations from simulator testing protocols.

Specific Aim 2.3: ***To obtain knee kinetics and kinematics of daily physical activities***

In order to assess the impact of physical activities in TKR wear testing, knee internal motions, rotations and forces must be known as input parameters for the knee simulator. In this aim, TKR patient's external knee moments and six degrees of freedom motions of the knee will be obtained using the point cluster technique (PCT) [18] while they repeat their activities of daily life in the motion laboratory. Internal knee contact forces will be determined using a parametric knee model developed in house [19].

Specific Aim 3: ***To assess the wear impact of physical activities in TKR wear testing***

In this aim, the impact of relevant daily physical activities in TKR wear (<u>overall hypothesis</u>) will be evaluated.

Specific Aim 3.1: ***To develop and validate a rapid wear scar identification method***

Wear scars generated through *in vitro* wear testing may take several million cycles (Mc) before they can be visually identified and analyzed. In this study, a rapid wear scar identification method will be developed and validated. In the proposed method, the articular surface of the tibial liners will be coated with a material that is easy to remove and that clearly and precisely delimits the boundaries of the tibiofemoral medial and lateral wear scar.

Specific Aim 3.2: ***To generate and compare wear scars from various physical activities with wear scars from ISO walking and retrieved polyethylene components***

Wear scars from various physical activities will be generated using knee kinetics and kinematics parameters that will be obtained in Specific Aim 2.3. Wear scars will be generated using a physiological knee wear simulator. Representative wear scars from the various physical activities will be analyzed using the artificial neural network model previously described in Specific Aim 1.

It is hypothesized that wear scars generated from physical activities, other than walking, will be clustered among retrieved components, away from walking-only simulator components, and closer to the center of the clustering map.

Specific Aim 3.3: ***To compare the wear impact of various physical activities through available wear models.***

The potential wear impact from various physical activities, other than walking, will be investigated and compared with standardized ISO walking. To do this, the axial joint load, sliding distance and cross-shear motion will be calculated for each physical activity. The wear impact comparison will be done using two analytical wear models. The first model will incorporate the activity frequency, axial load and sliding distance; while the second model will be based on the activity frequently, axial load and cross-shear motion.

It is <u>hypothesized</u> that when loading, sliding distance and cross-shear motion are taken into account; a higher proportional daily impact of various physical activities to walking will be achieved, than when considering the activities cycle frequency alone.

3. BACKGROUND and SIGNIFICANCE

3.1. Polyethylene Wear as One of the Major Causes of TKR Failure

About 450,000 total knee replacements (TKRs) are conducted annually in the United States. This number is expected to grow by about 670% by the year 2030 [20]. TKR is considered a highly successful procedure, with 90 to 95% patient satisfaction rate [5]. However, recent changes in demographics of TKR patients are challenging the components longevity, as TKR candidates are younger, heavier and more active [21]. Patients outliving their implant may require a revision surgery, which in addition to affecting the patient physically and emotionally, is more costly than the primary arthroplasty. It is anticipated that by the year 2030, revision procedures will increase from 38,300 in 2005 to 268,200 by the year 2030 [20].

Wear of the polyethylene component accounts for about 25% of TKR failure and revision [5]. In addition to the deterioration of the tibial component, wear particles may migrate to the implant-bone interface where the particles could cause chronic inflammation and bone resorption, which can result in implant loosening and ultimately, failure [22].

Wear performance evaluation of TKR components *in vivo* is rather difficult as the polyethylene component is not visible by the X-ray beam. *In vivo* wear volume estimations are therefore limited to yearly penetration rates of the metal component into the tibial liner or by computational modeling [23-26]. Semi-quantitative retrieval analysis is currently the only way to evaluate the wear performance of TKR components *in vivo*. However, estimation of wear volume from retrieved polyethylene components has proven to be difficult [27, 28] as the initial conditions of the component (weight, surface characteristics, and machining/molding error) are not known [29]. In order to evaluate the wear performance of TKR polyethylene components, *in* *vitro* wear testing protocols have been created with the objective of evaluating the materials and designs of TKR components pre-clinically.

3.2. Pre-Clinical Wear Performance Evaluation of TKR Polyethylene Components

With its six-degrees of freedom, the natural knee joint allows for translations and rotations between the femur and the tibia. Flexion-extension (F-E) is the primary motion of the knee; anterior-posterior (A-P) and medial-lateral (M-L) translations and internal-external (I-E) rotation are the knee secondary motions [18, 30]. An accurate re-creation of the motions and forces of the prosthetic knee joint is essential for the pre-clinical evaluations of the materials and designs used for TKR components. Currently, the wear performance of TKR polyethylene components is evaluated in mechanical simulators that mimic as close as possible the motions and forces of the knee during a normal walking cycle. There are two wear testing protocols developed by International Standards Organization (ISO) for the evaluation of TKR components. These protocols drive the secondary motions of the knee wear simulator by either displacement (ISO 14243-1) or load (ISO 14243-3). The differences between both testing protocols is that under load control mode an A-P shear force and a I-E torque are input to the simulator, while under displacement control mode an AP translation and a IE rotation are used. Both protocols input identical axial force and FE rotation (Figure 3-1).

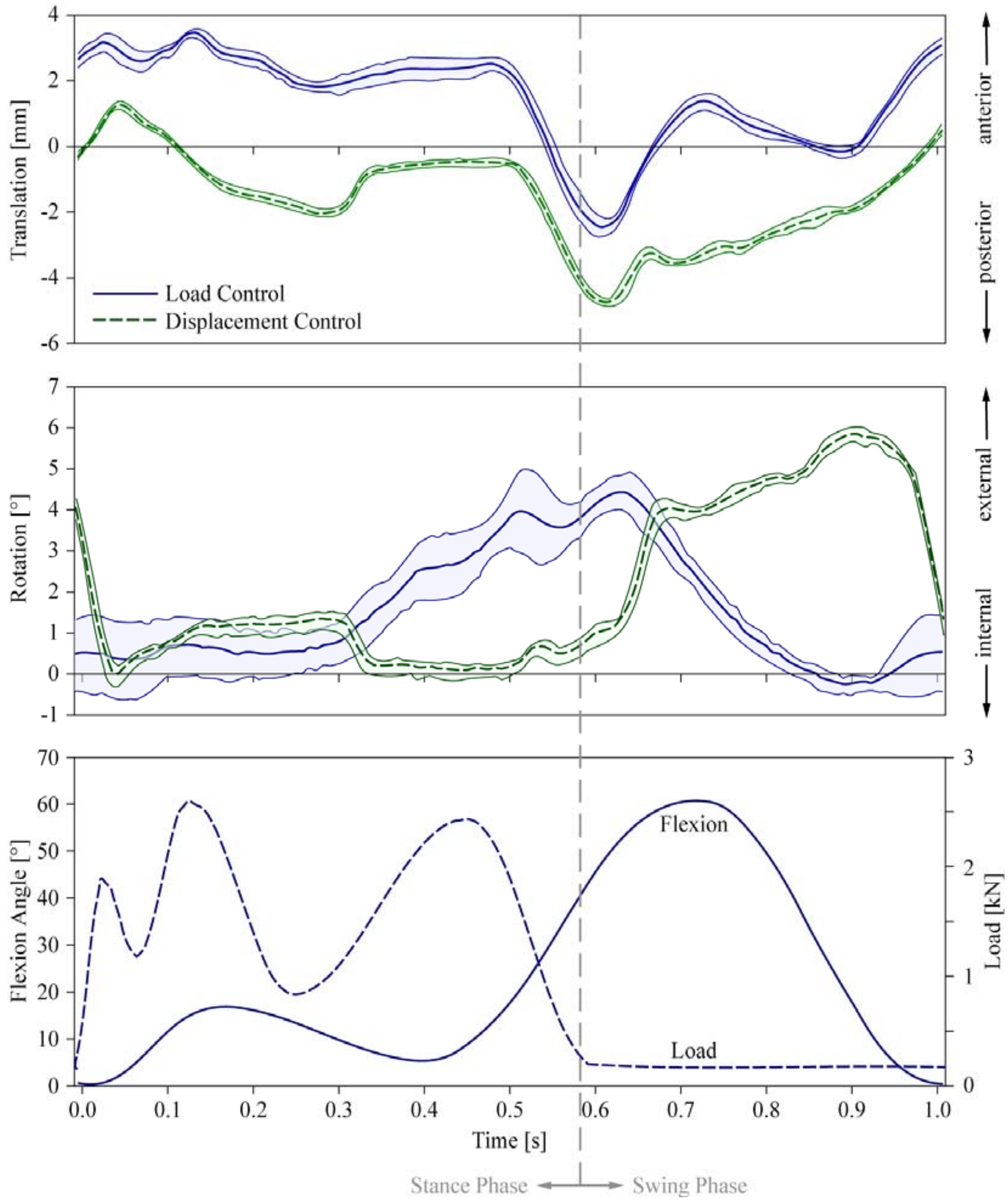

Figure 3-1: Differences in cross-shear motion between displacement and load control ISO tests. Wear rates from the load-controlled test were significantly higher than the wear rates generated during the displacement-controlled test. The amount of IE rotation occurring during the third maximum peak of the axial load (cross-shear effect) may explain the wear differences [9].

In order to evaluate the wear performance of TKR components, gravimetric measurements are conducted throughout the wear test (at the end of each test interval). Cleaning and gravimetric measurements are conducted in accordance to the ASTM standards 2025 and

F732, respectively. While gravimetric measurements allow for the quantification of material removed during the application of *n* testing cycles; these type of measurements only provide a global wear volume estimation and do not provide information from specific areas of the component (such as medial, lateral and back side). Wear volume estimates from specific areas of the component may be a key factor in the material selection or the component design as different wear factors (such as daily physical activities) may remove material from the tibial component differently.

3.3. Simulator vs. Retrieved Components

While both ISO wear-testing protocols (described above) are the gold standards for the evaluation of TKR components pre-clinically, their *in vivo* validity is questionable. Retrieval analysis has shown considerable differences in the wear scar formation (or damage pattern) between *in vitro* tested TKR components and components retrieved after either autopsy (postmortem) or revision surgery [13, 31, 32]. Since the wear scar is substantially influenced by the kinetics and kinematics of the knee joint [32-35], the findings of Harman et al. [32] and Wimmer et al. [34] suggest that the motions and loads generated during level walking do not account for the variability in wear scar size and location observed in retrieved components of the same design type. During their daily routine, TKR patients subject their components to not only walking cycles but to a complex combination of daily physical activities that, in spite of their lower frequency, may impose detrimental forces and motions to the TKR prosthetic components. The inclusion of daily physical activities other than walking may better recreate *in vivo* conditions in TKR wear testing.

3.4. Daily Physical Activities and Wear

Input kinematics in standardized knee wear tests (ISO 14243-1 and 3) are solely based on level walking, overlooking the inclusion of other daily physical activities that TKR patients perform regularly as part of their daily life [12, 14, 15]. While walking is the most representative physical activity, in the light of the above, it is questionable whether walking alone is the single most important activity that should be used in pre-clinical wear testing. There is evidence that other activities affect the wear performance of TKR components. Previous studies have shown that more representative wear scars as well as higher wear rates were obtained when bouts of stair ascend or descend were included in a typical ISO wear test [12, 36]. While the results from Benson et al. [14] and Cottrell et al. [12] support the inclusion of other physical activities in TKR wear testing, the *in vivo* representativeness of their has yet to be shown, as their testing protocol was conducted in an artificial manner, applying walking and stair steps in blocks, without having actual data of the stair activity. A realistic representation of physical activities is important as detrimental loading and motions, such as cross-shear motion, may occur. Furthermore, ratios of walking to other physical activities derived from a TKR population are needed, as these ratios may not be the same as those from healthy subjects.

3.5. Significance of Planned Studies

Current standards for wear performance evaluation of TKR components may not be representative of *in vivo* conditions as they address only level walking. While stair ascend or descend have been considered in previous testing protocols [12, 14, 15], their frequency and their kinematic/kinetic behavior as well as the inclusion of other physical activities has not been investigated. In this study, the impact of daily physical activities on TKR wear testing is assessed. The TKR patients' most common physical activities will be used to suggest a more realistic (physiological) testing protocol for wear performance evaluation of TKR tibial liners *in vitro*. In addition, by obtaining load and kinematics from specific activities and from their transitions, a mathematical model can be created to estimate the wear rate of a TKR patient based on their daily routine. Furthermore, by obtaining compartment-specific wear scars (from medial and lateral sides of the tibial liner) it may be found that different activities wear the compartments of the tibial components differently. Only one implant design has been selected (MG-II, Zimmer Inc., USA), because a vast retrieval collection is available, including some components with known knee kinetics and kinematics.

4. SPECIFIC AIM 1 - *To investigate and establish whether the in vivo wear scar patterning is closely reproduced in vitro by the application of only level walking cycles*

4.1. INTRODUCTION

Wear performance evaluation has become an important preclinical tool for the assessment of materials and designs of total knee replacement (TKR) components. To date, the International Organization for Standardization (ISO) has established two wear testing protocols to evaluate the long-term wear performance of TKR components [16, 17]. Both ISO protocols aim at replicating loading and motion characteristics of the natural knee during level walking, which is the most performed physical activity of daily living (ADL) [8]. As with any simulation tool, the ultimate goal of wear simulations is to recreate *in vivo* conditions as closely as possible. For knee wear simulation this means recreating wear damage characteristics (rates, modes, patterns, appearances, particle size and morphology) generated *in vivo*. However, despite the high reproducibility of *in vivo* wear damage characteristics of hip simulators, reproducing *in vivo* wear damage characteristics at the knee has proven to be very challenging. It has been reported that knee wear simulators generated tibial liner wear scars (envelope containing all damage patterns) that are less variable in size and location compared to those observed in retrievals of the same design type [37, 31].

Several factors influence wear of the TKR polyethylene tibial liner. Characteristics of the prosthesis (materials and designs), the patient (height, weight, joint loading during daily activities, and activity level) and the surgical technique (alignment and soft tissue balancing) all influence wear performance. Discrepancies between simulated and *in vivo* worn components can be identified by comparing their wear scar characteristics, which are substantially influenced by the kinetics and kinematics of the knee joint. Hence, wear scars are useful indicators of the physiological load and motion spectrum applied to the tibial liner during daily physical activity. However, the detailed analysis of wear scars is very complex. The mathematical description of wear scar patterns is nonlinear and multidimensional, which makes it very difficult to model these patterns using traditional mathematical or statistical methods. For instance, different geometric parameters including area, perimeter or centroid of the wear scar could be used to form the basis for a specific model. However, because a single geometric parameter may not sufficiently explain the overall wear scar architecture, the use of the wear scar as a whole was then proposed; using bitmap images for analyzing the complex patterns of *in vivo* and *in vitro* generated wear scar patterns.

In this study, the application of an Artificial Neural Network (ANN) model based on image information is implemented as a data mining tool to differentiate wear scars that originate from different loading histories. ANNs have been successfully used for similar models because of their ability to handle nonlinear behavior, to learn from experimental data and to generalize solutions [38-43]. From the pool of ANN models, the self-organizing feature map (SOFM) was selected for this study. SOFM is an unsupervised neural network (i.e. no *a priori* knowledge of the data structure and classification is used) and is frequently used for visualization of high-dimensional data and for data mining and knowledge discovery [39-42, 44, 45]. Self-organizing feature maps are particularly useful because of their ability to map non-linear statistical relationships between high-dimensional data onto a convenient and easily comprehendible two–dimensional map. This type of mapping preserves the topology of the data, meaning that points within close proximity in the high dimensional space are mapped to neighboring map units in the output space. While this modeling technology has been previously used for image mapping [46], to the best of our knowledge, it has not been used for wear pattern analysis and other applications in the orthopedic field.

4.2. PURPOSE

The purpose of the present investigation was to create a clustering structure of wear scar images based on similarities between retrieved (revision and postmortem) and simulator tested components of the same material and design type. Wear scars from postmortem-retrieved components were used to create a clustering structure, while the wear scars from simulator-tested components were assigned to the existing clustering structure based on their similarities to the retrieval components. Data mining was then performed to understand the similarities among wear scars clustered together, as well as to explain the differences between wear scars of different clusters. It was hypothesized that 1) despite using tibial liners of the same design that have been successfully implanted *in vivo* throughout the life of their hosts, there will be sufficient differences that clearly distinguishes components from each other by cluster generation, 2) using tibial liners that have been worn on simulators under ISO conditions [16, 17] will all end up in one cluster because only one activity is represented, and 3) the different ISO tests [16, 17] will be clustered in different groups since the two ISO tests were found generate different wear scar geometries [9].

4.3. MATERIALS and METHODS

4.3.1. Retrieved Components

An overview of the materials and methods used in this investigation has been presented in Figure 4-1.

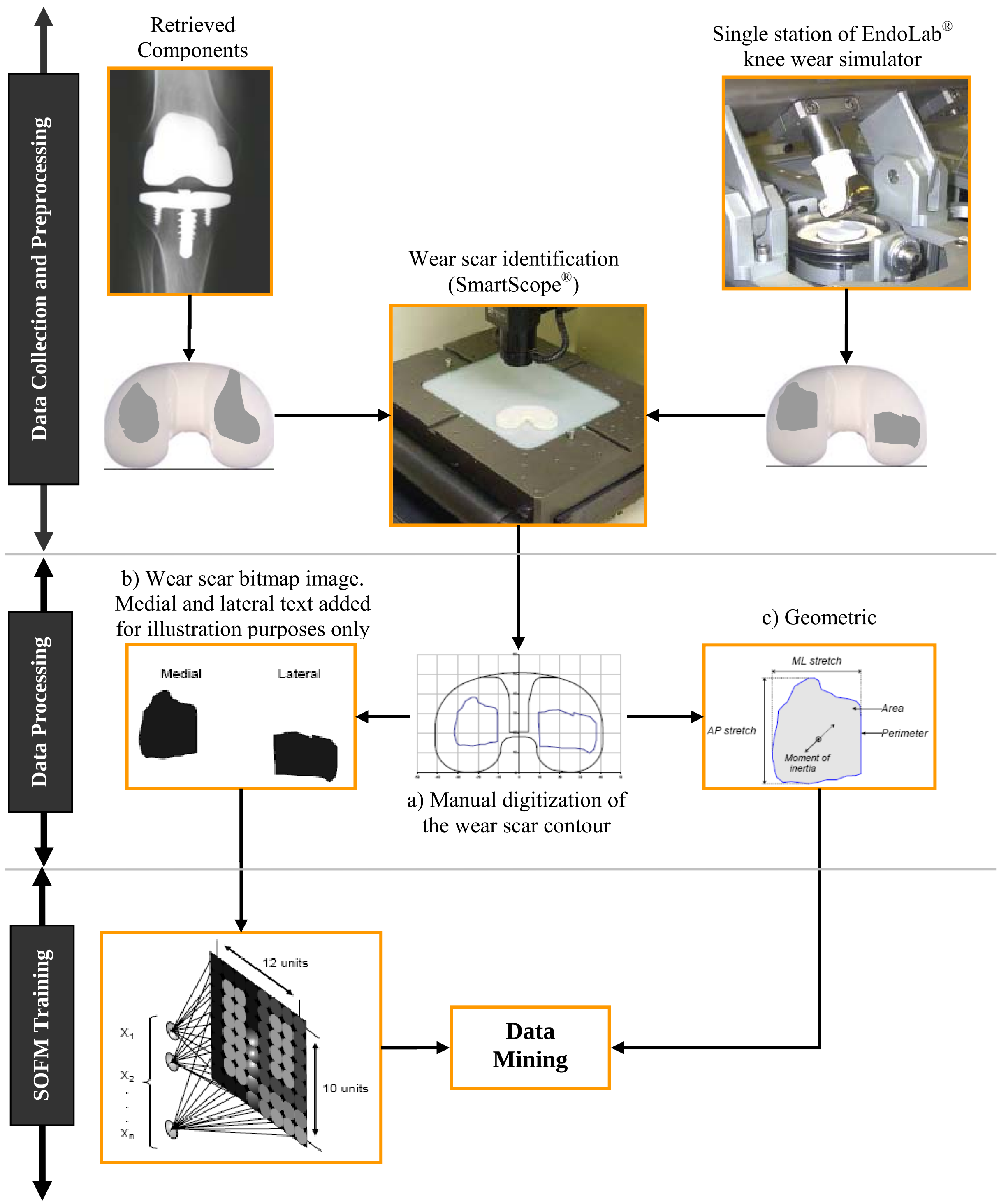

Figure 4-1: Wear scar identification and digitization process; creation of image and geometric information

Twenty-one postmortem and fifty-four revision retrieved tibial liners were selected from the Retrieval Repository at Rush University Medical Center (Table 4-1). Before being included in the study, components were screened for missing demographic information and for signs of delamination; heavily delaminated components were excluded. All retrieved components were of the MG-II design and were manufactured by the same company (Miller-Galante II, Zimmer, Inc., Warsaw, IN, USA).

Table 4-1: Demographic information of liner donors (postmortem and revision)

Implant Source (N)	Gender (N)	Side (N)	In-situ time (mo.)	Cause of failure (N)
Revisions (54)	Females (22) Males (26) Unknown (6)	Left (24) Right (23) Unknown(7)	Range (1-108) Mean (26) Unknown (16)	Infection (10) Maltracking (9) Loose (9) Instability (5) Synovitis (2) Fracture (1) Osteolysis (1) Failed liner (1) PE wear** (1) Unknown (15)
Postmortem (21)	Females (13) Males (8)	Left (11) Right (10)	Range (19-144) Mean (79)	Autopsy (21)
Simulator (6)	Not applicable	Left (6)	60 months*	Not applicable

**1 Million cycles representing 12 months of level walking* [16, 17].
*** PE = polyethylene*

4.3.2. Wear Testing

Wear testing was performed using eight tibial liners. The liners were of the same material and design type as the retrieved components (MG-II). Testing components were randomized into two equal groups. In each group, three samples were tested for wear performance and one sample served as a loaded soak control. The tibial plateaus were machined from ultra-high molecular weight polyethylene (UHMWPE), gamma sterilized and packaged in a nitrogen environment by the manufacturer. The boxes were opened immediately prior to testing. Wear performance tests were carried out in a four-station knee simulator (EndoLab®, Rosenheim, Germany). The simulator used met ISO standard requirements and was set up to run either in load-control mode (LCM) [17] or in displacement-control mode (DCM) [16]. The simulator motions were hydraulically actuated and closed-loop controlled. The difference in control mode refers to two degrees of freedom (anterior-posterior and internal-external, respectively) that are either load- or displacement–controlled. Each simulator station was comprised of a temperature-controlled chamber that contained test lubricant. The lubricant was based on a buffered mixture of bovine serum (Hyclone Inc., Logan, UT, USA) diluted with distilled water to achieve a final protein content of 30 g/l. All chambers were closed and sealed during the entire test to minimize fluid evaporation and contamination. The simulator was connected to a computer with a user interface for machine control, test supervision and data acquisition.

The first implant group of tibial inserts was tested in LCM while the second group was tested in DCM. The LCM and DCM tests followed the same general protocol and testing parameters previously described. Tests were conducted at 1.0 (±0.1) Hz cycle frequency for five million cycles (Mc). The load and displacement input represented one full walking cycle (60% stance and 40% swing phase) per test cycle and were taken from the respective ISO standards. The experiment was interrupted every 0.5 Mc to disassemble, clean and weigh the specimens following ISO standard specifications [47]. Wear scars on the tibial UHMWPE plateaus that developed during the test were analyzed after test completion [9].

4.3.3. Wear Scar Identification

Medial and lateral articulating surfaces were visually analyzed using a video-based microscope (SmartScope, OGP NY, USA). Wear scars were digitized by manually tracking their contours (i.e. the boundary between worn and unworn areas) on the liner surface (Figure 4-2a). Because the goal of this study was to compare wear scar patterns using images rather than discrete geometric parameters, black and white wear scar bitmap images (220x170 pixels) were generated for each component (Figure 4-2b). Each bitmap image contained medial and lateral wear scar shapes, with black pixels representing worn areas and white pixels representing unworn areas. Each bitmap image was converted to a 220 x 170 matrix with ones representing white pixels (unworn areas) and zeros representing black pixels (worn areas). Each matrix was then reshaped to a single-row vector size 37,400 which was used as input data for the SOFM model. While the component border was not kept in the image, the length and height of the image was adjusted to match the component size. Bitmap images were normalized to an equal size and implantation side (normalization was carried out only in retrieved- revision and -postmortem components. Each image was normalized to a predefined implant border size). Geometric wear scar parameters such as area, perimeter, centroid, bounding box, anterior/posterior stretch, medial/lateral stretch, moment of inertia and multiple shape factors were computed for each component (Figure 4-2c) and used for data mining and statistical analysis.

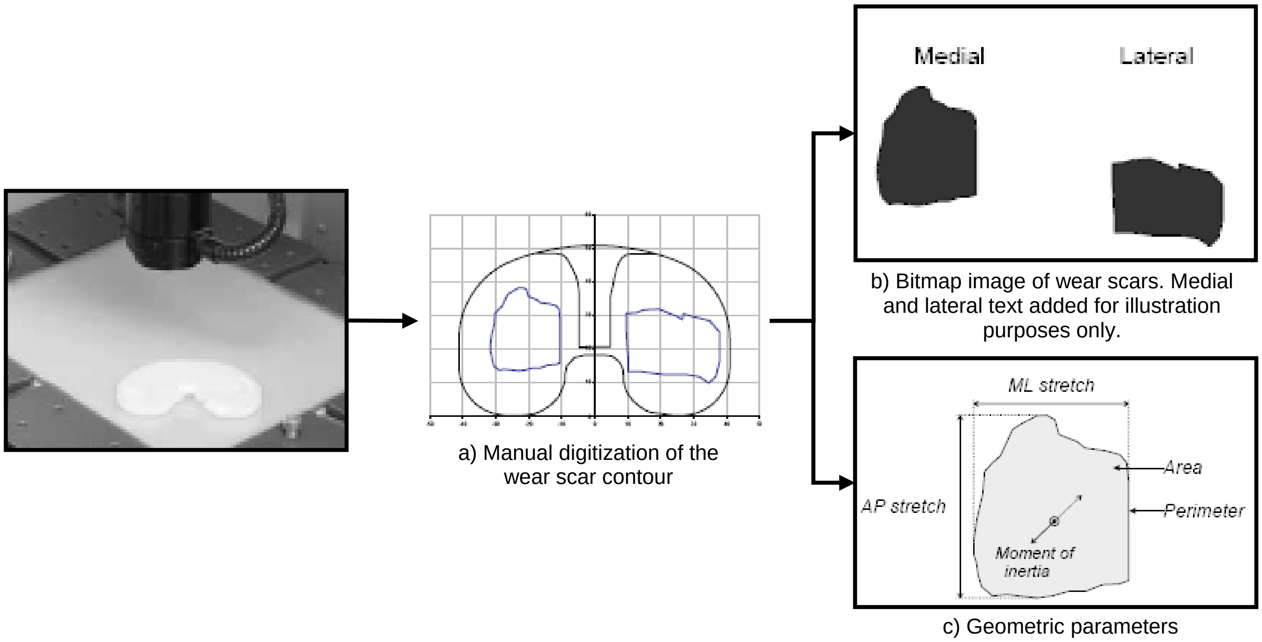

Figure 4-2: Wear scar identification and digitization process; creation of image and geometric information.

4.3.4. Clustering

Similar wear scar images from revision and postmortem retrievals and simulator components were identified and assigned to clusters using Kohonen's Self Organizing Feature Maps (SOFM) [48-51]. The SOFM network was designed and trained using the Matlab SOM Toolbox 2.0 (Helsinki University of Technology, Finland). A sensitivity analysis was conducted to identify ideal training parameters generating best mapping results. The networks consisted of an input layer of 37,400 dimensions (from image dimensions of 220x170 pixels = 37,400), a competitive layer, and an *n* x *m* neurons map or output layer (Figure 4-3). Five different networks with different map dimensions were generated. The sensitivity analysis was done by training SOFMs with different *n* x *m* map dimensions and different neighborhood radius (i.e. the number of neurons around the winning neuron that were trained to a specific input, Figure 4-3). Learning rate was linearly adjusted for all networks and the presentation of training samples was done in a random order. Training was performed using the postmortem retrieved components only. Subsequently, revision retrieval and simulator components were assigned to the already existing clusters. No network learning occurred from the clustering the revision retrieved and simulator wear scar patters. Training was done using the batch algorithm with Euclidian metric. Statistical analysis of the clustering structure was performed only from the map providing the smallest quantization error (which a measure of "fit" between input and output mapping) and a well defined clustering structure.

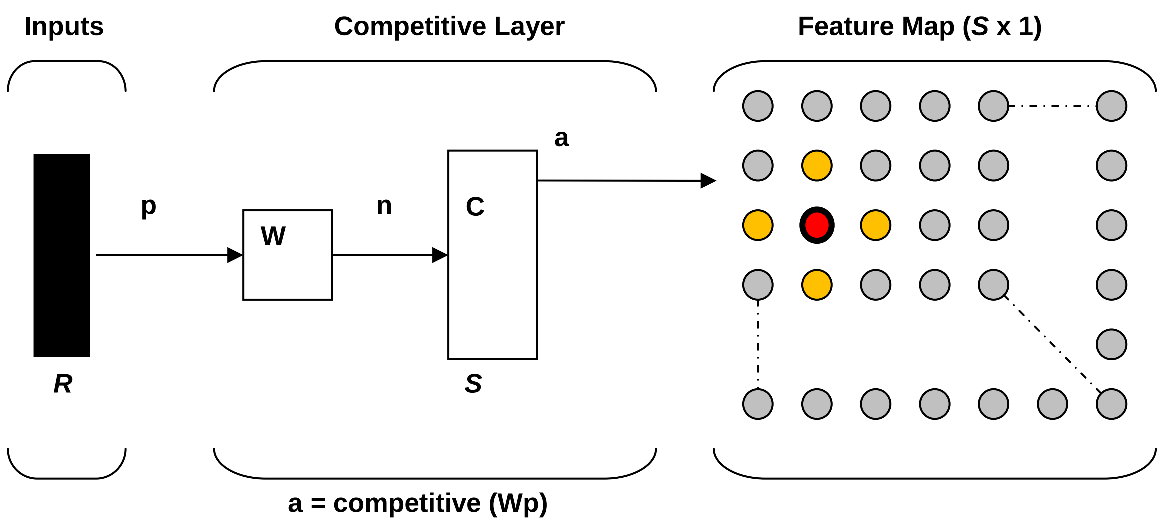

Figure 4-3: Self-organizing feature map (SOFM) neural network structure. Input vectors (wear scar images in this case) were assigned to a winning map neuron (red) which Euclidian distance to the input vector was the shortest. Neighboring neurons (orange) around the winning neuron will be also assigned the input vector. Similar input vectors will be assigned to neighboring neurons.

4.3.5. Clustering Visualization

The u-matrix method was used to visualize the distance of each map neuron to its neighbors. The shorter the distance between neurons was, the smaller the difference between them [49, 51]. This method was used to visually uncover the clustering structure in the SOFM. A two-dimensional color coded u-matrix is commonly used to identify cluster boundaries. However, in this study a topographic presentation was used where the distance between map neurons was represented by elevation values of a surface plot. The result was a topographic-like plot with high hills representing cluster boundaries and valleys representing clusters. Component planes (another commonly used visualization tool) were not created because the type of input data used in this study would have produced 37,400 component planes (one for each dimension), which would have not provided meaningful information for analysis.

4.3.6. Statistical Analysis

Clustering robustness was evaluated by producing multiple versions of the map with the best mapping results. The goal of this process was to detect mapping irregularities caused by the inherent mapping error that arises when clustering data from a high dimensional space onto a significantly smaller dimensional space. To detect clustering irregularities, three network versions were created and trained until they converged. The networks were created and analyzed by an independent internal investigator. The networks' map size, learning rate and neighborhood radius were left unchanged. The only training parameters that differed between networks were the initial values of the map neurons and the presentation of the training samples, which were both randomly chosen. The clustering structure was visualized and compared between network versions. The map neurons assigned to each wear scar in each of the networks were recorded and used for comparison. Cohen's Kappa analysis was carried out to investigate if each component was consistently clustered with the same group of components.

Linear regression analysis was conducted to investigate mapping correlations between clustered components and their wear scar geometry. Analysis of variance (ANOVAs) was used to detect differences within and among clustered wear scar images. The geometric parameters computed for each medial and lateral wear scar were used in the statistical analysis. All statistical analysis was performed in SPSS 10.0 for Windows (SPSS Inc., Champaign, IL, USA).

4.4. RESULTS

4.4.1. Sensitivity Analysis

A network with a 12x10 map size and initial and final neighborhood radii of 4 and 1, respectively, was found to provide the lowest quantization error (q_e= 11.14) and a well defined clustering structure (i.e. clearly identifiable clusters). The other network configurations evaluated were: 20x10/4 to 1, 20x10/4 to 1, 10x10/4 to 1, 10x10/5 to 3.5 and 7x7/4 to 1 (map size/initial to final neighborhood radius). The 20x10 network had a lower quantization error ($q_{e\ (20x10)}$ = 10.9) than the network selected for the final analysis; however, its clustering structure was not well defined. The remaining evaluated networks had higher quantization errors: $q_{e\ (10x10/4\ to\ 1)}$ = 12.7; $q_{e\ (10x10/5\ to\ 3.5)}$ = 15.3; and $q_{e\ (7x7)}$ = 17.1.

4.4.2. Robustness

The clustering robustness analysis showed substantial inter-rater reliability for the different SOFMs created with a Kappa value of 0.69 (p <.0.001), 95% CI (0.667, 0.712). Despite the random initial values of map neurons and the random presentation of the training samples, tibial components were consistently clustered with the same components. Because of mapping errors, some components were assigned to different neighboring clusters. However, on average, 84% of all components were consistently mapped with the same components.

4.4.3. Clustering Results

Using the u-matrix visualization method, eleven clusters (A-K) became evident. Each contained at least one retrieved component and a maximum of 18 retrieved components (Figure 4-4). Wear scar images assigned to all clusters can be found in Appendix 1-I. While 54 revision-retrieved components were assigned to nine of the eleven clusters, all but one of the six simulator-tested components were placed in cluster G, which contained only a small number of retrieved components (Figure 4-5). Cluster G was one of the more isolated clusters on the map with relative high boundaries separating this cluster from others. The remaining simulator component was assigned to cluster 'D'. Interestedly, this outlier represented a component from a simulator station, which experienced rotatory actuator failure during testing.

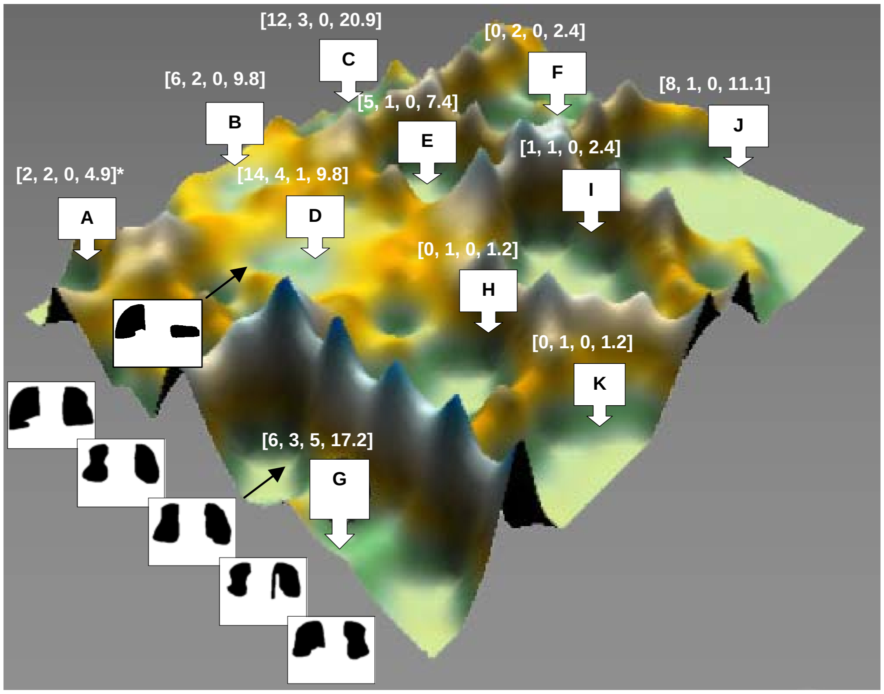

Figure 4-4: Topographic visualization of the SOFM after training. Eleven wear pattern clusters were identified ('A-K'). Five out of six *in vitro* tested components were assigned to cluster 'G'. For each cluster, the number of revision (R), postmortem (P), simulator (S) and percent of total components are provided.

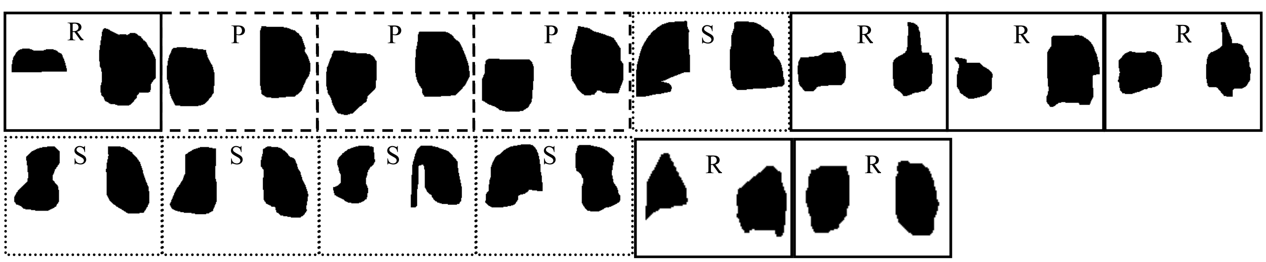

Figure 4-5: Cluster '1' contains six revision, three postmortem and five simulator components (three force control and two displacement control).

When looking for clustering correlations, linear regression analysis revealed that geometrics parameter could not significantly explain the difference between wear scars of one cluster and those of other clusters (Table 4-2). It was found that although the SOFM network established cluster G as one of the most isolated clusters, cluster G was not significantly different from the other clusters based on wear scar geometric parameters. The largest number of significant differences in wear scar geometry was found between cluster J and all the other clusters. For simulator components only, their medial and lateral wear scars were more anteriorly located and more symmetrical. However, only the anterior location differed significantly from all other clustered retrieved components ($\alpha < 0.05$). Wear scar symmetry did not differ significantly between all clustered retrieved components. A summary of area and perimeter per cluster is presented in Table 4-3.

Table 4-2: Geometric parameters that differed significantly between clusters.

Dependent variable	(i) cluster	(j) cluster	Dependent variable	(i) cluster	(j) cluster
M. Area	B	C, E, F, G, J	Time *in situ*	F	C, J
M. Perimeter	B	C, E, F, J	Comp. Type	F	C, J , D
M. Ml distance	B	K , J	M. Area	F	B, J
M. AP distance	B	C, E, G, J	M. Perimeter	F	B
M. Moment inertia x	B	C, E, F, J	M. Moment inertia x	F	B
M. Moment inertia y	B	C, E, F, J	L. AP distance	F	B
L. Area	B	C, E, G, J	L. Moment inertia x	F	B, G
L. Perimeter	B	C	Time *in situ*	G	J
L. AP distance	B	C, E, F, J	M. Area	G	B, J
L. Moment inertia x	B	E, F, K, J	M. AP distance	G	B
L. Moment inertia y	B	C, E, G, J	M. Moment inertia x	G	E
M. Centroid	B	G	M. Moment inertia y	G	B, J
L. Centroid	B	G	L. Area	G	B
Time *in situ*	C	F	L. AP distance	G	E
Comp. Type	C	F	L. Moment inertia x	G	E, F, K, J
M. Area	C	B, J	L. Moment inertia y	G	B
M. Perimeter	C	B	M. Centroid	G	B, C, E, D
M. AP distance	C	B	L. Centroid	G	B, C,
M. Moment inertia x	C	B	M. Ml distance	K	B
M. Moment inertia y	C	B, J	L. Moment inertia x	K	B, G
L. Area	C	B	Time *in situ*	J	F, G
L. Perimeter	C	B	Comp. Type	J	F
L. AP distance	C	B	M. Area	J	B, C, F, G, D
L. Moment inertia x	C	E	M. Perimeter	J	B
L. Moment inertia y	C	B	M. Ml distance	J	B
M. Centroid	C	G	M. AP stretch	J	B
L. Centroid	C	G	M. Moment inertia x	J	B
M. Area	E	B	M. Moment inertia y	J	B, C
M. Perimeter	E	B	M. Moment inertia y	J	G, D
M. AP distance	E	B, D	L. Area	J	B
M. Moment inertia x	E	B, G, D	L. AP distance	J	B
M. Moment inertia y	E	B	L. Moment inertia x	J	B, G
L. Area	E	B	L. Moment inertia y	J	B
L. AP distance	E	B, G	Comp. Type	D	F
L. Moment inertia x	E	B, C, G, D	M. Area	D	J
L. Moment inertia y	E	B	M. AP distance	D	E
M. Centroid	E	G	M. Moment inertia x	D	E
			M. Moment inertia y	D	J
			L. Moment inertia x	D	E
			M. Centroid	D	G

Table 4-3: Summary of geometric parameters for retrieved and simulator components.

Mean (StDev)	***MEDIAL***				***LATERAL***			
Cluster no.	**Area (mm^2)**	**Perimeter (mm)**	**ML stretch (mm)**	**AP stretch (mm)**	**Area (mm^2)**	**Perimeter (mm)**	**ML stretch (mm)**	**AP stretch (mm)**
A	498.21 (78.26)	83.56 (4.40)	24.39 (4.66)	26.15 (3.32)	566.35 (80.80)	89.47 (2.84)	12.25 (28.34)	27.06 (1.99)
B	712.27 (185.35)	100.02 (12.20)	26.87 (2.88)	32.92 (5.23)	754.24 (180.98)	102.73 (11.72)	0.93 (29.67)	33.26 (5.72)
C	374.52 (108.82)	75.28 (9.46)	23.33 (3.76)	21.05 (4.33)	392.90 (124.16)	74.99 (10.18)	3.62 (23.54)	21.97 (5.55)
D	416.07 (146.55)	78.78 (1.51)	23.12 (3.37)	23.68 (4.87)	421.97 (165.74)	79.01 (12.56)	-3.67 (26.80)	22.86 (6.32)
E	179.84 (34.29)	54.08 (6.05)	17.21 (1.75)	14.83 (3.31)	143.83 (76.49)	46.72 (12.10)	3.17 (15.72)	13.87 (3.19)
F	363.73 (15.08)	73.69 (0.83)	22.83 (3.82)	21.21 (5.66)	308.54 (46.11)	68.10 (6.71)	-7.98 (28.02)	16.16 (3.08)
G	391.84 (135.11)	79.18 (13.54)	23.59 (3.51)	21.87 (6.03)	460.96 (166.04)	84.25 (12.78)	-12.77 (20.80)	25.64 (4.97)
H*	283.47	62.59	22.63	16.71	337.01	67.39	-20.51	21.38
I*	355.69	71.44	19.39	23.58	436.42	76.99	-26.19	21.71
J	129.36 (88.82)	45.12 (18.78)	13.76 (5.50)	13.53 (6.04)	241.70 (136.61)	58.06 (26.35)	8.61 (15.45)	16.62 (7.67)
K	418.87 (101.98)	77.46 (6.04)	21.78 (0.63)	24.22 (3.62)	412.37 (121.97)	76.86 (10.95)	-23.54 (2.06)	22.74 (3.61)

StDev = standard deviation, ML stretch = Medial-Lateral stretch, AP stretch = Anterior-Posterior stretch,
**StDev not available n(cluster) = 1*

4.5. DISCUSSION

In this study, the relationship between wear scar images of simulator tested and retrieved TKR tibial components was investigated. A non-traditional qualitative modeling approach was used to project the non-linear relationships of a high dimensional data set (wear scar images) onto a two-dimensional map. The Self-organizing Feature Map algorithm was used as a data mining and knowledge discovering tool and served as visual aid in the discovery of wear scar characteristics.

The mapping results showed that after successful training of the network with the wear scars of retrieved components, eleven clusters were created. These findings support the first hypothesis of this study, as wear scars from retrieved-postmortem components generated several clusters of similar wear scars, mimicking the variability of wear scar patterns that characterizes retrieved components [31, 37]. Furthermore, the second hypothesis of this study was also supported since wear scars generated through mechanical simulation were clustered together, but only with a small percentage of retrieved components, reflecting that the sole application of normal gait cycles may not be sufficient in mimicking the greater variability of wear scar patterns observed on retrieved components [12, 14]. The successful training of the SOFM is a milestone in the analysis of wear scars, because the proposed approach is able to generate meaningful results.

Previous studies reported that wear scar patterns from simulator tested components differed from those observed on retrievals [13, 31]; similar results were found in this study. Simulator components were clustered with only 10.8% of retrieved components, indicating that standardized wear testing recreates only about 11% of wear scar patterns generated *in vivo* during daily physical activities. The modeling approach proposed in this study proved to be very useful in quantifying the proportion of reality being recreated by knee wear simulators. The already trained SOFM network could be used to cluster wear scars from tibial liners generated in future wear tests.

All but one of the simulator-tested components were clustered together; thus suggesting that both ISO testing protocols produce similar wear scar patterns. These finding do not support our third hypothesis, which stated that simulator components from the different ISO test were going to be clustered in different groups. Further, the SOFM network appears to be capable of clustering wear scars with similar loading and motion history. Figure 4-6 shows the six simulator tested components that were assigned to cluster G and D. One of the simulator components (the one assigned to cluster D) clearly differs visually from the other simulator components. This difference was not unknown, as it was previously noticed that one of the A-P actuators of the simulator was faulty during one of the wear tests. However, this information was not used as input into the SOFM. The only data and information used as input into the SOFM network was the medial and lateral wear scar images from both retrieved and simulator tested components, which were all presented to the network in a random order during the training process. The identification of faulty simulator tested component is another application of the SOFM network. Ideally, standardized wear testing should generate repeatable wear scars. By analyzing the clusters each tested component is assigned to, testing error could be identified. Furthermore, the SOFM network is able to directly compare wear scars of simulator and retrieved components. This comparison provides an estimate of how closely wear scars from components worn *in vivo* are replicated through preclinical wear testing.

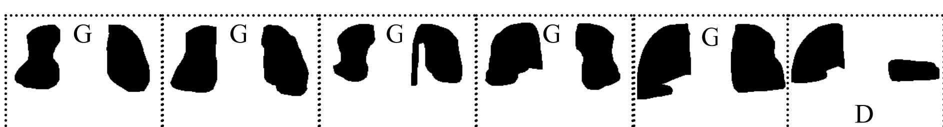

Figure 4-6: five out of six simulator components were clustered together in cluster G.

When comparing wear scars from simulator and retrieved components, it was found that wear scars from simulator components were located more anteriorly, which relates to the home position selected during wear testing. In addition, wear scars on the medial and lateral side of simulator components were more symmetrical when compared to retrieved components. This difference, however, was not statistically significant. These findings suggest that the amount of internal-external rotation as well as the center of the rotation applied in mechanical simulations may not be representative of the rotational motion pattern that an implanted device experiences during activities of daily living (ADL). Because wear scars are substantially influenced by the kinetics and kinematics of the knee joint, these findings indicate that it might be important to consider other ADL to achieve wear scar patterns that better resemble *in vivo* patterns. Cottrell et al. and Benson et al.. found that the inclusion of one cycle of stair ascent (Cottrell) or descent (Benson) for every seventy cycles of level walking during wear testing (corresponding to a 70:1 ratio) produced higher wear rates and more *in vivo* like wear scars than those generated by walking alone [12, 37]. When considering walking only, Ngai et al. [52] reported that the motion pattern of TKR patients was not only different from those applied by the displacement control standard [17], but that it was also highly variable between patients [52], raising the need for selecting a more representative TKR motion pattern. The variability of wear scars observed in retrieved components may not just be the result of the range of physical activities performed by the patient but also the outcome of different walking patterns that are characteristic for each individual.

4.6. LIMITATIONS

There are limitations of using the SOFM, which produces a qualitative representation of the data analyzed. The network does not identify the variable or variables that characterize each cluster and best discriminate between clusters [39]. In addition, the clustering created by the SOFM is a projection of the non-linear and high dimensional input space, and therefore, the clustering results may not be fully explained by traditional linear statistical models. This is particularly true in this study because of the nature of the clustered data. Typically, cluster correlations created by a SOFM are performed using component planes; however, since our data sets were based on pixel information, this analysis was not applicable. This fact is both a limitation and strength of study: clustering the wear scar geometric parameters resulted in a completely different clustering structure where simulator tested components were not clustered together. Furthermore, the high dimensionality of the input dataset representing wear scars affected the training time of the SOFM, which ranged from four hours to almost a full day, until network convergence was achieved. Smaller bitmap images or a different representation of the wear scar pattern may be used to limit the computational time spent on training the SOFM. Smaller bitmap images may also reduce the quantization error, as this error depends directly on the dimensionality of the input space and the output map; where a greater dimensionality reduction will result in a greater quantization error.

4.7. CONCLUDING REMARKS

In conclusion, a non-traditional modeling approach has been suggested for the comparison of wears scar images of simulator-tested and retrieved TKR tibial liners. This modeling approach proved to be robust and repeatable when using the wear scars of the same retrieved tibial liners. The model, which was based on the Self-Organizing Feature Map network, can be used to directly compare wear scars from simulator and retrieved tibial liners. This qualitative analysis was useful in finding similarities between wear scars clustered together. The results generated by the SOFM network revealed that 1) the wear scars from simulator components are only representative for a small part of the retrieval population, 2) wear scars generated by the two ISO standards are comparable, and 3) the wear scars from retrieved components are highly variable and complex, generating eleven clusters of similar wear scars. The model created in this study can be used as the baseline for future analysis. For instance, the wear scars of future ISO wear tests can be compared with previous wear tests using the SOFM created. This will allow us to verify whether new ISO-generated wear scars match those previously generated using the same wear testing protocols or whether new wear testing protocol generate wear scars that share more features with retrieved components (i.e. move more into the center of the feature map). There is ample room for investigation of the wear scar generation process using the proposed model, as any wear scar parameter can be potentially used to investigate relationships among groups.

5. SPECIFIC AIM 2 - *To assess the frequency and duration of daily physical activities and their potential impact on TKR polyethylene wear*

The objectives of this Specific Aim are: 1) to identify and validate an activity monitoring device able to acquire TKR relevant physical activity parameters during activities of daily living (ADL) (Specific Aim 2.1), 2) to measure the frequency and duration of ADL in a sample TKR population during their daily routine (Specific Aim 2.2), and 3) to measure the kinetic and kinematics of ADL in a laboratory setting (Specific Aim 2.3). The ADL and parameters identified and measured in this study will be of relevance to the wear assessment of TKR prosthesis components.

5.1. SPECIFIC AIM 2.1 - *To identify and validate an activity monitoring device able to acquire TKR relevant physical activity parameters during ADL*

5.1.1. INTRODUCTION

In section 4, it was found that wear testing base on the application of level normal walking cycles only, recreated about 11% of the wear scar patterning observed in retrieved tibial component of the same design and material type. This suggests that the contribution of activities of daily living (ADL), other than walking, play a significant role in the wear scar damage created *in vivo*. In order to evaluate whether activities other than walking (e.g. stair ascent and descent, chair sitting and rising, squatting and stop-and-go motions) generate a more physiological wear scar pattern, and thus potentially wear rates, through *in vitro* testing, TKR patient specific activities have to be identified, measured and put in perspective so that they can be used for wear testing evaluation.

5.1.2. PURPOSE

The objective of this Specific Aim was to validate the Intelligent Device for Energy Expenditure and Activity (IDEEA, MiniSun, Fresno, CA, USA) and the Advanced Activity Monitoring Pod (AMP-331, Dynastream Innovations Inc., Cochrane, Alberta, Canada) activity monitors and to compare them with an optical tracking system and instrumented treadmill.

5.1.3. MATERIALS and METHODS

5.1.3.1. Demographics

Eleven (5 female; 6 male) healthy volunteers participated in this IRB approved study (Table 5-1). Volunteers had no history of any neurological and/or orthopedic disorders and were without any pain at the day of the experiment.

Table 5-1: Demographics of healthy study participants.

Participant	Gender	Age (years)	Weight (lb)	Height (m)	BMI (kg/m^2)
1	Female	27	132	1.67	22
2	Male	30	182	1.87	24
3	Male	28	154	1.68	25
4	Female	26	140	1.67	23
5	Female	32	220	1.60	39
6	Male	41	156	1.80	22
7	Male	27	205	1.75	30
8	Female	19	134	1.75	20
9	Male	27	191	1.89	24
10	Female	31	126	1.65	21
11	Male	31	175	1.77	25
	Average	29	165	1.74	25
	StDev	5.3	31.8	0.09	5.3

5.1.3.2. IDEEA Activity Monitor

The IDEEA monitor (Figure 5-1) collects motion data from the upper body and the lower extremities to determine a variety of activities including walking and running [53, 54]. The battery-operated, pager-sized IDEEA recorder is connected to three thin, 2mm flexible wires that transmit the output signals of five sensors to the recorder. The sensors monitored and measured the angle and acceleration of body segments in two orthogonal directions. The different combinations of signals from the five sensors represented different physical activities. The position, side and orientation of the sensors are important factor for accurate motion data acquisition.

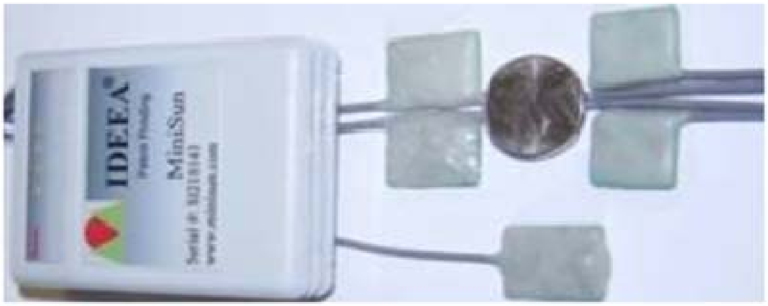

Figure 5-1: Photo of IDEEA monitoring system depicting recorder box and cables connecting five sensors.

The five sensors of the IDEEA system are placed on the chest (4 cm below the clavicle, midline), right and left thighs (half the distance between the iliac crest and patella, in the midline), and soles of the right and left feet (below the 4th toe, Figure 5-2). Once all five sensors are placed and the individual demographics have been entered (ID, age, gender, height and weight), the monitor is ready for calibration. Calibration is performed in a sitting position. An adjustable stool or chair can be used to align the sensors to the horizontal and vertical planes (Figure 5-3). Calibration is accomplished by aligning all sensors within 15° from the horizontal (feet and thighs sensors) or vertical (chest sensor) planes. The raw data are transferred to a personal computer via a USB port. ActView software (MiniSun, Fresno, CA, USA), which is provided with the activity monitor, downloads and preprocesses the data and reports duration and, if applicable, intensity results for each physical activity (PA). In addition, gait-related parameters, such as step count, distance, power and speed are estimated.

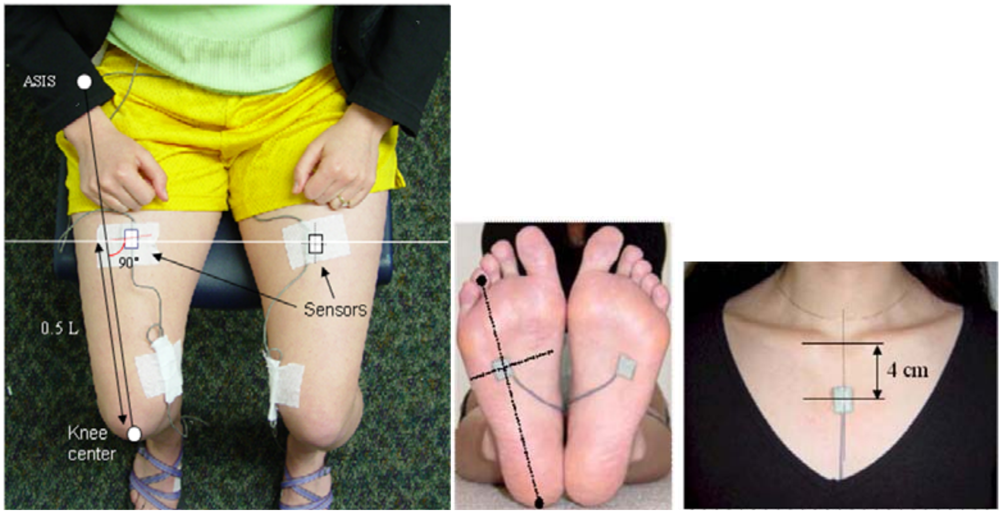

Figure 5-2: Activity monitor sensor placement. Thigh sensors (left), foot sensors (middle) and chest sensor (right)

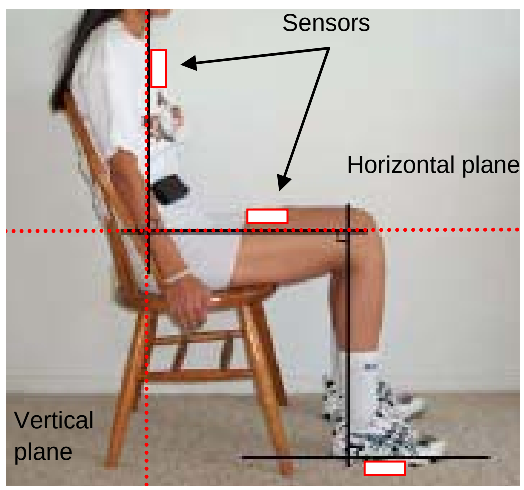

Figure 5-3: Subject position and orientation used for calibration of sensor**.**

5.1.3.3. AMP-331 Activity Monitor

The AMP monitor is mounted in a neoprene bag, worn at the ankle along the Achilles tendon, and measures vertical and horizontal accelerations of the shank (Figure 5-4). The data is stored in a 5MB hard-disc at adjustable epochs. A display provides elapsed time, duration of data collection, total walked distance, average speed and the total consumed energy. The AMP monitor does not require calibration. Data analysis is performed through an Excel macro (Microsoft Corporation, Redmond, WA, USA) provided by the manufacturer. The Excel macro processes the raw data and outputs time intervals, which are then classified into inactive (<20 sec without steps detected), active (sporadic steps) and locomotion (>19 consecutive steps) categories. Within each class (except inactive), step count, distance, average speed, step length, cadence and energy consumption values are estimated.

Figure 5-4: AMP activity monitor placement (top) and data transfer setup (bottom).

5.1.3.4. Validation of Spatiotemporal Parameters

All eleven volunteers were asked to ambulate on a split-belt treadmill (Series 1800, Marquette Electronics, Milwaukee, Wis., USA) (Figure 5-5) at self-selected normal and fast walking and running speeds, while simultaneously wearing both activity monitors. Both activity monitors were applied and setup following the procedures previously described. A fixed distance of 300 meters was traveled at each self-selected locomotion speed. An optical tracking system (Motion Analysis Corp, Santa Rosa, CA, USA) was used for comparison of the monitors' step count and cadence, while speed was compared to the speed of the treadmill motor. Data synchronization was performed manually by activating the event micro switches located in the IDEEA data logger (1–walking, 2–fast walking and 3–running). Accuracy of step count, speed and cadence, measured by both activity monitors, were evaluated.

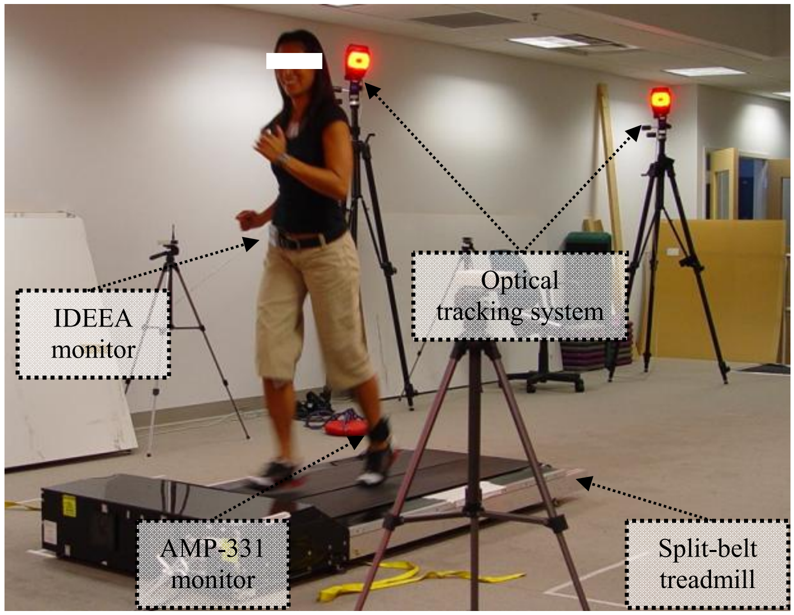

Figure 5-5: Test setup (Clinical Biomechanics and Rehabilitation Laboratory, Department of Kinesiology and Nutrition, UIC).

5.1.3.5. Validation of Activity Recognition and Measurement

The IDEEA monitor is capable of measuring 32 ADL [54]. Among these activities, level walking, running, stair ascent and descent, chair sitting and rising, squatting and activity transitions are of particular interest due to their effect on the knee joint motions and loading. Even though the IDEEA monitor has been previously validated and has shown an overall accuracy of 98% [53], a short validation was conducted to verify that the monitor performed to specifications and provided reliable and accurate identification and measurement of the activities of interest. The validation consisted on videotaping a series of activities (Table 5-2) performed by three of the eleven volunteers participating in this study (Table 5-1). Each volunteer wore the IDEEA monitor and was instructed to execute all activities in an ordered and timely manner. The results were analyzed by two independent observers who analyzed the activity recordings and documented the occurrence and frequency of each identified activity.

Table 5-2: Series of activities performed for validation of IDEEA monitor.

Activity	Description	Activity	Description
(1) - Stand	3 sec	(11) - Sit	5 sec
(2) – Sit	5 sec	(12) - Stand	3 sec
(3) - Stand	3 sec	(13) - Run	Beginning of hallway
(4) - Walk	End of hallway (approximately 100 feet)	(14) - Stand	3 sec
(5) - Stand	3 sec	(15) - Jump	Both feet
(6) – Sit	5 sec	(16) - Hop	Right foot
(7) - Stand	3 sec	(17) - Hop	Left foot
(8) - Ascend stairs	6 stair steps	(18) - Turn back	Turn 180 degrees to start stair descent
(9) -Stand	3 sec		
(10) -Turn back	Turn 180 degrees to start stair descent		

5.1.3.6. Processing and Analysis

Raw activity data collected by the IDEEA monitor was pre-processed and analyzed using the manufacturer's software (ActView). Locomotion activities were identified by finding the 'event' marks generated by the micro switches. Similarly, the AMP raw data was analyzed using the manufacturer's Excel macro.

5.1.3.7. Statistical Analysis

Intraclass correlation analysis (ICC(2, 1), absolute agreement) was used to evaluate the concurrent agreement between the two monitoring devices against the 'gold standards': the treadmill for speed and distance, and the optical tracking system for step count and cadence; ICC values greater than 0.75 represented good concurrent agreement [55, 56]. Repeated Measures ANOVA was performed to identify differences between speed groups for all parameters. Bland-Altman plots were generated to visualize the measuring bias and the level of agreement between the two monitors for normal walking, fast walking and running [57, 58, 59]. Cohen's Kappa analysis was carried to investigate the agreement between activities identified by the IDEAA monitor and the two independent observers.

5.1.4. RESULTS

5.1.4.1. Validation of Spatiotemporal Parameters

The participants' self-selected speed during normal walking, fast walking and running were 1.2±0.2, 1.6±0.2 and 2.1±0.3m/s (mean±SD), respectively. ICC values for all measured parameters are provided in Table 5-3.

Table 5-3: Mean, standard deviations (SD) and intra class correlations (ICC) during normal walking (NW), fast walking (FW) and running (R) for speed, step count and cadence.

Parameter		IDEEA			AMP		
		Mean	StDev	ICC	Mean	StDev	ICC
Speed (m/s)	NW	1.2	0.19	0.96	1.10	0.18	0.83
	FW	1.5	0.17	0.89	1.41	0.21	0.50
	R	2.3	0.25	NS	1.47	0.35	NS
Steps (count)	NW	468	58	0.99	472	55	0.98
	FW	408	74	0.99	407	74	0.99
	R	347	44	0.70	373	39	0.74
Cadence (steps/min)	NW	108	7	0.99	107	7	0.99
	FW	121	6	0.97	119	12	0.83
	R	154	9	NS	145	10	NS

NS = non-significant ICC

The measurement error for gait parameters did not differ significantly between normal and fast walking activities (p>0.1). In contrast, for running, the measurement errors for most gait parameters were significantly greater for both monitors compared to errors for the optical tracking system, except for distance (IDEEA, p>0.100) and for step count (AMP, p>0.100) (Table 5-4).

Table 5-4: Mean relative error of speed, step count, distance and cadence measurements for normal walking (NW), fast walking (FW) and running (R).

% Error (mean ± StDev)	IDEEA			AMP		
	NW	**FW**	**R**	**NW**	**FW**	**R**
Speed (m/s)	-0.2±5.1	5.3±3.3	-4.5±12.6*	-9.6±7.5	-9.0±10.6	-29.6±17.6*+
Steps (count)	0.8±1.4	-0.3±1.6	-9.1±8.2*+	1.5±2.4	-0.1±3.6	-2.3±8.7
Distance (m)	3.6±5.7	4.5±16.9	1.1±8.3	-4.2±8.8	-3.1±11.3	-24.3±15.3*+
Cadence (steps/min)	0±1.1	0.4±2.3	-4.1±15.5*+	-0.4±0.9	-2.6±7	-7±19.3*+

* Significantly different from NW ($p<0.05$), + Significantly different from FW ($p<0.05$)

Degree of agreement between both monitors and the gold standards for all parameters are shown in the Bland-Altman plots provided in Figure 5-6.

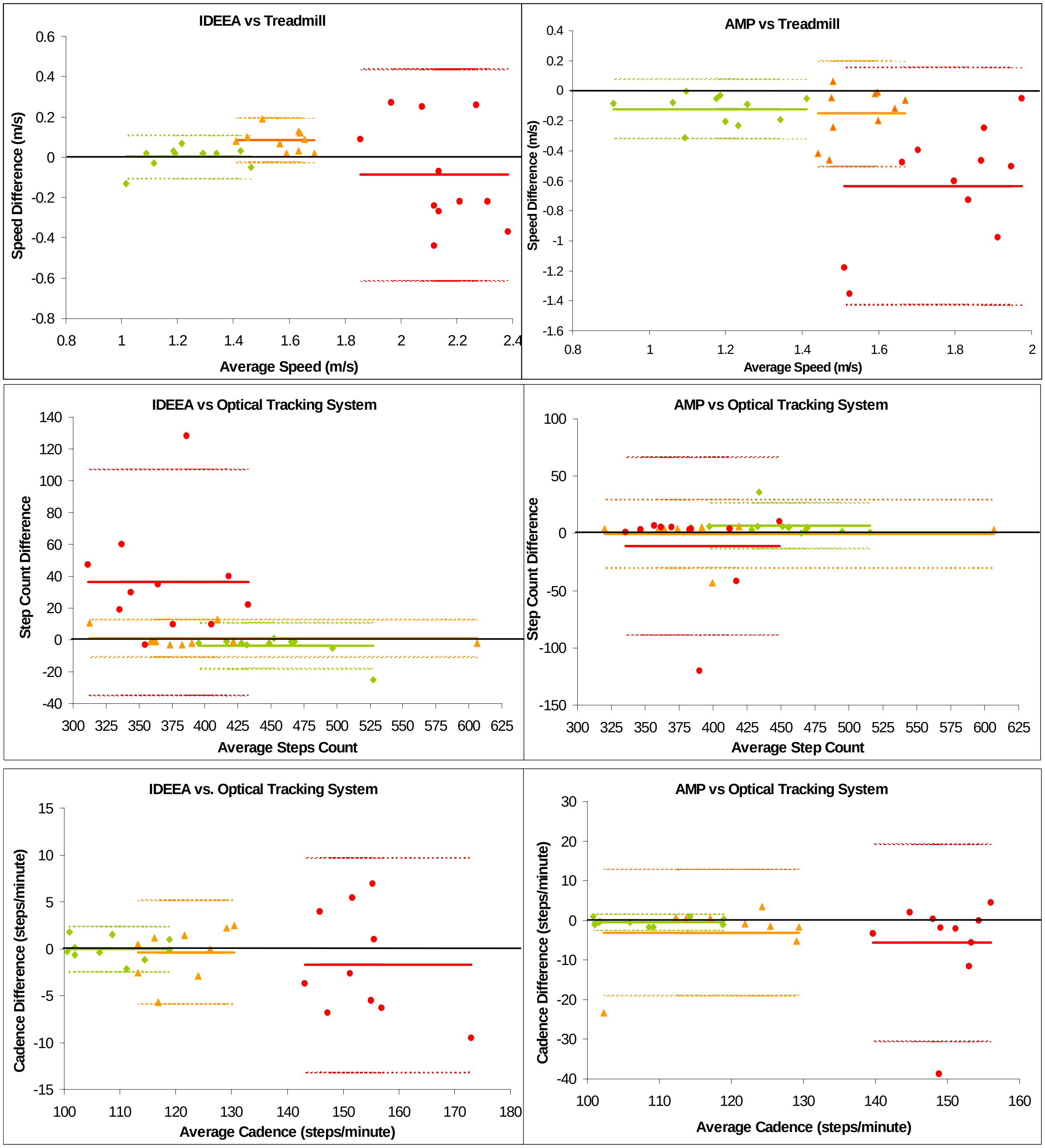

Figure 5-6: Bland-Altman plots depicting measurement error for speed (top row), step count (middle row) and cadence (bottom row) for the IDEEA (left column) and AMP (right column) activity monitors. Solid lines depict average measurement bias. Interrupted lines depict confidence intervals (±2 SD). Normal Walking is depicted by 'green rhombuses', fast walking depicted by 'orange triangles' and running by 'red circles'.

5.1.4.2. Activity Identification Reliability

The IDEEA video-based validation analysis indicated substantial inter-rater reliability with a Kappa value of 0.69 ($p < 0.001$, 95% CI: 0.667, 0.712). Based on these results, the IDEEA monitor was deemed appropriate to perform activity identification and measurements in a sampled TKR population.

5.1.5. DISCUSSION

The results of this validation study demonstrated good to excellent concurrent agreement for gait parameter measurements at walking speeds between 1.0 and 1.8m/s, which are the minimum and maximum self-selected normal walking speeds, respectively, for both activity monitors. The IDEEA monitor is well suited for estimating distance over a range of ambulation speeds. The AMP monitor, on the other hand, is the better choice in settings that require high step count accuracy. However, the devices' cost and setup requirements are also important criteria in the selection process. The IDEEA monitor costs about three times more than the AMP monitor, requires a trained technician for setup and is able to identifying up to 32 physical activities [54], compared to the AMP monitor that only measures ambulatory activities. When assessing the ability and accuracy of the IDEEA monitor to identify and measure ADL, it was found that the monitor exhibited substantial inter-rater reliability with a Kappa value of 0.69 ($p < 0.001$). The IDEEA monitor was therefore considered suitable to perform activity identification and measurements in a sampled TKR population.

Most other accelerometer-based monitors, especially those mounted at the waist line, have shown poor accuracy at walking speeds below 1.1m/s [60, 54]. The lowest normal walking speed recorded in this study was 0.9 m/s and was slightly underestimated by the IDEEA (0.8 m/s) and AMP (0.7 m/s) monitors. However, step count and cadence were estimated accurately by both monitors (±1.8% error). Because participating volunteers did not walk at speeds lower than 0.9m/s, accuracy information for these speeds is not available. Walking speeds below 1.0 m/s are often observed in older adults [60] and in persons with lower extremity trauma or pathology [61, 62]. However, these persons may also present altered gait mechanics, and hence the results of this study involving healthy subjects cannot be extrapolated to these populations. It is expected that results would be similar for over-ground walking and running.

It is possible that rotation of the AMP monitor along the ankle may be related to the poor accuracy of measurements during running. The AMP manufacturer used athletic tape during their validation procedure to secure the monitor in place [63] and prevent the monitor from shifting position. However, the position of the AMP monitor was closely monitored. Hence, the measurement error likely lay in the AMP stride detection algorithm, as it may not be robust enough to detect varying kinematic patterns. In contrast, one reason for the significant reduction in accuracy of the IDEEA monitor could be related to the motions exerted by the upper body during locomotion. With high accelerations and speeds, measurement errors may be more sensitive to sensor placement [64] than at lower ambulation speeds, and there might be a discrepancy between information from the thigh and chest sensors and that provided by the foot sensors. However, the algorithms used by the IDEEA monitor have not been disclosed. The AMP superior accuracy in step counts may be related to the use of the "smart" stride detection algorithm [63]. This algorithm uses the shank angle and angular velocity throughout the gait cycle in addition to acceleration peaks, which could produce erroneous stride detections caused by outside vibration.

5.1.6. CONCLUDING REMARKS

Based on the results of this investigation, it was concluded that: 1) the IDEEA monitor is well suited for the identification and measurement of ADL such as level walking, running, stair ascent and descent, chair sitting and rising, squatting and activity transitions, and 2) the IDEEA and AMP monitors are well suited for the measurement of locomotion parameters such as speed, distance, cadence and step count throughout a variety of locomotion speeds. Due to the easy setup the latter also allows self-application by patients and hence is easier on handling when large cohorts are studied over a period of several days. Both activity monitors will be used in the measurement of ADL and locomotion parameters in a TKR population (Specific Aim 2.2).

5.2. SPECIFIC AIM 2.2 - *To measure the frequency and duration of activities of daily living of relevance to TKR wear*

5.2.1. INTRODUCTION

The activity profile of total knee replacement (TKR) patients is very useful in determining the pre- and post-surgical outcome of the arthroplasty procedure [65]. Activity profiles are also useful when comparing the activity level of TKR patients with their healthy counterparts [66-68]. Furthermore, frequency and duration of physical activities are key parameters used in the wear evaluation of TKR prosthesis *in vitro*. Current standardized wear testing protocols simulate level walking cycles only, which are continuously performed at 1±0.1 Hz for a duration of 5 million repetitions [16, 17]. While walking is the most frequent physical activity during the day [8], analyses of retrieved tibial liners have shown that the contact damage patterns generated *in vivo* (wear scars and appearances) differ from those generated *in vitro*, through mechanical simulators. This suggests that the kinetics and kinematics used as input in contemporary wear testing protocols do not reflect physiological conditions. Human life incorporates a greater variety of daily physical activities, with even more complex combinations and transitions. These activities, in spite of the lower frequency, may generate loads and motions that are detrimental to the articulation of the TKR prosthesis.

5.2.2. PURPOSE

The objective of this study was to investigate the frequency and duration of daily physical activities of relevance to TKR polyethylene wear; from a sample TKR population. Activity frequency and duration will be measured using the two activity monitoring devices validated in the previous section (section 6.1). Rations of walking to other physical will be used to form the basis of a multi-activity wear testing protocol.

5.2.3. MATERIALS and METHODS

5.2.3.1. Demographics

Qualifying TKR patients were gathered from the Rush Orthopedic database. All patients gave their consent to participate in this IRB approved study. The inclusion criterion for patient selection was a successful primary TKR of a posterior cruciate retaining design (NexGen CR, Zimmer, Inc., Warsaw IN, USA) in the left and/or right knee with at least twelve months *in situ* (for both sides if bilateral). All patients lived in the Chicagoland area and needed to be active in the workforce or household and report participation in moderate exercise (1 to 2 times a week). Patients were excluded if they had rheumatoid arthritis, significant lumbar spine disease, neurological disorders, undergone revision surgery of the original implant or a history of total hip arthroplasty.

5.2.3.2. Test-Day Activity Measurements

Frequency and duration of level walking, running, chair sitting and rising, stair ascent and descent, squatting and activity transitions were measured using the IDEEA system. The IDEEA activity monitor was setup and calibrated following the procedures previously described in <u>Specific Aim 2.1</u> (section 6.1). Data collection took place at the patient's house and it was synchronized to start at the beginning of their daily routine and stop right before bedtime (12+ hrs. of data collection was sought). All patients immersed in their regular daily activities. The

IDEEA device did not affect or impede the proper execution of any daily activity, including sports and recreational activities. Patients were able to change clothes but were not allowed to shower or swim as this would have damaged the activity monitor.

5.2.3.3. Week-Long Activity Measurement

Right after the IDEEA monitor was set up, the step monitor (AMP 331, Dynastream Innovations, Cochrane, AB) was applied to the patient's ankle, along the Achilles tendon of the operated knee (or the knee with higher in-situ time in bilateral patients). The step monitor collected data for seven consecutive days, including IDEEA the test day. The mean average activity level (steps count, distance, cadence and speed) the AMP step monitor collected for the seven-day period of time was computed and then compared to the activity level measured by the IDEEA monitor during the test-day. This provided knowledge of how representative the test day was for each patient and provided an overall weekly activity level for each patient. As in the study of Tudor-Locke et al. [68], patients were classified as active, some-what active or sedentary based on their activity level (i.e. number of daily steps).

5.2.3.4. Statistical Analysis

Data normality tests were performed to validate that the activity data were normally distributed. A two-sample t-test was performed to evaluate whether the test day was significantly different from a regular weekday or weekend day. Repeated measures ANOVA was performed to identify differences between groups with different levels of activity (e.g. sedentary and somewhat active), gender and BMI (normal, overweight and obese). The significance level was set *a priori* to $\alpha=0.05$. All statistical analyses were carried out in Minitab 15 for Windows (State College, PA, USA).

5.2.4. RESULTS

5.2.4.1. Demographics

A total of 27 patients average age 60.9±6.6 (range 50 to 82 years) were recruited, out of which 11 were males and 16 were females. There were 11 right, 4 left and 12 bilateral TKR patients. Mean average time *in situ* was 41.7±29.1 months (range 12 to 119 months). The Patient population had a mean average BMI 30.6±7.82 (range 20.8 to 51.5 BMI). Table 5-5 provides patient specific demographic.

Table 5-5: Participating patient demographics.

Patient No.	Gender	Age (years)	Implantation Side	Time *in situ* (mo)	Height (in)	Weight (lb)	BMI (lb/in^2)
1	Male	59	Left	93	71	194	27.1
2	Female	50	Right	37	68	227	34.5
3	Male	64	Right	35	73	234	30.9
4	Female	67	Left	27	68	137	20.8
5	Female	63	Left	119	64	183	31.4
6	Female	69	Right	46	66	134	21.6
7	Female	67	Right	21	60	119	23.2
8	Female	50	Bilateral	43	64	300	51.5
9	Male	64	Right	18	75	203	25.4
10	Female	55	Right	18	66	159	25.7
11	Female	60	Right	19	67	209	32.7
12	Male	62	Bilateral	20	69	183	27.0
13	Female	51	Right	39	64	250	42.9
14	Female	58	Right	60	66	216	34.9
15	Female	67	Left	49	65	192	31.9
16	Male	82	Bilateral	43	68	150	22.8
17	Male	57	Bilateral	108	60	223	43.5
18	Female	59	Bilateral	102	59	205	41.4
19	Male	60	Bilateral	40	69	198	29.2
20	Male	59	Bilateral	32	75	201	25.1
21	Male	65	Bilateral	34	68	194	29.5
22	Female	59	Bilateral	38	62	154	28.2
23	Female	57	Bilateral	23	67	174	27.2
24	Male	67	Right	16	69	163	24.1
25	Female	64	Right	12	66	227	36.6
26	Female	65	Bilateral	21	63	238	42.2
27	Female	58	Bilateral	22	67	139	21.8

5.2.4.2. Frequency and Duration of ADL

Twenty-six out of twenty-seven patients were successfully measured. One patient's activity data was corrupted and was therefore not included in the study. The average total activity measurement duration was 12.3±2.6 hours (range 8.4 to 14.8 hours). The majority of the activities performed during the day were of static nature (standing 29.6% and sitting 52.2%). Walking was the dominant dynamic activity, followed by stop-and-go motions, then stair, chair and running activities (Figure 5-7). Activity occurrences and ratios of level walking cycles to chair and stair activities are provided in Table 5-6. Detailed daily activity information from each patient is presented in Figure 5-8.

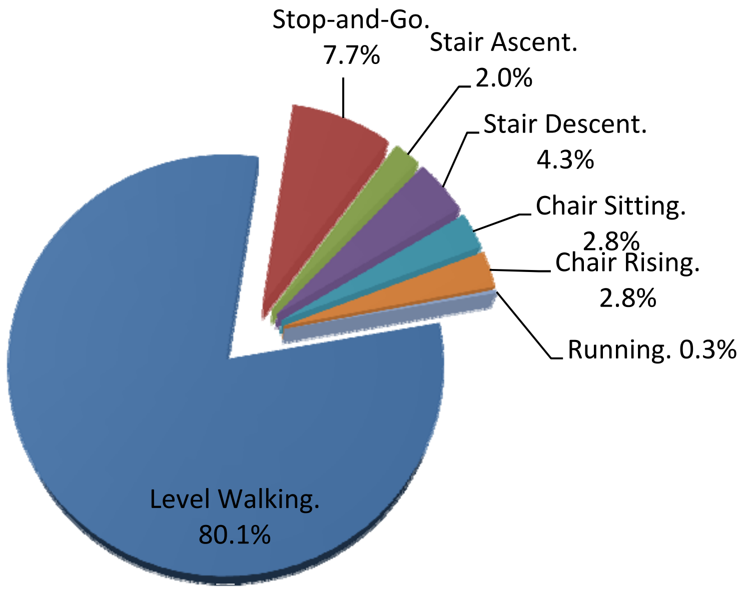

Figure 5-7: Population average of walking, stop-and-go motions, chair sitting-rising, stair ascent-descent and running (based on test-day data).

Table 5-6: Test day activity occurrences for the investigated TKR patient population.

counts/occurrences	**Average**	**StDev**	**Min.**	**Max.**	**Walking : ADL ratio**
Level Walking	2599	1220	222	4888	1:1
Stop-and-go	251	118	60	542	10:1
Stair Ascent	66	63	0	244	39:1
Stair Descent	139	138	4	554	19:1
Chair Sitting	90	59	6	336	29:1
Chair Rising	90	59	6	336	29:1
Running	8	28	0	139	306:1

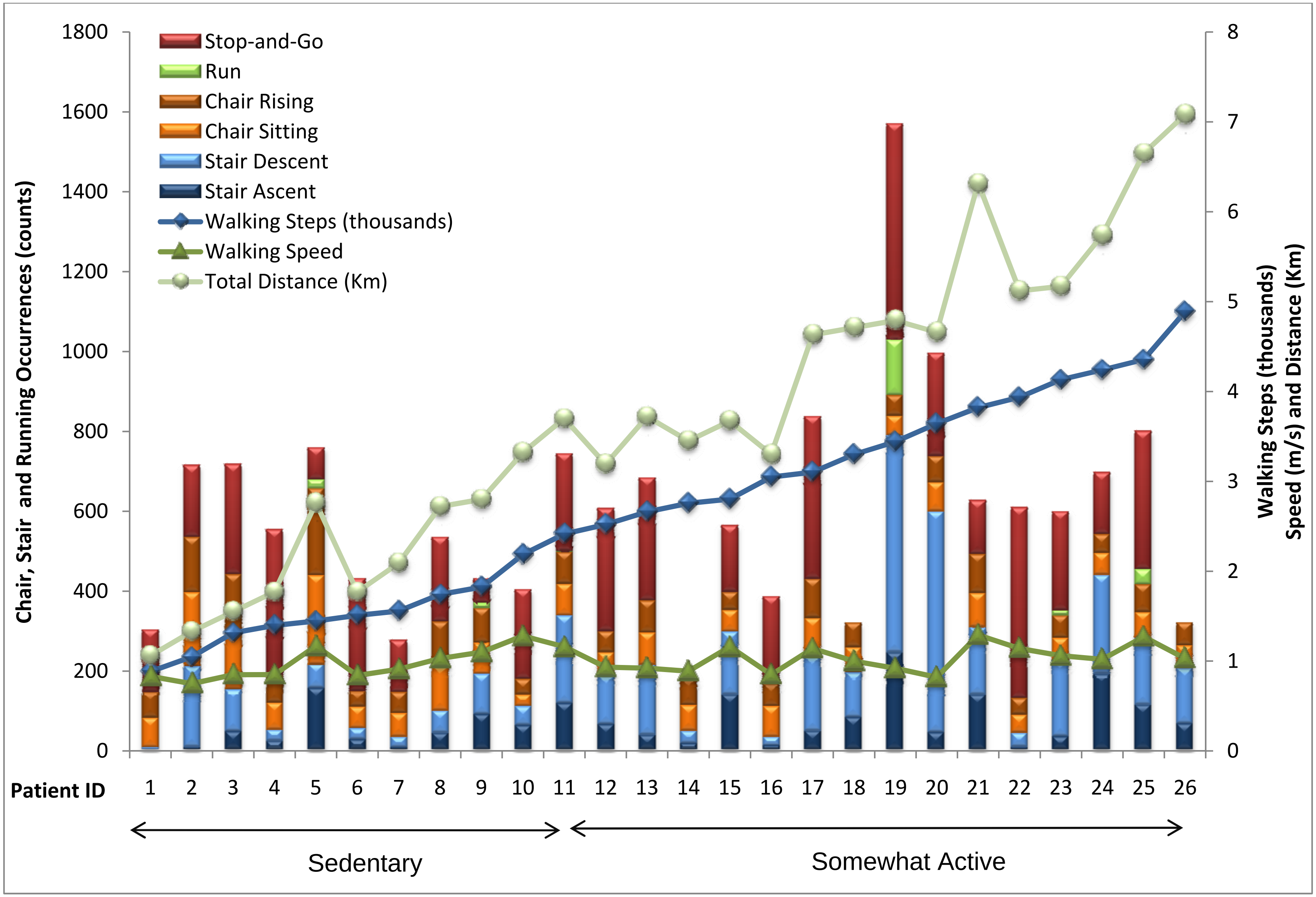

Figure 5-8: Stacked bars provide summary of running, stair and chair activities for each patient. Line plots provide walking steps, walking speed and traveled distance.

5.2.4.3. Step Count Distribution

Both the test-day and the week-long step count data were normally distributed, as indicated by the significance level of the Kolmogorov-Smirnov test (Table 5-7). A histogram depicting a normal distribution for level walking cycles, measured on the test day and throughout the week, are provided in Figure 5-9.

Table 5-7: Kolmogorov-Smirnov test of normality (KS-test).

steps/occurrences	*KS-test level*	p *value*
IDEEA test day	0.122	> 0.15
Average week day	0.104	> 0.15
Average weekend	0.165	0.089

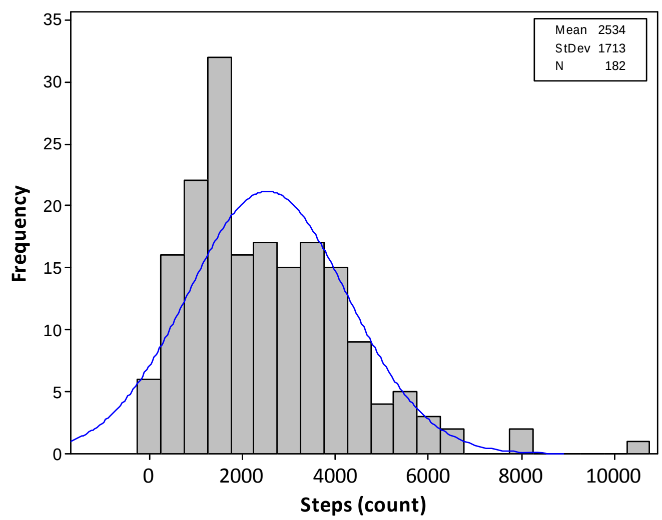

Figure 5-9: Frequency distribution of level walking and stair steps throughout the week (n=26)

5.2.4.4. Representativeness of Test Day

Step count measurements for the test day were not significantly different from the average weekday (p=0.164) or average weekend day (p=0.174) (Table 5-8).

Table 5-8: Test day, weekday and weekend step counts.

Patient No.	IDEEA test day	AMP test day	AMP weekday average	AMP weekend average
1	2187	1820	5310	9048
2	4355	3364	2338	1305
3	2661	3633	3712	NA
4	4240	5284	3111	1754
5	3643	4947	2146	1747
6	1823	997	2797	2549
7	4133	5964	3789	4968
8	1557	747	1366	2145
9	1742	2923	2950	2411
10	2520	3278	2192	1396
11	3936	3997	2746	3285
12	2756	ME	ME	ME
13	2414	3942	3090	4730
14	884	1441	1439	1172
15	1314	1433	678	192
16	3821	NA	2776	3490
17	1047	1441	1439	1172
18	3103	4077	3580	956
19	4888	6311	2628	2730
20	3441	3533	1204	492
21	2803	3448	2613	3048
22	1509	1931	982	854
23	1398	1440	3856	2232
24	3048	4277	2917	2458
25	1447	2253	2179	2156
26	3299	4812	4639	4335
Average	2691	3221	2659	2526
St. Dev.	1146	1596	1128	1880
p-value	AMP test day vs. weekday average			0.164
	AMP test day vs. weekend average			0.174
	IDEEA test day vs. AMP test day			0.188

ME=measurement error

5.2.4.5. Activity Levels

Based on Tudor-Locke et al. [68], eleven patients were classified as sedentary (<5000 steps) and fifteen as somewhat active (5,000 – 9,999 steps). Two-sample t-tests (with a confidence level of 95%) showed that patients classified as sedentary, performed significantly less total stair steps (p=0.01), less stair descent steps (p=0.01) and less stop-and-go motions (p=0.01) (Figure 5-10). While not significantly different, sedentary patients tended to spend more time sitting, less time standing and performed more chair sitting/rising maneuvers than somewhat active patients.

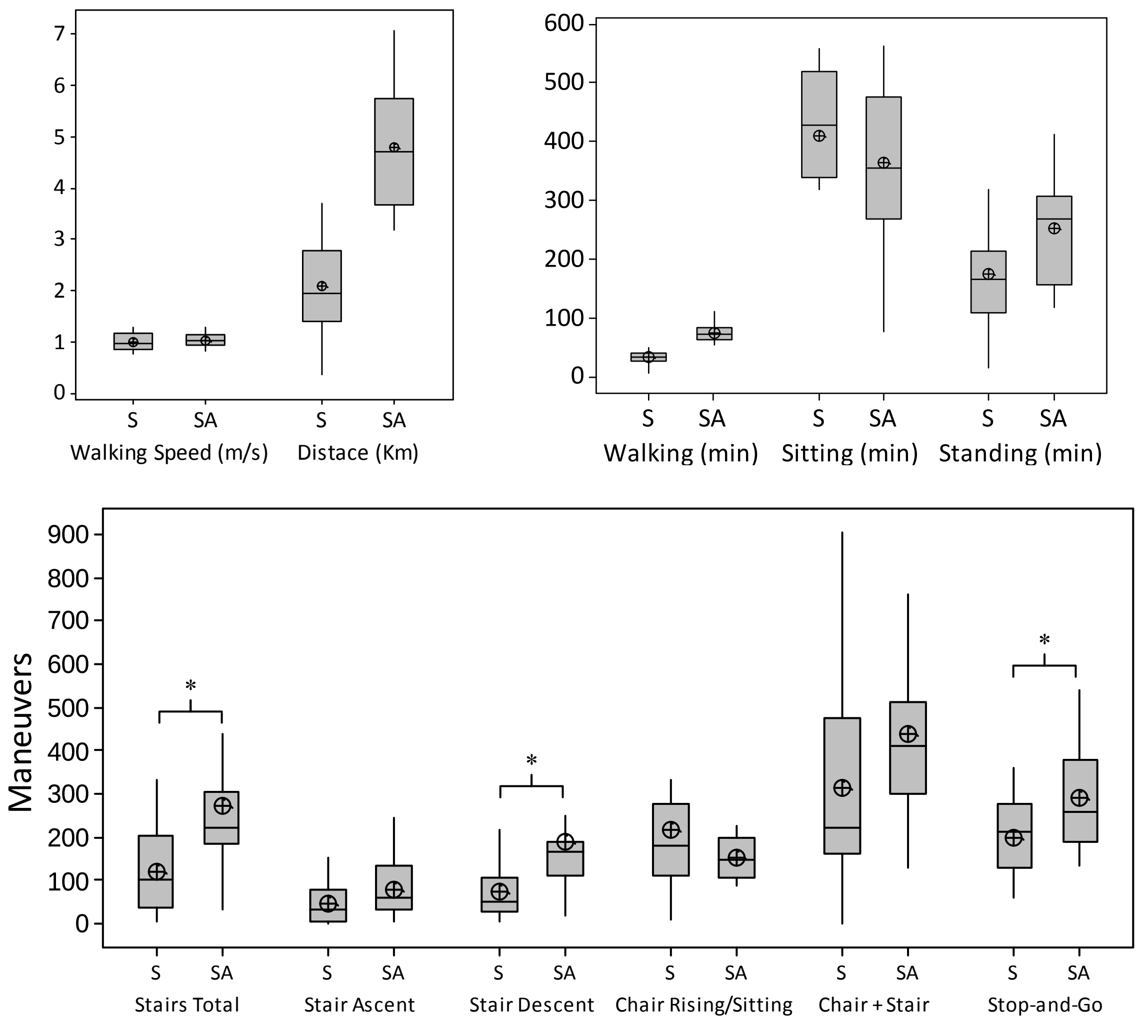

Figure 5-10: Differences between sedentary (S) and somewhat active (SA) patients. * indicates S parameters were significantly lower than SA parameters.

5.2.5. DISCUSSION

The majority of the activities performed during the day were of static nature (standing 30% and sitting 52%). Walking was the dominant dynamic activity (80.1%), followed by stop-and-go motions (7.7%), stair ascent/descent (ascent 2.0%, descent 4.3%) and chair (sitting 2.8%, rising %2.8) maneuvers. When relating walking to other activities, ratios of 10:1 for stop-and-go, 39:1 for stair ascent, 19:1 for stair descent and 29:1 for chair sitting or rising were obtained. These ratios were all smaller than the 70:1 walking to stair ascent ratio Benson et al. used to investigate the impact of stair descent in TKR wear [14]. By means of *in vitro* wear simulation, Benson et al. found that the wear of conventional (non crosslinked) polyethylene was significantly higher when one stair step was added for every 70 level walking steps; thus suggesting that as stair stepping frequency increases, so does the wear rate. The result of this investigation found considerably lower ratios of walking to not only stair steps, but also to stop-and-go motions and chair maneuvers, suggesting that the impact of these activities in TKR wear may be more significant than previously thought.

Based on week-long step counts, it was found that patients subjected their TKR components to an average of 0.95±0.45 million steps/year (Ms/yr) (extrapolated from average of 2,651 steps/day), which agrees well with the 1 Ms/yr commonly used by standardized wear testing protocols for the knee and hip [8]. The most active patient walked an average of 2.29 Ms/yr, which would account for about 2.3 times more walking steps when compared with 1 Ms/yr commonly used. The 5 Ms test duration suggested by standardized wear testing protocols would then represent 2.18 years of walking for somewhat active patients (5,000 – 9,999 steps/day), 43.6 % of the 5-year test duration currently suggested by standardized wear testing protocols. As the TKR patient population becomes younger and more active [21], new yearly step count estimates will be needed to provide realistic polyethylene wear rates and implant survivorship duration.

Patients walked the most steps, walked faster and traveled the longest distance during the test day than any other day of the week (Figure 5-11). This difference, however, was not significant for most variables but walking speed, as the average walking speed on the test day was significantly higher than the average Sunday walking speed (Table 5-9). When looking at the daily step counts, it was noticed that the patients' level of activity exhibited a sinusoidal pattern at the beginning of the week, with activity level decreasing from Mondays to Tuesdays and increasing from Tuesdays to Wednesdays. After Wednesdays, the level of activity consistently decreased day by day until Sunday. This weekly activity pattern differs from the activity pattern observed in healthy individuals [66], which exhibited a sinusoidal activity pattern that was maintained throughout the week and which level of activity was opposite to the pattern exhibited by the TKR patients (Figure 5-12).

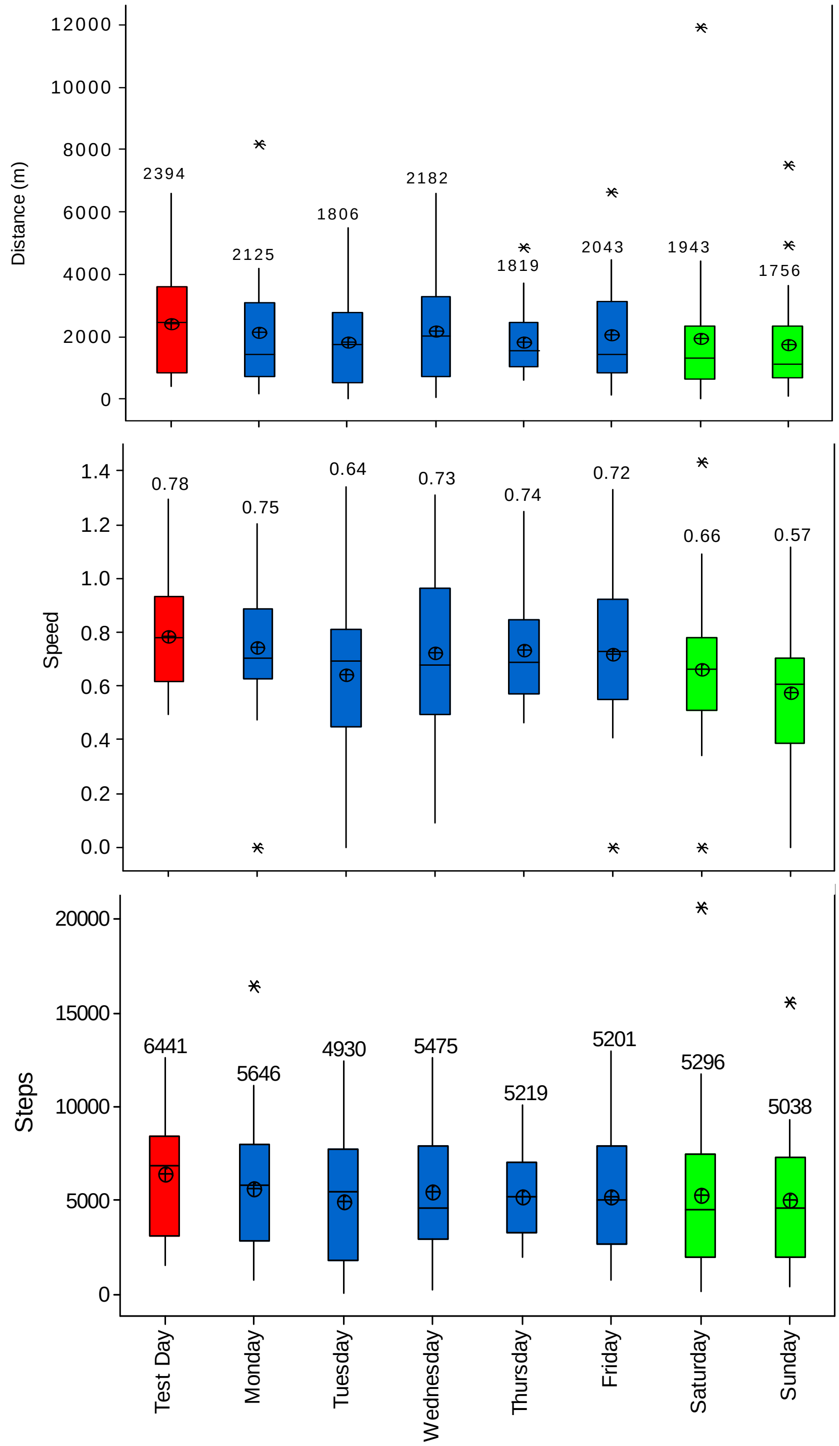

Figure 5-11: Test-day and week-long distribution of step count (bottom), speed (middle) and traveled distance (top). ⊕ symbol and boxplot top values represent group mean results.

Table 5-9: Test-day vs. average week days (two-sample t-test *p* values).

	Test day vs. Average Week days (p *values, α=0.05)*						
Variable	**Mo**	**Tu**	**We**	**Th**	**Fr**	**Say**	**Su**
Steps	0.43	0.11	0.33	0.13	0.19	0.32	0.18
Speed	0.54	0.09	0.39	0.40	0.36	0.09	**0.01**
Distance	0.57	0.18	0.66	0.14	0.45	0.44	0.20
Cadence	0.90	0.73	0.84	0.49	0.96	0.39	0.34

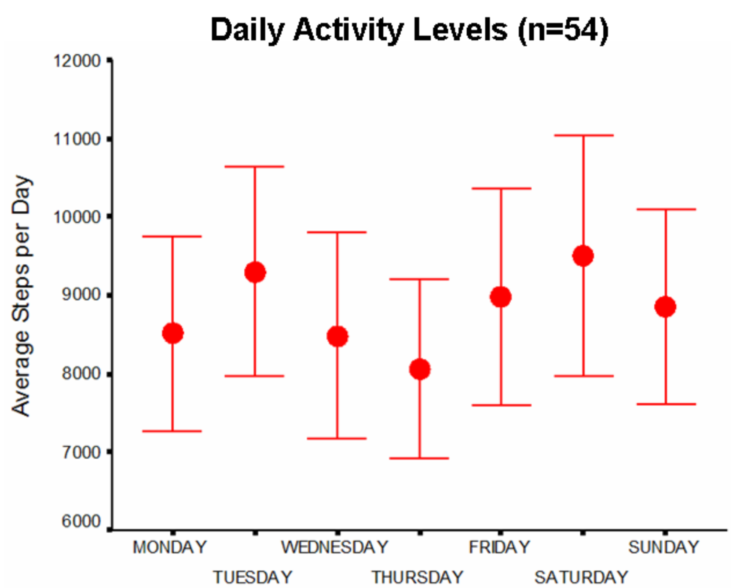

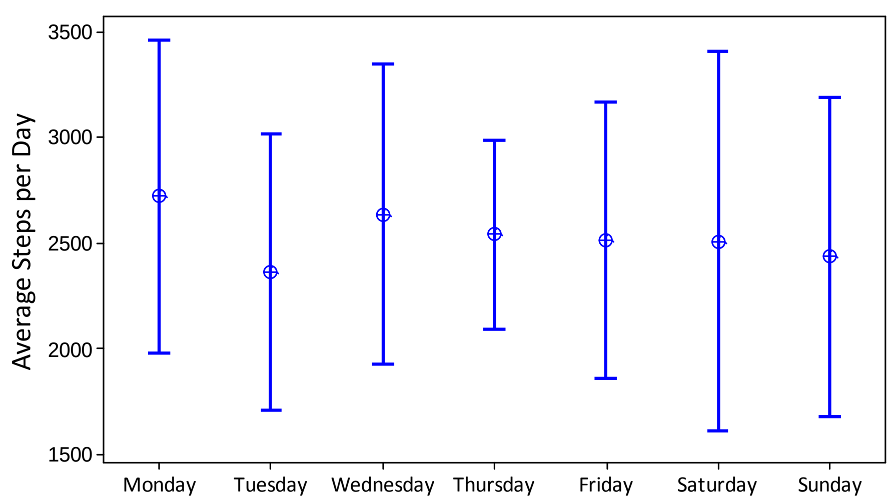

Figure 5-12: Average daily step count for the TKR population investigated in this study (top) and for the healthy group investigated by Thorp et al. [66] (bottom).

Based on self-reported activities, patients also engaged in sports and recreational activities, in addition to performing chair and stair maneuvers (Figure 5-13 top). Both sedentary and somewhat active patients reported participation in a variety of sport activities, however, only somewhat active patients reported walking for exercise (Figure 5-13 bottom). This may explain the reason why somewhat active patients performed more walking cycles than sedentary patients.

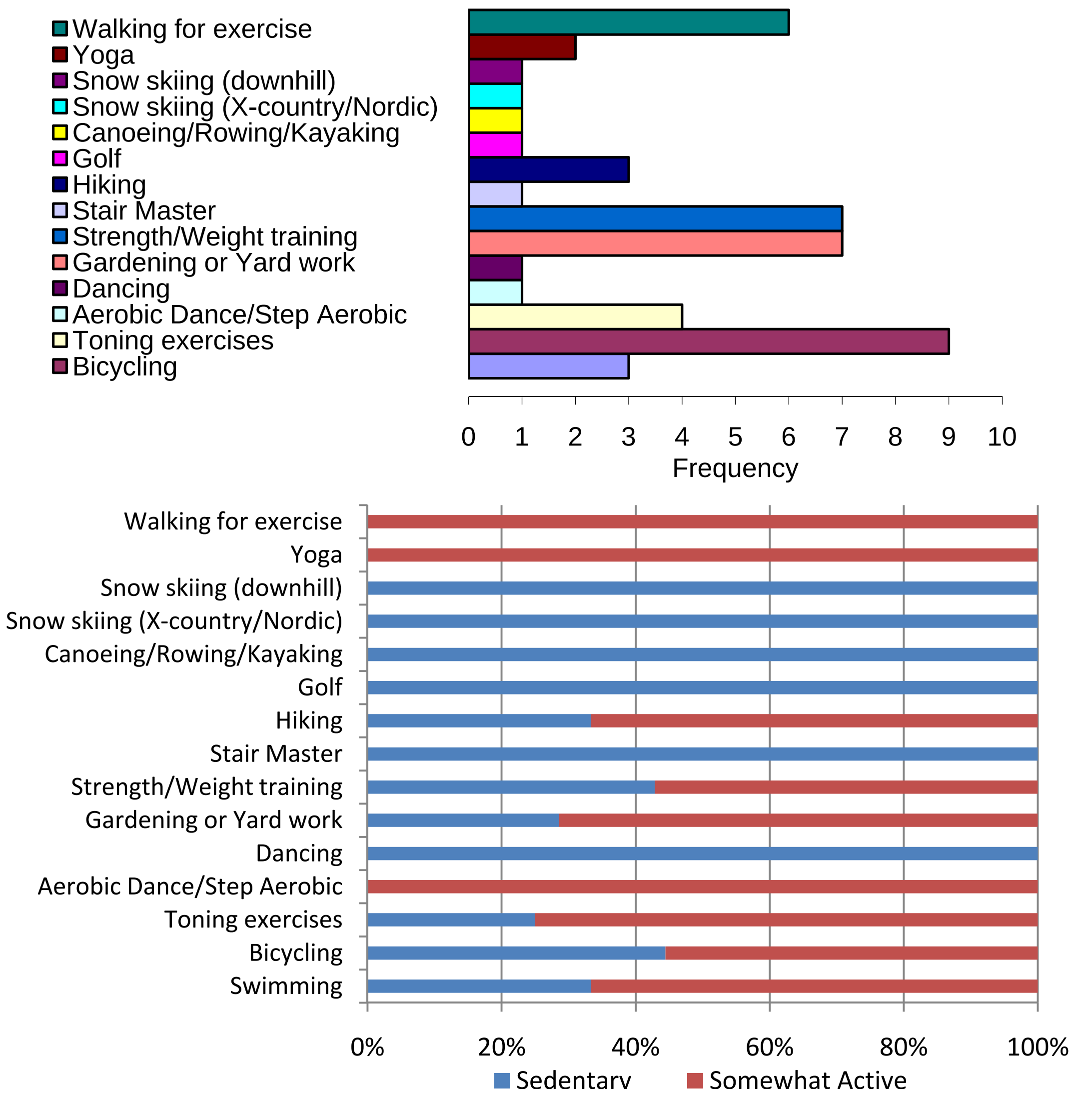

Figure 5-13: Self-reported recreational and sport activities by patients (top) and patients were classified as sedentary of somewhat active (bottom).

The self-reported activities add on to the cyclic motions and loads patients subject their TKR components to. While the frequency of recreational and sport activities may be low compared to walking, activities such as gardening and golf have demonstrated significantly higher knee joint loading and motions, which could have detrimental effects in the wear of TKR components [69-71]. These activities, while they do not represent the norm, they could provide the basis for the creation of worst case wear testing scenarios.

Patient recruitment was a limiting factor because of the acceptance criteria and demographic area selected. All patients lived and worked in a highly urbanized setting with a rather flat landscape. A previous activity study, conducted in Switzerland, showed that individuals living in a more challenging landscape (mountainous terrain) engaged in a more active life style and subjected their TKR components to higher walking cycles [72]. Even though the TKR population investigated by Wimmer et al. was older than the TKR population investigated in this study (74.6±10.4 and 60.9±6.6 yeas, respectively), patients walked significantly more (mean of 2.5 Ms/yr) than the patients that participated in this study (mean of 0.95 Ms/yr). Geographic landscape as well as cultural characteristics of the population investigated may play a significant role in the amount of walking steps TKR patient subject their components to.

In this study, different ratios of stair ascent and descent were identified. While this difference could be related to patients feeling more comfortable descending than ascending stairs, it may also be related to the activity monitor not being able to correctly identify stair ascent steps due to the abnormal kinematics exerted by TKR patients. This study investigated only stop-and-go motions, sitting and chair maneuvers. There are other activities of relevance to TKR, such as gardening (and thus squatting), bicycling, and unclassified stepping maneuvers, with noticeable frequencies that may challenge the wear performance of knee prosthetic devices [73-75].

5.2.6. CONCLUDING REMARKS

This study suggests that ADL other than walking, such as chair and stair activities, may be a significant source of TKR wear and should therefore be further evaluated.

5.3. SPECIFIC AIM 2.3 - *To obtain knee kinetics and kinematics of daily physical activities*

5.3.1. INTRODUCTION

In the previous section (section 5.2) it was found that activities, such as stop-and-go motions and chair, stair and squatting (self-reported) maneuvers, contribute approximately 18% of the dynamic activities performed during the day. These activities, while not as frequent as walking, may impact the wear performance, and therefore survivorship of TKR components due to the higher loads, sliding distances and cross shears generated. In order to evaluate the impact on TKR wear from daily activities other than walking, the kinetics and kinematics from each activity needs to be measured.

5.3.2. PURPOSE

In this study, the primary (flexion-extension) and secondary (anterior-posterior and internal-external) motions and external moments of the TKR joint were determined during chair, stair and squatting maneuvers. The objectives were to: 1) identify significant differences between the joint motions and moments of each activity in comparison to walking, and 2) provide support for the development of a multi-activity wear testing protocol. It was hypothesized that the secondary motions and moments generated during chair, stair and squatting maneuvers will be significantly higher than those generated during walking gait.

5.3.3. MATERIALS and METHODS

5.3.3.1. Demographics

Knee kinetics and kinematics where measured on subjects that had also participated in the activity frequency and duration study (section 5.2). In total, twenty-three TKR subjects (9M/14F, 60.8±7.1 years old, 41.8±29.7 months post-op) with a NexGen-CR prosthesis (Zimmer Inc., Warsaw, IN USA) participated in this IRB approved study. All participants were able to function independently without assistive devices.

5.3.3.2. Gait Testing

Using the point cluster technique (PCT), flexion-extension (F-E), anterior-posterior (A-P) translation and internal-external (I-E) rotation joint motions of the TKR joint were obtained. By palpating bony landmarks, the femur and tibia were defined as individual segments with separate anatomical coordinate systems. Two cluster groups with corresponding orthogonal sets of axes, referred to as the cluster coordinate systems [30], were then created by adhering twenty-one reflective markers on the thigh and shank (Figure 5-14). The cluster and anatomical coordinate systems were related by defining zero positions (origin). The origin of the anatomical femoral coordinate system was the midpoint of the transepicondylar line of the distal femur. The origin of the anatomical tibial coordinate system was located at the midpoint of the line connecting the medial and lateral points of the tibial plateau [30]. A-P translation and I-E rotation motions were measured based on displacements between the origins of the tibial coordinate system relative to the femoral coordinate system. The displacements were then projected onto the axis of the tibia in order to obtain and define the motions of the tibia relative to the femur.

The movements of the reflective markers were tracked using a four-camera optoelectronic system (Qualisys, Gothenburg, Sweden). A force plate (Bertec, Columbus, USA) was used to record foot-ground reaction forces (GRF), which were then used to calculate 3-dimensional external knee moments via inverse dynamics. A computer system was used to acquire and process the motion data (CFTC, Chicago, USA).

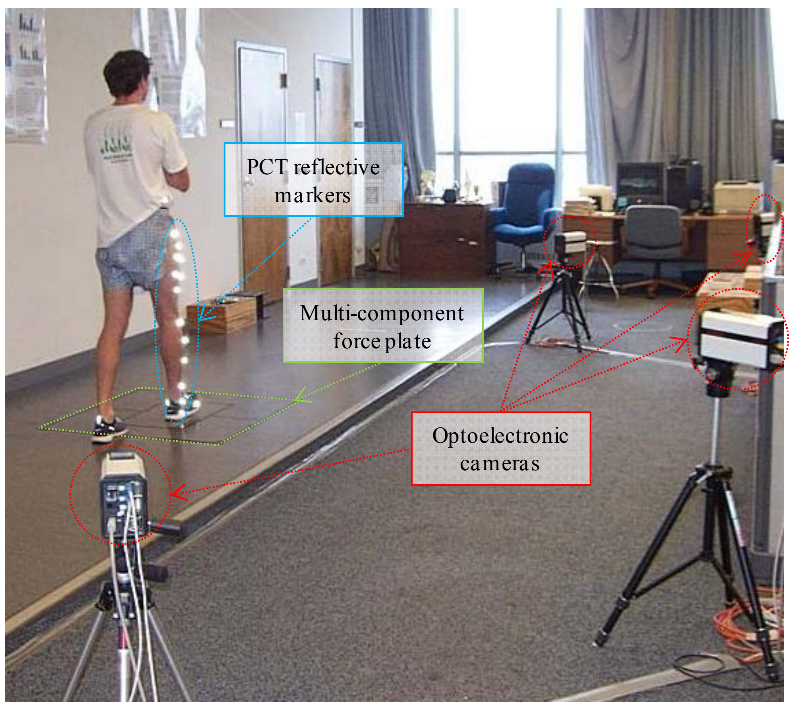

Figure 5-14: Point cluster method for acquisition of joint kinematics and kinetics.

5.3.3.3. Kinetics and Kinematics of the TKR Joint

For each subject, three-dimensional knee motions (F-E rotation, A-P translation and I-E rotation) and three external moments (flexor (flex), extensor (ext), adductor (add), abductor (abd) and internal (int), external (ext) rotators) were collected for 3 separate trials of stair ascent, stair descent, chair sitting, chair rising and squatting; totaling 15 activity trials. For stair ascent and descent, a 3-step staircase unit was positioned on the force plate. During stair ascent, subjects approached the staircase unit with 2 normal walking steps and did not use a handrail. Knee motions were acquired on all 3 steps and external moments were calculated from the first to second step. Conversely for stair descent, subjects started at the top of the staircase unit and descended without use of a handrail. On the last step, subjects were instructed to continue walking in the same direction. Primary and secondary knee motions were again acquired on all 3 steps and external moments were calculated from the second step descending to the first step. For chair rising and chair sitting activities, an armless chair with adjustable seat height was strategically placed at the perimeter of the force plate to allow only the tested foot to be placed on the force plate, however ensuring no interference with the movements. Seat height was adjusted to the tibiofemoral joint line of each subject as measured from the floor to a standing position. For chair rising, subjects started in a seated position prior to data collection. The tested leg was slightly raised, relieving the force plate of contact. Once instructed, the subject lowered the tested leg and stood up to a vertical position without use of any aids. For chair sitting, the subject started in an erect position with the tested leg slightly lifted to again ensure no contact with the force plate. Upon data collection, the subject lowered the tested leg and sat onto the chair. Knee motions were recorded for the entire sequence of movements and knee moments were calculated once contact with the force plate occurred. During squatting, subjects started standing erect with the tested leg slightly lifted. Data collection started as soon as the subject was instructed to lower the tested leg onto the force plate and squat to a comfortable depth, keeping heels on the ground and feet shoulder's width apart.

All five activities (chair, stair and squatting) were compared to normal walking gait cycles (at normal walking speed) [52]. Walking gait was measured using the same patient population, during the same period of time, and with the same method and equipment.

5.3.3.4. Data Post-Processing and Analysis

Average F-E, A-P and I-E motion profiles per subject and activity were generated by averaging the three trials from each activity; since the objective of this study was obtain relative knee motions. A unique reference point for the motion data were established, allowing comparison between subjects and activities. For this, the average A-P and I-E motions were set to zero at the time point when knee F-E reached 45 degrees (this data adjustment/normalization allowed for a relative comparison of the motion data between activities, which was one of the main objectives of this study). Moment data were normalized to body weight times height (Bw · Ht). Peak moments were obtained for each moment direction. Peak moments were used to identify any significant differences between activities.

5.3.3.5. Statistical Analysis

For each adjusted motion profile, range of motion and descriptive statistics (average, standard deviation, minimum and maximum) were computed. Based on the motion ranges, outliers were identified and excluded using Grubb's test of outliers. Peak external moment values were computed and compared between activities. Two-sample t-tests were conducted to identify differences in kinematics and kinetics between activities. A *p*-value of 0.05 or less was considered significant. Statistical analysis was performed using Minitab 15.1 for Windows.

5.3.4. RESULTS

5.3.4.1. Primary and Secondary Motions of the TKR Joint

Depending on the activity (chair, stair or squatting), subject data were excluded from the analysis either because of corrupted kinematic/kinetic data or because the data collected were classified as outliers per Grubb's test of outliers. For two subjects, squatting kinetic/kinematic data were also collected. This activity was not part of the overall study design; however, it is reported here since the results are interesting for future investigations. Average A-P displacement, I-E rotation and F-E motion values for each measured subject and activity are provided in Table 5-10. Range of motion and average motion profiles were calculated for chair sitting and rising (Figure 5-15), stair ascent and descent (Figure 5-16) and squatting (Figure 5-17). Full data sets are provided in Appendix 2-I.

In comparison to normal walking, chair and stair activities generated significantly higher A-P displacements and I-E rotation (secondary motions), except for A-P and I-E motions generated during chair sitting and stair descent (p-values > 0.05), respectively. Statistical significance *p*-values are provided in the last row of Table 5-10.

Table 5-10: Average A-P, I-E and F-E range of motion for chair sitting and rising, stair ascent and descent, squatting and normal walking [52].

	Chair Sitting			Chair Rising			Stair Descent			Stair Ascent			Squatting			Normal Walking		
ID	**A-P (mm)**	**I-E (deg)**	**F-E (deg)**	**A-P (mm)**	**I-E (deg)**	**F-E (deg)**	**A-P (mm)**	**I-E (deg)**	**F-E (deg)**	**A-P (mm)**	**I-E (deg)**	**F-E (deg)**	**A-P (mm)**	**I-E (deg)**	**F-E (deg)**	**A-P (mm)**	**I-E (deg)**	**F-E (deg)**
1	11.4	16.2	66.2	15.6	20	91.7	14.5	12.6	91.7	13.6	16.6	71.1	--	--	--	18.5	13.2	42.3
2	+	+	+	33.3	20.1	93.4	34	15.9	93.4	32.4	14.1	72.3	--	--	--	20.0	16.1	34.6
3	46.3	*	96.2	31.8	46.8	103.3	28.8	32.2	103.3	41.5	30.6	83.7	--	--	--	32.8	17.7	25.5
4	40.5	10.7	70.2	32.7	6.2	85.4	33.1	10.5	85.4	49.4	18.6	67.1	--	--	--	21.1	19.4	32.3
5	19.6	34.6	82.4	20.3	40.4	97.5	26.4	20	97.5	22	21.2	63.2	--	--	--	14.2	9.5	28.4
6	+	+	+	*	*	*	*	*	*	+	+	+	--	--	--	+	+	33.5
7	66.9	15.9	89	83	16.9	105.6	73.7	15.9	105.6	120	11.1	91.3	--	--	--	47.5	8.9	30.9
8	21.6	7.4	64.6	29.1	5	85.3	50.2	16.2	85.3	35.1	8.3	62.4	--	--	--	17.1	6.8	42.1
9	*	*	*	81.3	+	132.5	52.8	35.8	132.5	36.9	50.6	103.8	--	--	--	25.2	19.2	30.7
10	29	25.7	95.7	36.4	29.1	99.6	18.1	18.1	99.6	14	18.3	62.9	--	--	--	33.0	7.7	33.3
11	40.5	15.9	98.7	48.8	16.6	117.4	36.8	10.2	117.4	32	12.1	89.8	--	--	--	19.7	6.0	43.6
12	36.7	11.3	91.7	37.8	6.6	96.7	47.6	12.6	96.7	57.3	12.9	70.4	--	--	--	20.2	9.1	35.5
13	20.3	23.4	81.9	20.3	22.8	82.5	16.3	13.6	82.5	26.2	20.2	76.2	--	--	--	22.8	16.1	33.8
14	18.5	9.1	77.6	20.8	20.2	95.3	17	15.4	95.3	14.3	12.1	57.1	--	--	--	18.0	10.1	36.4
15	10.5	16.5	87.6	13	16.4	92.9	27.3	17.9	92.9	18.9	7.9	64.5	--	--	--	21.6	8.9	47.4
16	12	16.8	72.1	21.5	14.3	80.4	26	21.3	80.4	26.8	6.2	59.8	--	--	--	+	+	56.9
17	23.2	8.4	75.9	28.8	12.1	87.4	31.3	7.4	87.4	37.3	8.8	65.9	--	--	--	14.0	6.0	36.1
18	*	43.4	*	60.2	41.2	*	102.3	*	*	*	*	*	--	--	--	--	11.4	24.3
19	19	25.7	87	21.3	31.2	92.8	13.4	13.6	92.8	22.7	8.4	57.4	--	--	--	10.5	10.4	43.5
20	44.4	15.5	96.5	20.4	9.9	66.7	30.5	10	66.7	25.4	10.7	75.5	--	--	--	+	+	+
21	23.6	5.6	90	19.1	5	89.4	10.8	7.1	89.4	27.5	8.8	57.9	20.5	1.4	82.6	+	+	+
22	26	16.2	99.5	28.5	14.4	96.3	40.9	14.3	96.3	47.8	13	70.6	28.1	3	89.8	+	+	+
23	+	+	+	+	52.3	111.8	*	37.2	111.8	*	*	*	+	+	+	+	+	+
Ave	**28.3**	**17.7**	**84.6**	**33.5**	**21.3**	**95.4**	**34.8**	**17.0**	**95.4**	**35.1**	**15.5**	**71.1**	**24.3**	**2.2**	**86.2**	**22.3**	**11.6**	**36.4**
SD	**14.8**	**9.8**	**11.3**	**19.6**	**13.9**	**13.9**	**21.8**	**8.4**	**13.9**	**23.4**	**10.1**	**12.6**	**5.4**	**1.1**	**5.1**	**9.0**	**4.5**	**8.0**
***p*-value**	0.16	**0.02**	**0.00**	**0.03**	**0.01**	**0.00**	**0.02**	**0.02**	**0.00**	**0.03**	0.13	**0.00**	--	--	--	1.0	1.0	1.0

**Outliers per Grubb's method, + Not available / Corrupted data, -- Activity not measured / Analysis not performed*
p-values based on a two-sample t-test p values with 95% confidence interval

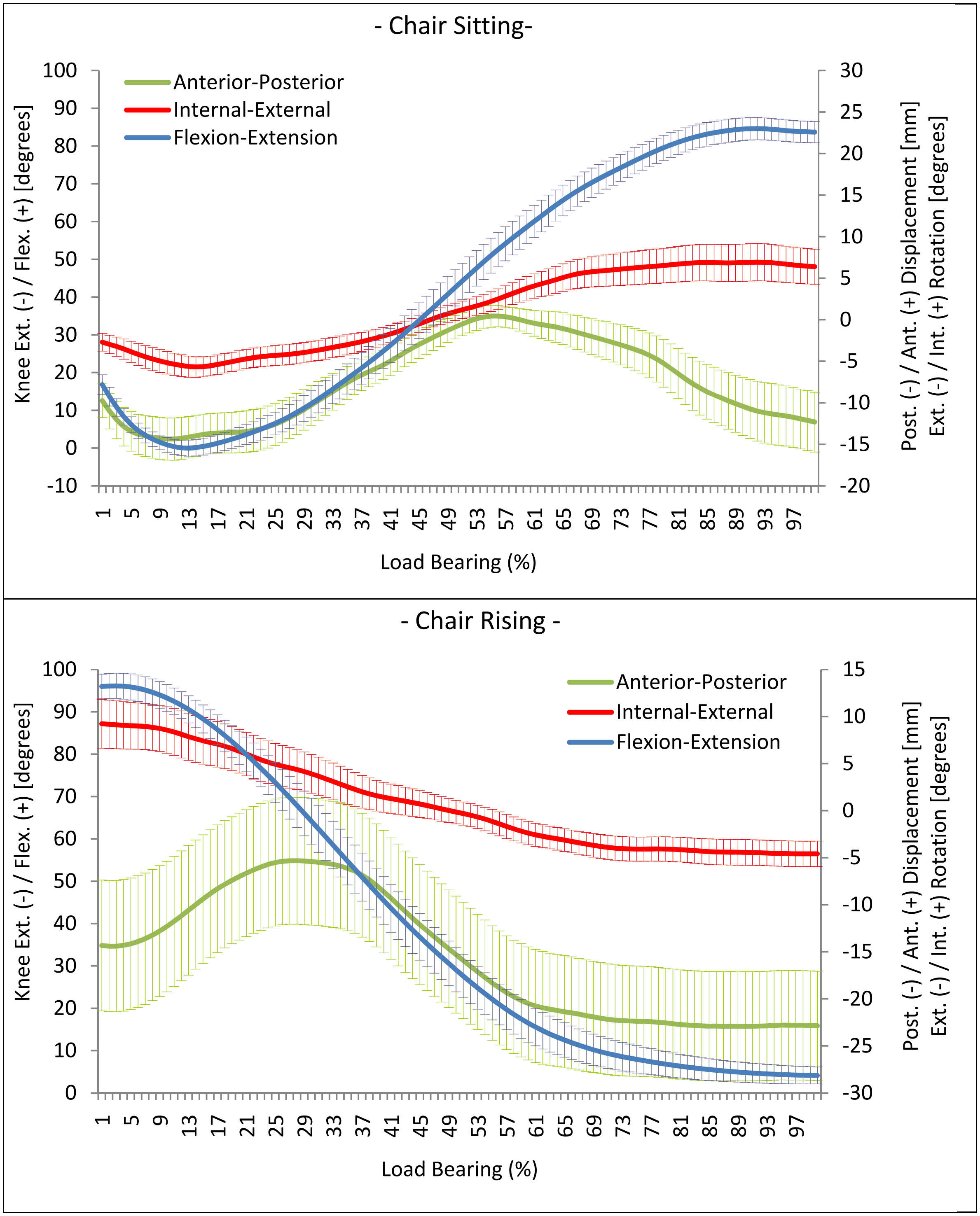

Figure 5-15: Primary (F-E) and secondary (A-P and I-E) motions of the TKR joint during chair sitting (top) and rising (bottom) from twenty-three patients. Error bars depict the standard error of the mean (SE).

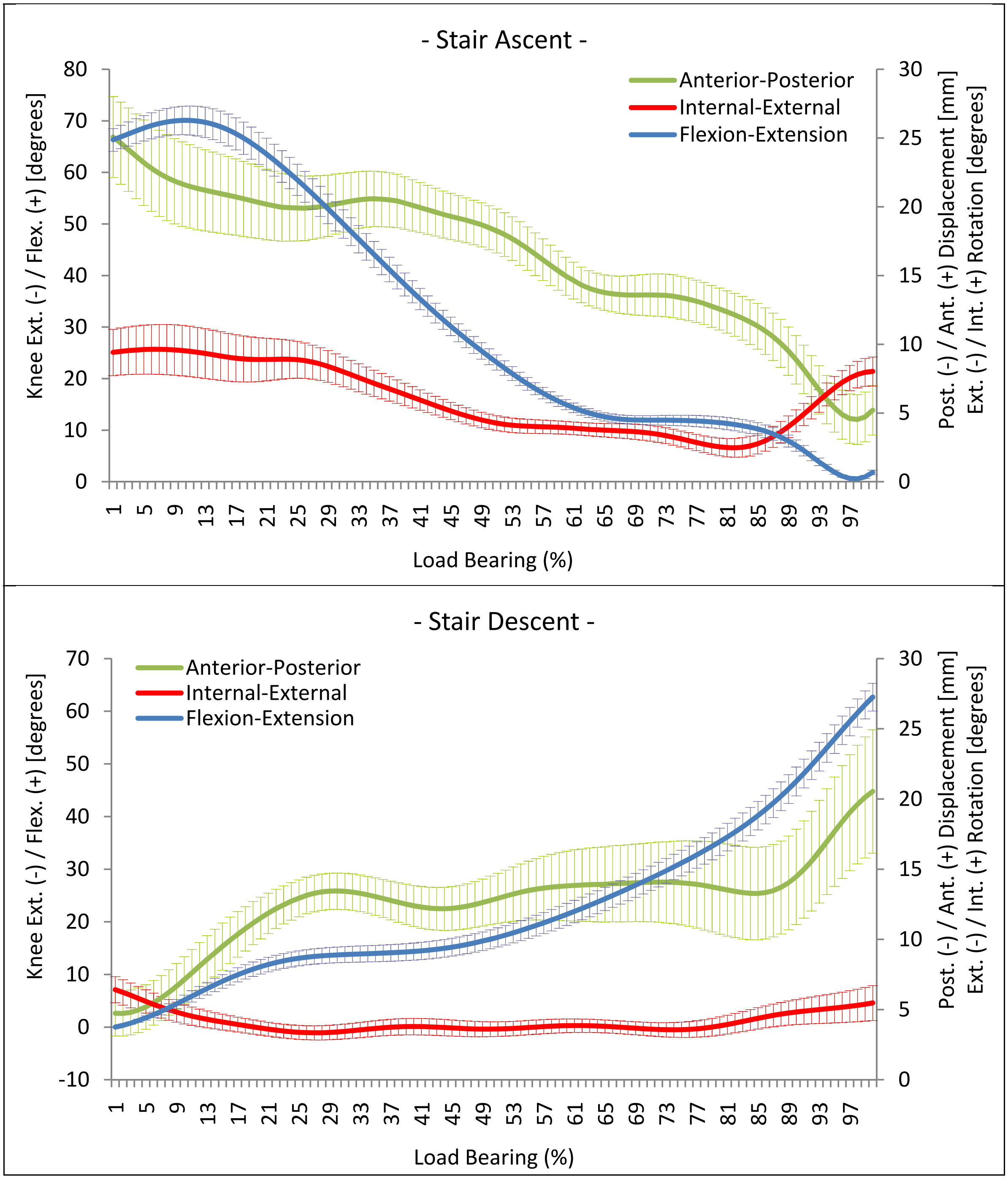

Figure 5-16: Primary (F-E) and secondary (A-P and I-E) motions of the TKR joint during stair ascent (top) and descent (bottom) from twenty-three patients. Error bars depict the standard error of the mean (SE).

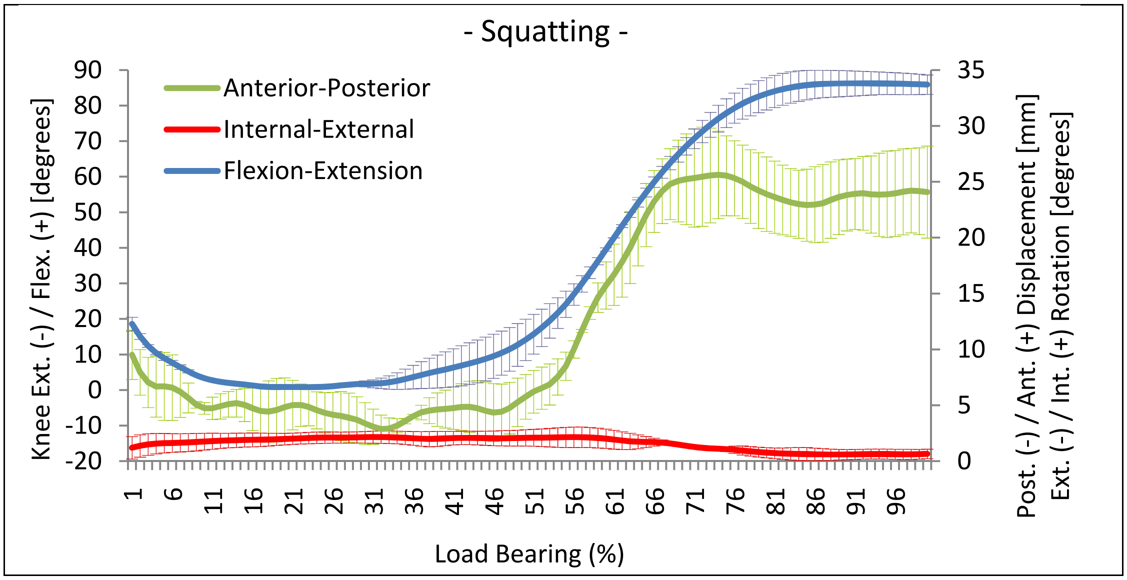

Figure 5-17: Primary (F-E) and secondary (A-P and I-E) motions of the TKR joint during squatting from two patients. Error bars depict the standard error of the mean (SE).

5.3.4.2. External Knee Moments of the TKR Joint

Peak external knee moments generated during chair, stair and squatting activities were calculated (Figure 5-18). In comparison to walking, chair and stair activities generated significantly higher external knee moments across all moment directions (Table 5-11).

Table 5-11: Walking normal vs. chair and stair activities (two-sample t-test *p* values).

Moment direction	*p values, α=0.05*			
	Chair Sitting	**Chair Rising**	**Stair Ascent**	**Stair Descent**
Flex	0.00*	0.00*	0.00*	0.00*
Ext	0.001*	0.00*	0.002*	0.055
Add	0.001*	0.00*	0.43	0.316
Add	0.00+	0.00+	0.689	0.339
IR	0.00*	0.00*	0.002*	0.220
ER	0.339	0.001+	0.00*	0.175

* *significantly higher,* + *significantly lower*

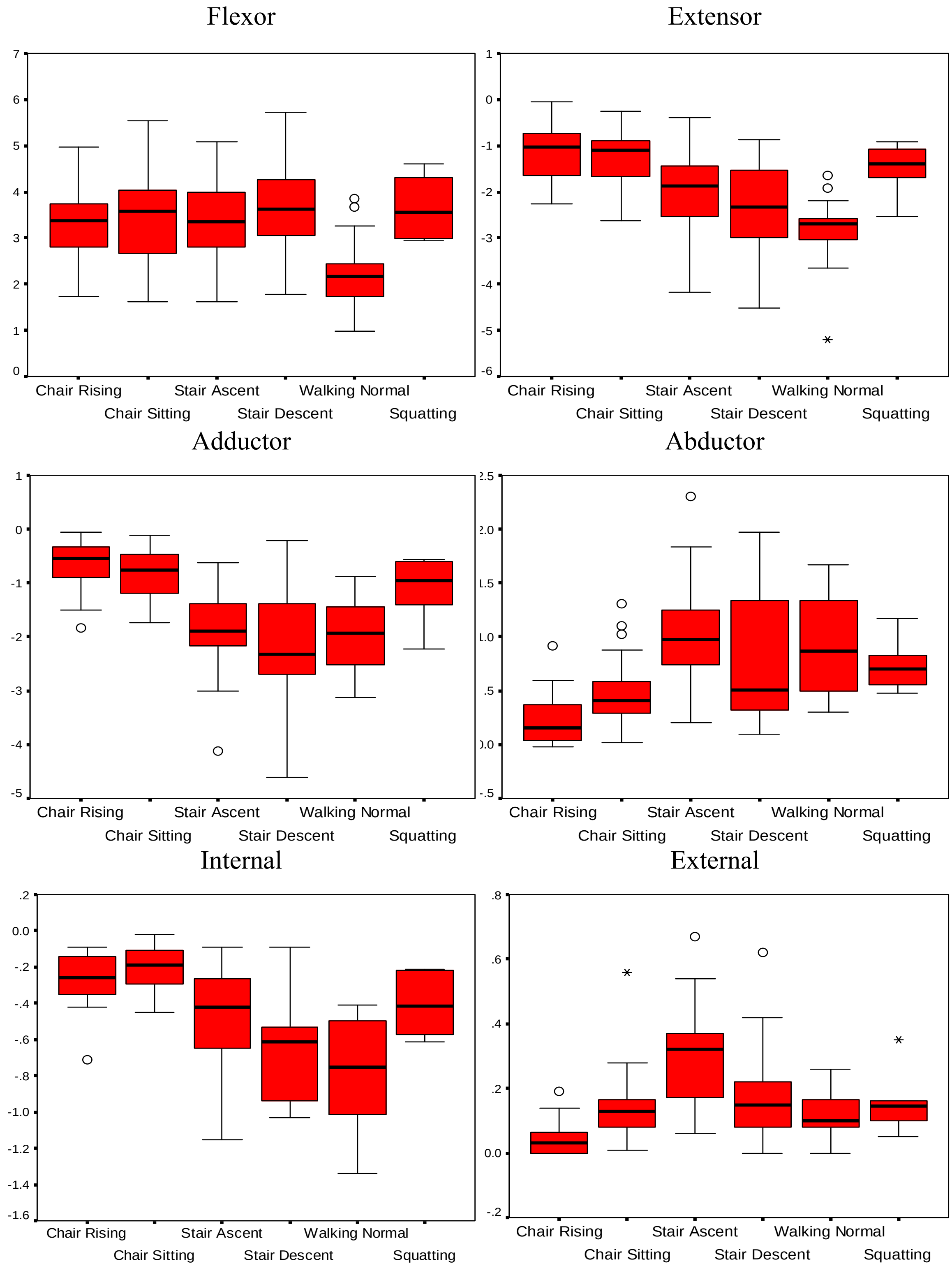

Figure 5-18: External knee moments (BW·m) of the TKR joint during chair sitting/rising, stair ascent/descent, squatting and walking normal. Graph created using three measurements per activity per patient.

5.3.5. DISCUSSION

5.3.5.1. Chair and Stair vs. Normal Walking

In this investigation, the primary (flexion-extension) and secondary (anterior-posterior and internal-external) motions and external moments of the TKR joint of 23 patients were measured during chair sitting and rising, stair ascent and descent and squatting maneuvers. All primary motions and all but two secondary motions (A-P from chair sitting and I-E from stair descent) generated during chair and stair activities were significantly higher than those generated during normal walking. With regards to the external peak knee moments generated during chair and stair activities, about 54% were significantly higher, 13% significantly lower and 33% were not significantly different from the peak knee moments generated during normal walking. These findings suggest that significantly higher amounts of motion and loading conditions are exerted during chair and stair activities than during normal walking. The results of this investigation partially support our hypothesis, as not all secondary motions and external moments generated during chair and stair maneuvers were significantly higher than those generated during normal walking.

Given that polyethylene wear is a function of load, sliding distance, and cross-shear, it is clear that the range of motion and thus sliding distance under load is much larger for chair, stair and squatting activities than for normal walking. Walking is currently the only activity being simulated in standardized wear testing [16], however, other activities such as chair, stair and squatting should also be considered when assessing the preclinical wear performance of TKR components.

5.3.5.2. Multi-Activity Wear Testing Scenario

A comprehensive multi-activity motion profile has yet to be developed for pre-clinical wear evaluation of TKR joint components. Cottrell et al., Benson et al. and Popoola et al. have all evaluated the effects of activities other than walking on TKR polyethylene wear and delamination [12, 14, 77]. However, the kinematics, kinetics or activity frequency and duration used in these studies were collected from a variety of different studies from different patient populations, measuring methods and characteristics. The kinetics and kinematic data generated in this investigation, together with the frequency and duration data previously provided (section 6.2), provide a comprehensive data set that will be useful in the establishment of a population-representative multi-activity protocol for the wear testing of TKR components. Figure 5-19 provides the motion profiles for such a multi-activity wear test. Figure 5-19 differs from Figure 5-15 and Figure 5-16 in that chair and stair activities were grouped based on their primary and secondary motions. Worst case testing conditions may be also generated using the kinetics and kinematics information from the TKR patients who were the most active, walked the most or had significantly higher TKR joint kinetics while performing ADL. With younger, heavier and more active TKR patients [21], more stringent and specialized wear testing protocols for preclinical evaluation of TKR components is palpable and a necessity. One could refer to the experience with metal-on-metal (MoM) hip prosthesis [78, 79], where standardized wear testing was not able to recreate clinical experience; partially due to the omission of physical activities which lead to more challenging contact conditions than those generated by walking.

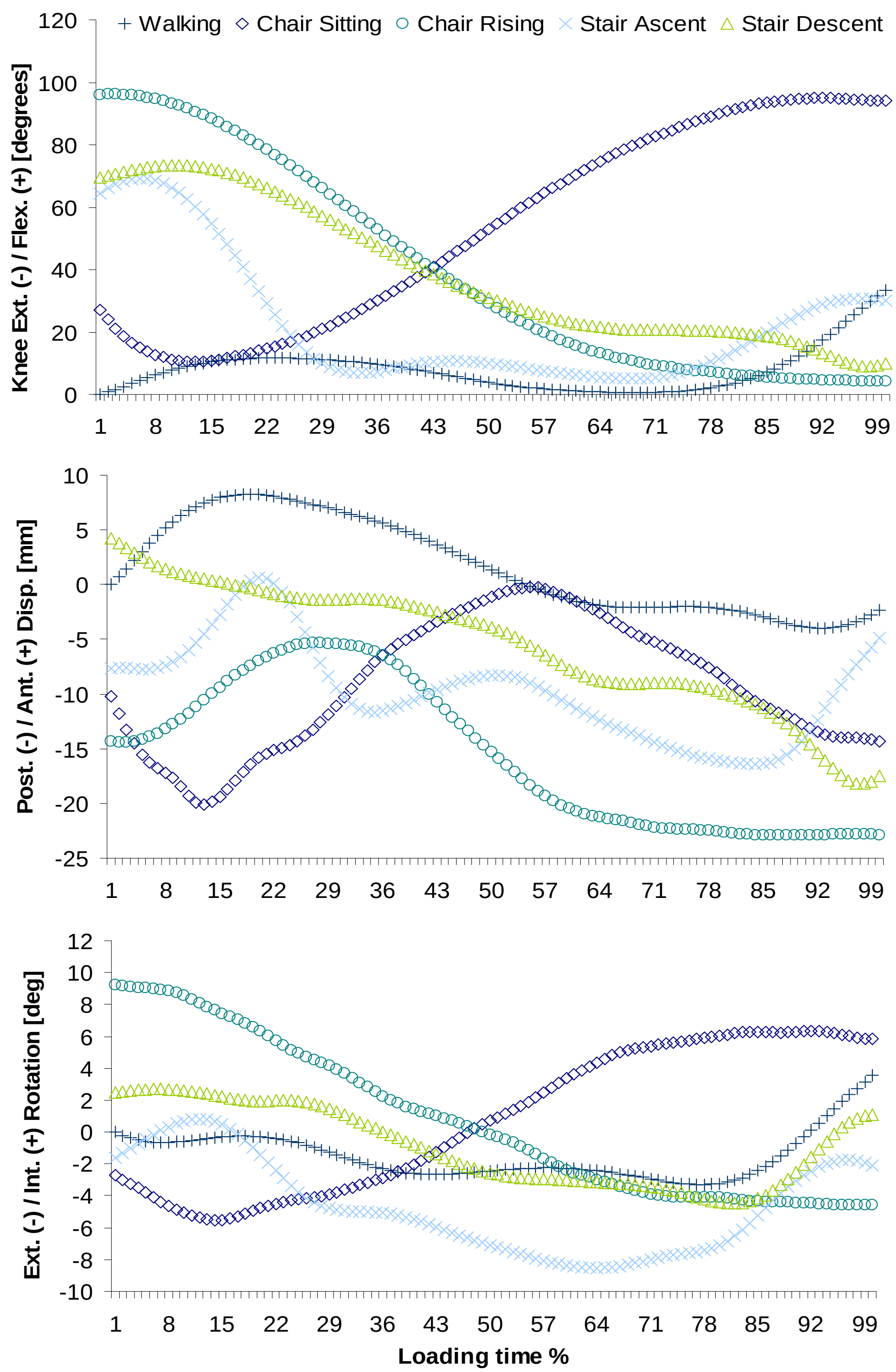

Figure 5-19: Multi-activity motion profile. Average knee F-E (top), A-P (middle) and I-E (bottom) motions of 23 TKR subjects. The SEM ranged from 1.39 – 3.91 for F-E, 0.24 – 6.30 for A-P and for 1 – 1.68 for I-E.

5.3.6. LIMITATIONS

All participating patients came from the same geographic location, with the majority of patients having an office-related job. While this facilitated patient recruitment, it may also have impacted the type and level of activity performed by each patient. Another limitation of the study is that the data generated can only be analyzed in a relative sense.

While chair and stair were identified as the most common activities of daily living in the investigated population; there are also other leisure and sport activities that this study did not cover. Activities such as cycling, golfing and skiing have been found to generate high knee joint loading [70, 71, 80, 81]. A multi-activity wear testing protocol may also consider the contribution to TKR wear of leisure and recreational activities [82].

5.3.7. CONCLUDING REMARKS

This study provided a range of TKR joint kinetic and kinematic data during chair sitting and rising, stair ascent and descent and squatting, which were, for the most part, significantly higher than the kinetic and kinematics generated by normal walking. This information will be utilized to create a multi-activity wear testing profile to obtain contact wear scars patterns (Specific Aim 3.2) and to generate a wear model (Specific Aim 3.3) combining the kinematic, kinetic and frequency data from Specific Aim 2.

6. SPECIFIC AIM 3 - *To assess the impact of chair and stair in TKR wear testing*

6.1. SPECIFIC AIM 3.1 – *To develop and validate a rapid wear scar identification method*

6.1.1. INTRODUCTION

The contact damage pattern, referred to as wear scar, may not be visually identifiable on *in vitro* wear tested tibial components but after about one million walking cycles (Mc), which when performed at the standard suggested frequency of 1.0±0.1 Hz [16], could take over two weeks of uninterrupted testing. The wear scar is typically used to describe the extent of contact damage generated by the femoral component on the articular surface of the tibial component. In the case of a simulator study where the main goal is to analyze the wear scars only, without description of wear appearances, a rapid wear scar identification method may be useful as it will expedite wear scar analysis while minimizing testing duration and resources.

6.1.2. PURPOSE

In this study, a rapid wear scar creation and identification method will be developed. The rapid wear scar identification method will coat the articular surface of the tibial liners with a material that is easy to remove and that clearly and precisely delimits the boundaries of the tibiofemoral medial and lateral wear scars. The ultimate goal of this study is to develop a method to generate, identify and analysis wear scar patterns created by chair and stair activities.

6.1.3. MATERIALS and METHODS

6.1.3.1. Tibial Components

Four NexGen TKR pairs (femoral and tibial component) were used in this investigation. Components were made from ultra-high-molecular-weight-polyethylene (UHMWPE) and were of the CR (cruciate retaining) design type. All components were manufactured by the same company (Zimmer, Inc., Warsaw, IN, USA).

6.1.3.2. Rapid Wear Scar Generation and Identification

The articular surfaces (medial and lateral) of each tibial component was uniformly coated with small dots using a permanent marker (Newell Rubbermaid Office Products, Oak Brook, IL), which was selected as an easy to apply, non-water soluble coating material (Figure 6-1).

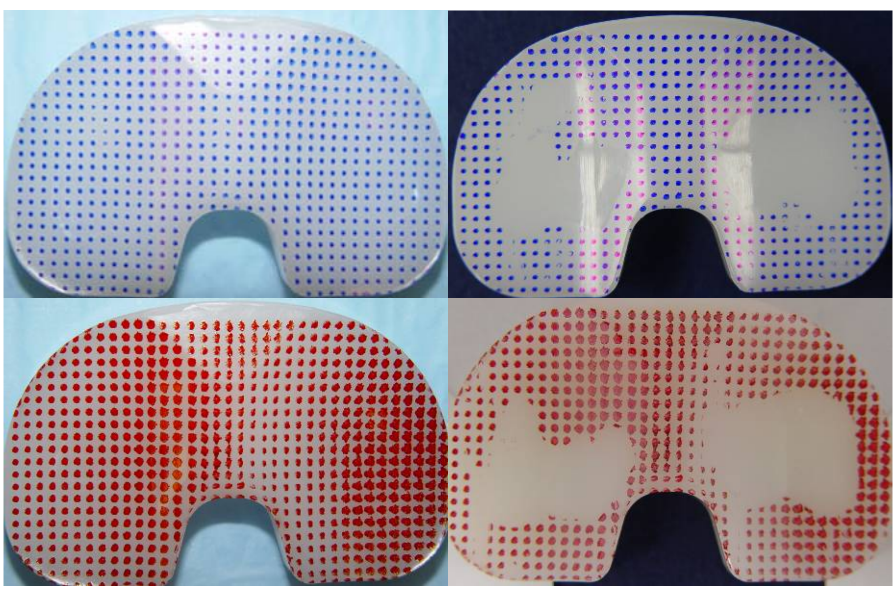

Figure 6-1: Rapid wear scar generation method: pre-test (left) and post-test (right) NexGen CR tibial components.

Wear scars were generated by performing a short-term wear test ($5x10^3$ walking cycles) using the ISO walking standard profile [16]. Wear simulation was performed in displacement control mode. After each tibial component was coated, the TKR couples were setup in a four-station knee simulator (Figure 6-2), following the procedure previously described in section 4.3.2. Distilled water was used as lubricant instead of bovine calf serum, which is what the ISO standard requires [16]. This was done to facilitate cleaning of the tibial components and analysis of their wear scars. Since displacement was applied and wear volume was not evaluated, the lubricant had no effect on the output. Testing stations were not sealed to prevent evaporation of the test lubricant given that the test duration was not long enough for evaporation to be relevant. Distilled water was added anytime the level was considered too low to provide sufficient coverage of the tibiofemoral articulating interface.

Figure 6-2: EndoLab (Rosenheim, Germany) four-station knee simulator. Lubricant in the test stations for this study was distilled water.

6.1.3.3. Wear Scar Identification and Digitization

Wear scar identification and digitization were performed following the method previously described in section 5.3.3. The wear scars generated (medial and lateral) were visually identified and digitized to black and white bitmap images. Geometric parameters were also calculated and used for statistical analysis. Geometric parameters were obtained using ImageJ 1.44p (National Institutes of Health, Bethesda, Maryland).

6.1.3.4. Short-term vs. Full-term ISO Wear Scars

Validation of this method was performed by comparing the wear scars from the short-term ISO wear test ($5x10^3$ cycles, n=4) with the wear scars from a full-term ISO wear test ($5x10^6$ cycles, n=4) which was previously performed in the same simulator under identical testing parameters (except the lubricant). The TKR components (femoral and tibial) were identical (design and material type) to components used for the short-term wear test. Two-sample t-tests (at 95% confidence level) was performed to evaluate whether the wear scars (area and perimeter, medial-lateral (M-L) and anterior-posterior (A-P) stretch) generated by the short- and the full-term wear tests were significantly different.

6.1.4. RESULTS

A comparison of the wear scars from the short- and full-term wear tests is provided in Figure 6-3. Two-sample t-tests (based on the area, perimeter M-L and A-P stretch) indicated that the medial and lateral wear scars generated by the short-term ISO wear test were not significantly different (p-values > 0.055) from the wear scars generated by the full-term ISO wear test (Table 6-1).

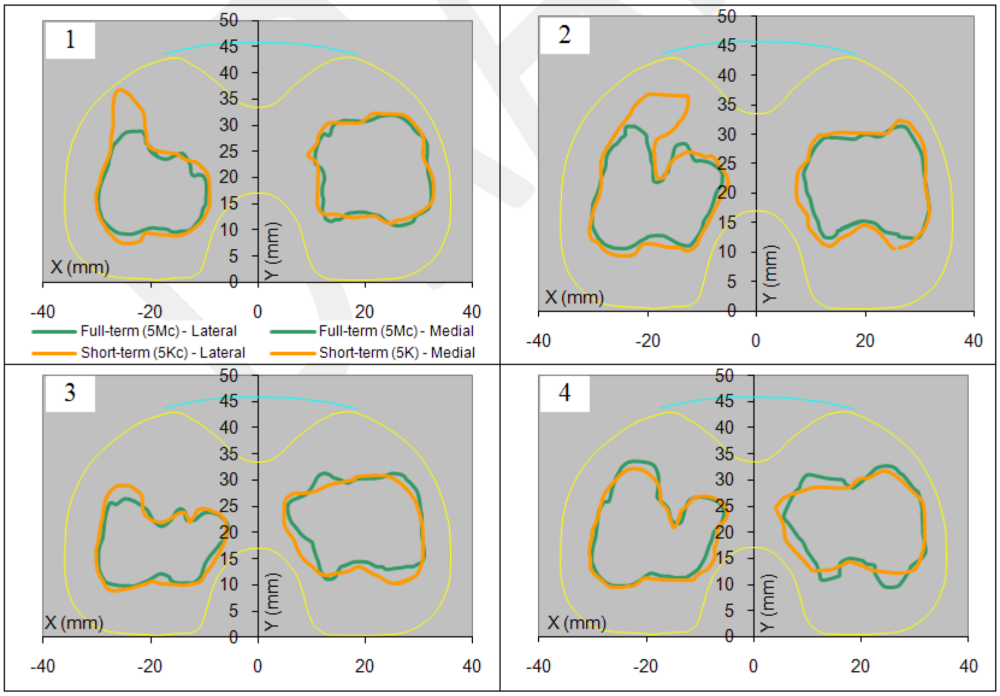

Figure 6-3: Wear scars from the full-term (green) and short-term (orange) ISO wear tests.

Table 6-1: Full-term vs. short-term wears scars

Component	Test	Side	Area	Perim.	M-L stretch	A-P stretch
1	Full-term	Lateral	267.87	69.93	12.20	21.75
2	Full-term	Lateral	327.33	89.72	11.50	19.22
3	Full-term	Lateral	278.30	79.27	11.97	24.41
4	Full-term	Lateral	357.23	91.81	11.61	17.10
		Ave.	307.68	82.68	11.82	20.62
		StDev	41.99	10.12	0.32	3.16
1	Short-term	Lateral	348.37	85.73	11.55	13.91
2	Short-term	Lateral	418.37	107.74	11.08	14.03
3	Short-term	Lateral	335.07	85.07	11.50	21.46
4	Short-term	Lateral	385.58	91.62	11.02	18.45
		Ave.	371.85	92.54	11.29	16.96
		StDev	37.67	10.55	0.28	3.67
		p-value	**0.072**	**0.235**	**0.055**	**0.191**
1	Full-term	Medial	346.40	77.16	52.41	18.57
2	Full-term	Medial	326.60	77.07	49.99	19.57
3	Full-term	Medial	365.88	82.53	47.28	19.40
4	Full-term	Medial	406.33	91.88	47.22	18.04
		Ave.	361.30	82.16	49.23	18.90
		StDev	34.03	6.96	2.49	0.72
1	Short-term	Medial	368.60	77.20	50.99	18.22
2	Short-term	Medial	386.91	82.75	48.75	18.51
3	Short-term	Medial	420.91	82.81	46.45	19.57
4	Short-term	Medial	397.58	82.29	45.81	19.04
		Ave.	393.50	81.26	48.00	18.84
		StDev	21.84	2.72	2.36	0.60
		p-value	**0.172**	**0.825**	**0.505**	**0.903**

6.1.5. DISCUSSION

A rapid wear scar generation and identification method was successfully developed and validated. This study provides a method to speed up the creation and analysis of tibiofemoral wear scars from *in vitro* wear testing protocols for which the wear rate or the wear appearances are not of interest. Wear scars that would otherwise take one million or more cycles (depending on the testing parameters) to be visually distinguishable, can now be visualized in a fraction of the time and without the need to utilize a brand new tibial component for each testing condition.

It is important to note that the method proposed does not substitute standardized wear testing, which main objective is to quantify the amount of material loss (i.e. wear) of the tibial component. Furthermore, this test is susceptible to the condition of the articulating surfaces, as they may affect the contact interaction between the femoral and tibial component. Tibial components which have been significantly deformed due to creep should not be used to obtain wear scars using the rapid wear scar generation and identification method described in this study.

The rapid wear scar generation and identification method developed here will be used to accelerate the creation and analysis of wear scar patterns from chair and stair activities, which is a task that will be undertaken in the following section.

6.2. SPECIFIC AIM 3.2 - *To investigate whether in vitro wear scars from chair and stair activities compare better with in vivo wear scar*

6.2.1. INTRODUCTION

As with any simulation tool, the ultimate goal of preclinical wear simulations is to recreate *in vivo* conditions as closely as possible. For knee wear simulation this means recreating wear damage characteristics (rates, modes, patterns, appearances, particle size and morphology) generated *in vivo*. This, however, has proven challenging for knee wear simulators despite the high reproducibility of *in vivo* wear damage characteristics of hip simulators. As previously mentioned in section 4, it has been reported that knee wear simulators generated tibial liner wear scars (envelope containing all damage patterns), which are less variable in size and location in comparison to those observed in postmortem and revision retrievals of the same design type [37], [31]. Since wear scars are substantially influenced by the kinetics and kinematics of the knee joint, current standardized knee wear tests are limited in that they apply loads and motions from only one of the many activities TKR patients perform throughout the day, normal walking [16]. Cottrell et al. and Benson et al. found that when one stair ascent [12] or descent [14] was combined with seventy cycles of normal walking (a 1:70 walking to stair ratio), more *in vivo* like wear scars and higher wear rates were generated. Popoola et at. evaluated the wear and delamination effects of stair ascent, chair rising and deep squatting activities [77] on polyethylene articular surfaces. While the author found significantly higher wear rates for stair, chair and squatting activities in comparison to normal walking, wear scars from individual or from combinations of activities were not investigated or compared with retrieved TKR components. Determining what and how physical activities, other than walking, better recreate the wear scar patterns observed on retrieved TKR components may be useful in creating more representative, *in vivo* like preclinical wear testing conditions.

6.2.2. PURPOSE

In this study, wear scars from chair sitting and rising and stair ascent and descent were generated using the primary (flexion-extension) and secondary (anterior-posterior and internal-external) motions of the TKR joint. The TKR population average motions obtained in section 5.3 were used. The wear scars generated by each activity, as well as those from multiple combinations of activities, were compared with the wear scars generated by revision-retrieved, postmortem-retrieved and ISO simulator generated components [16] of the same design type. It was hypothesized that: 1) either as a single activity or as a combination of activities, the wear scars generated by chair and stair activities will have significantly different geometric characteristics than those generated by ISO standardized testing, and 2) wear scars from chair and stair will not be assigned to the same cluster group of ISO generated wear scars.

6.2.3. MATERIALS and METHODS

6.2.3.1. Retrieved and Simulator Tested Components

The digitized wear scars (images and geometric data) from the twenty-one postmortem retrieved, fifty-four revision retrieved and six ISO simulator components used in section 4 (Table 4-1) were used in this study. In addition, three mildly used components (used less than 5,000 cycles for tuning) were used to generate wear scars from chair and stair activities. All retrieved and simulator components used in this study were of the same MG-II design type and were manufactured by the same company (Miller-Galante II, Zimmer, Inc., Warsaw, IN, USA).

6.2.3.2. Knee Simulator Input Parameters

The average activity motion profiles generated in section 5.3 (Figure 5-19) were used to create input profiles for the EndoLab (Rosenheim, Germany) four-station knee simulator. Ranges of motion for each activity are provided in Table 6-2**.**

Table 6-2: TKR ranges of motion during chair and stair activities.

Activity	Chair Sitting			Chair Rising			Stair Descent			Stair Ascent		
Motion	A-P (mm)	I-E (deg)	F-E (deg)	A-P (mm)	I-E (deg)	F-E (deg)	A-P (mm)	I-E (deg)	F-E (deg)	A-P (mm)	I-E (deg)	F-E (deg)
Range	28.3	17.7	84.6	33.5	21.3	95.4	34.8	17	95.4	35.1	15.5	71.1

The knee simulator imparts tibial liner anterior-posterior displacement (A-P) and internal-external rotation (I-E) via two linear actuators (actuator A and actuator B, Figure 6-4). Average flexion-extension (F-E), A-P and I-E patient motion profiles were converted to simulator input profiles using the equation provided by the manufacturer (Table 6-3). Since this study focused on obtaining wear scars and not wears volumes, a constant axial force of 1,000 N was used with all activities. The simulator applied the activity primary (F-E) and secondary (A-P and I-E) motions of the TKR joint in displacement control mode.

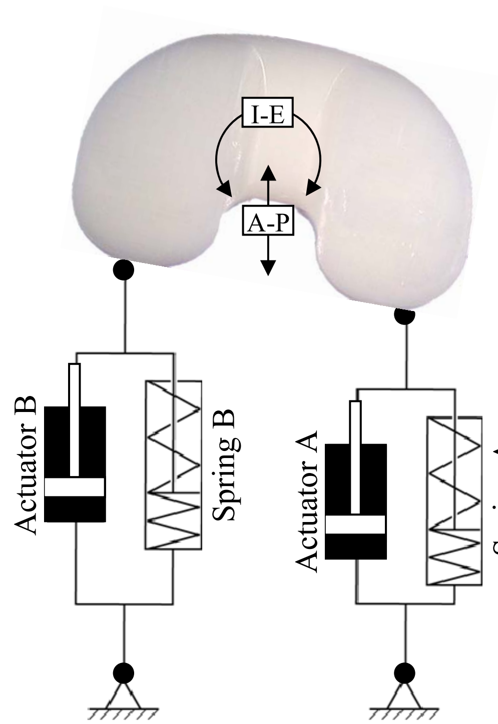

Figure 6-4: Knee simulator A-P and I-E actuation concept.

Table 6-3: Conversion of patient kinematics and kinetics to simulator input profiles.

Patient Kinetics and Kinematics	Patient to Simulator conversion	mm, deg, N to mV
A-P (mm)	$Act.\ A_{(mm)}=A\text{-}P_{(mm)}-(L2*\tan(I\text{-}E_{(deg)}))$ $Act.\ B_{(mm)}=A\text{-}P_{(mm)}+(L1*\tan(I\text{-}E_{(deg)}))$	$Act.\ A\ or\ B_{\ (mV)}=(Act.\ A\ or\ B_{\ (mm)}*250)+5000$
I-E (degrees)		
F-E (degrees)	N/C	$F\text{-}E_{(mV)}=F\text{-}E_{(deg)}*100$
Axial (N)	N/C	$Axial_{\ (mV)}=Axial_{\ (N)}*2$

Act = actuator. L1 and L2 are the distances from the Act A and B to the center of rotation of the articular component. N/C= no conversion needed.

6.2.3.3. Knee Simulator Modifications

The knee simulator was modified to allow more than 60 degrees of knee F-E (i.e. the default manufacturer configuration). The modifications reversed the F-E direction (allowing maximum available range of motion), changed the attachment location of the F-E actuator (providing sufficient torque throughout the range of motion) and changed the F-E sensor attachment location (measuring and controlling F-E angles through the range of motion). After modifications were made, the knee simulator was able to reach a maximum F-E range of motion of 105 degrees (Figure 6-5). The femoral components were setup with 60 degrees of hyper-flexion in order to use the new maximum F-E range of motion of the simulator (Figure 6-6).

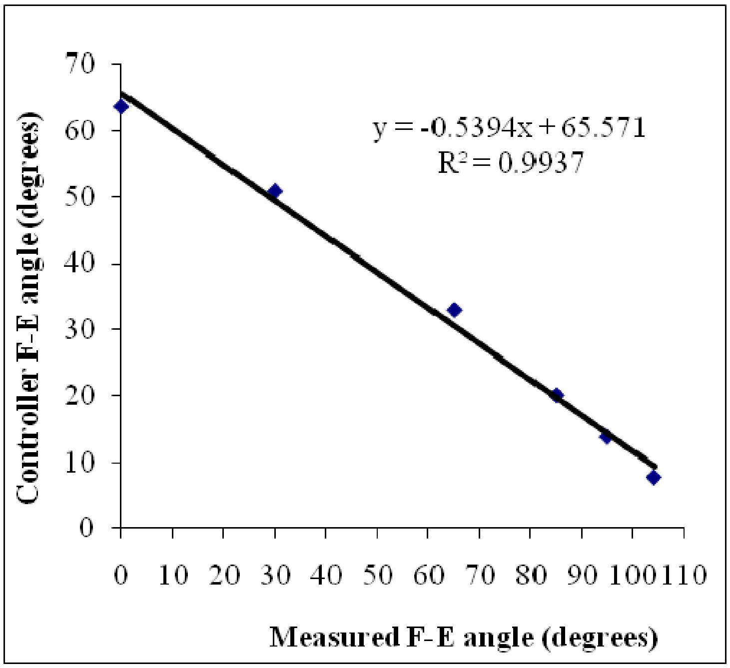

Figure 6-5: Controller readout after modifications were done. F-E response exhibited a nearly linear pattern. Because the F-E motion direction was reversed, the measured angle increased while the controller angle decreased.

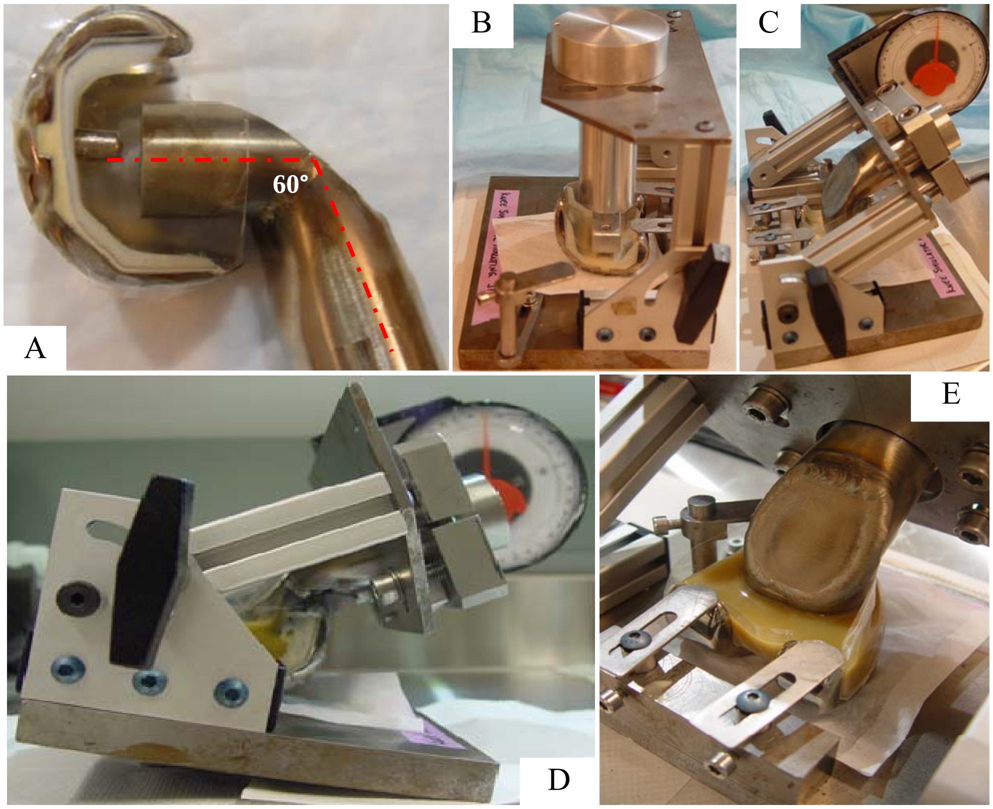

Figure 6-6: Femoral component setup: A) femoral component was prepared (taped and sealed) for potting with hyper-flexed (60 deg) attachment fixture; B) femoral component was aligned at zero deg F-E angle; C) hyper-flexed fixture was setup and aligned with the femoral component; and D/E) fixture and femoral component are attached together using a two-phase glue.

6.2.3.4. Rapid Wear Scar Generation

Only three pairs of MG-II TKR (femoral and tibial) components were available for this study. Since the objective of this investigation was to obtain wear scars from four different activities (chair sitting, chair rising, stair ascent and stair descent), all TKR component pairs needed to be reused every time a new activity was evaluated. To do this, the rapid wear scar generation and identification method described in the previous section (section 6.1) was implemented.

6.2.3.5. Wear Scar Identification and Digitization

Wear scar identification and digitization were performed following the method previously described in section 4.3.3. The wear scars (medial and lateral) generated by each activity were visually identified and digitized using ImageJ 1.44p (National Institutes of Health, Bethesda, Maryland) to black and white bitmap images (220x170 pixels). These wear scar images were used for clustering analysis using the previously developed Self-Organizing-Feature-Map (SOFM) model presented in section 4. Geometric parameters were also calculated for each activity wear scar and used for data mining and statistical analysis.

6.2.3.6. Clustering and Cluster Visualization

Wear scars from individual and combination of activities were compared with wear scars from postmortem-retrieved, revision-retrieved and ISO-generated wear scars. Wear scar comparison was done using the SOFM model developed in section 4. It is important to note that the SOFM was not re-trained; wear scars from individual and combination of activities were assigned to the eleven clusters created from the wear scars of postmortem-retrieved components. Cluster visualization was done using the u-matrix method described in section 5.4.5.

6.2.4. RESULTS

6.2.4.1. Chair and Stair Wear Scars

Four medial and lateral wear scars (3 individual + 1 combined) were generated for each activity. In addition, wear scars from different combinations of activities were created by overlapping two or more activities (Figure 6-7). Based on geometric parameters, chair rising generated the largest combined medial and lateral wear scars; followed by chair sitting, stair descent and stair ascent. Chair maneuvers generated medial wear scars that were larger than the lateral wear scars. Stair maneuvers, on the other hand, generated lateral wear scars that were larger than the medial wear scars (Table 6-4). These differences, however, were statistically significant only for chair rising and sitting when compared with stair ascent (p<0.01).

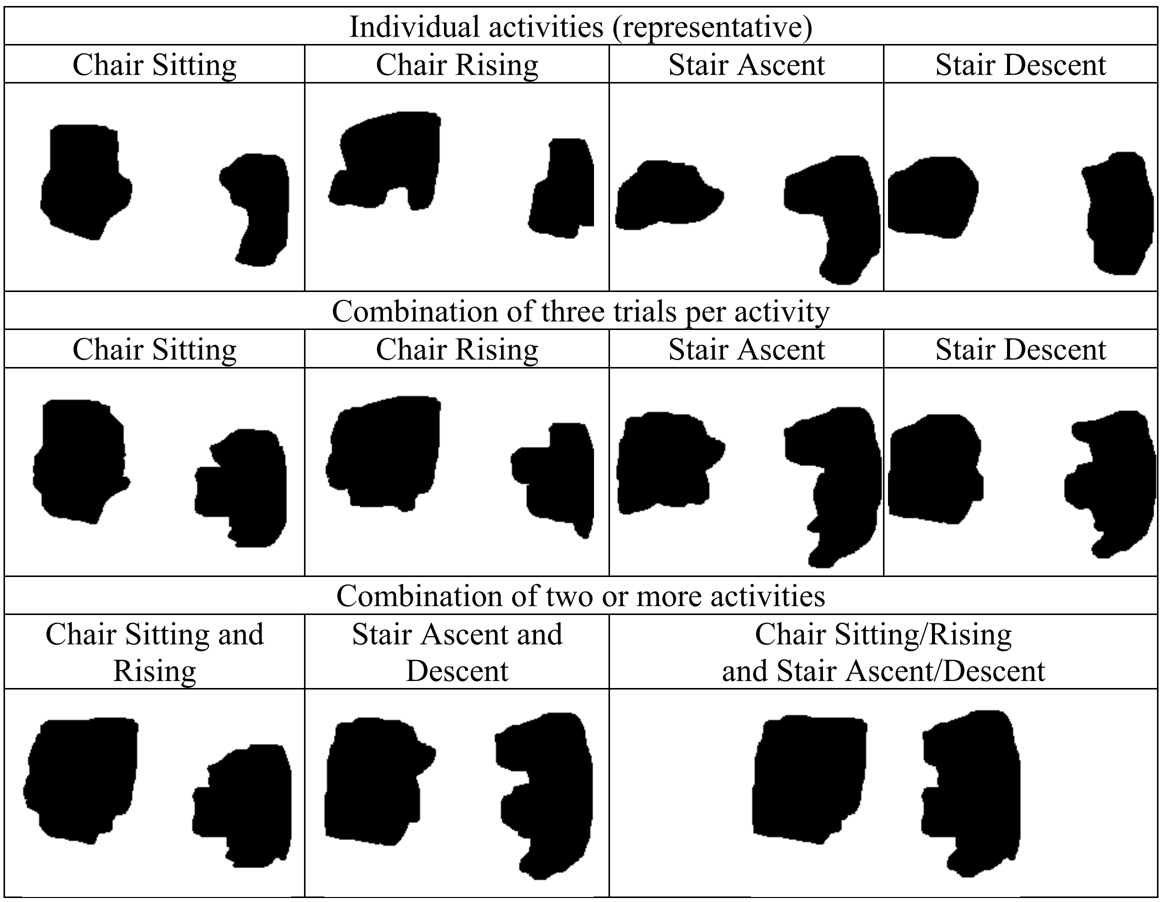

Figure 6-7: Individual and combined wear scars from chair and stair activities.

Table 6-4: Wear scar geometric features.

Average (StDev)	Lateral				Medial			
	Area (mm^2)	**Perim.** (mm)	**M-L stretch** (mm)	**A-P stretch** (mm)	**Area** (mm^2)	**Perim.** (mm)	**M-L stretch** (mm)	**A-P stretch** (mm)
CR/I	541.3 (37.5)	98.7 (6.5)	27.2 (0.6)	25.2 (1.3)	314.2 (15.6)	76.2 (2.8)	18.3 (3.0)	23.6 (1.5)
CS/I	444.0 (62.2)	87.4 (9.6)	21.4 (1.7)	27.8 (2.6)	349.8 (61.1)	85.5 (7.8)	19.1 (3.0)	26.4 (1.7)
SA/I	306.2 (40.4)	73.4 (5.5)	25.2 (2.3)	16.7 (0.5)	431.6 (81.4)	97.0 (14.5)	21.5 (4.1)	30.0 (2.0)
SD/I	367.1 (2.5)	74.4 (0.9)	22.3 (1.1)	20.3 (0.2)	419.9 (2.3)	90.6 (4.3)	20.2 (2.4)	30.1 (0.2)
CR/C	639.5	102.4	28.2	28.5	559.2	96.4	24	30.6
CS/C	512.7	94.2	26.7	25.2	531	90.8	23.4	27
SA/C	701.8	105.6	28.2	31.2	665.9	105.2	27.3	31.5
SD/C	756.7	108.6	28.2	31.8	394.5	89.2	20.4	28.5
CR-CS/C	502.8	98.5	22.5	29.1	630.4	122.8	24	39.6
SA-SD/C	575.2	114.6	22.5	36.3	574.9	102.4	24.3	30.3
Chair-Stair/C	731.8	128.7	24	41.1	795.7	128.3	24.3	41.1

CR=chair rising, CS=chair sitting, SA=stair ascent, SD=stair descent, I=individual, C=combined

6.2.4.2. Clustering of Wear Scars

The wear scars generated by chair and stair activities were assigned to two different clusters, cluster A (Figure 6-8) and cluster D (Figure 6-9). None of the wear scars generated by chair or stair were assigned to cluster G (Figure 6-10), which contains all but one of the ISO simulator components (Figure 6-11). The wear scars resulting from the combination of chair sitting and rising (CS-CR), stair ascent and descent (SA-SD) and chair and stair (CS-CR-SA-SD) were also assigned to cluster D.

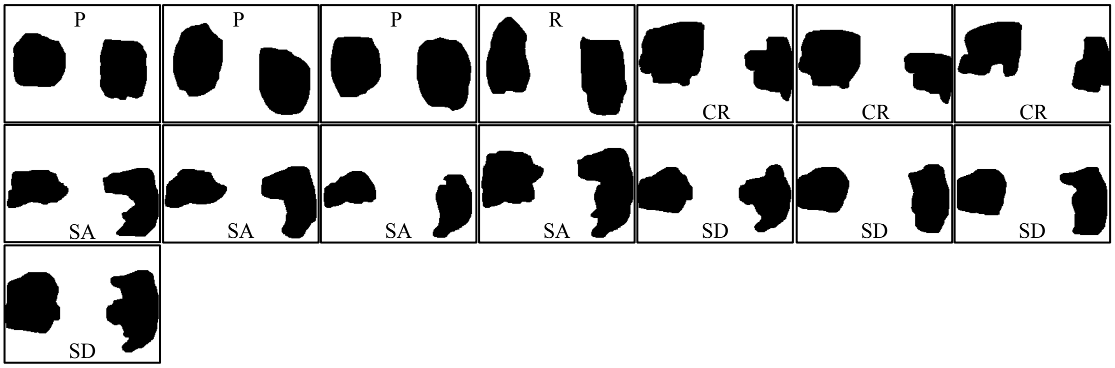

Figure 6-8: Cluster A contains wear scars from 2 revision (R), 2 postmortem (P), 3 chair rising (CS), 4 stair ascent (SA) and 4 stair descent (SD) components.

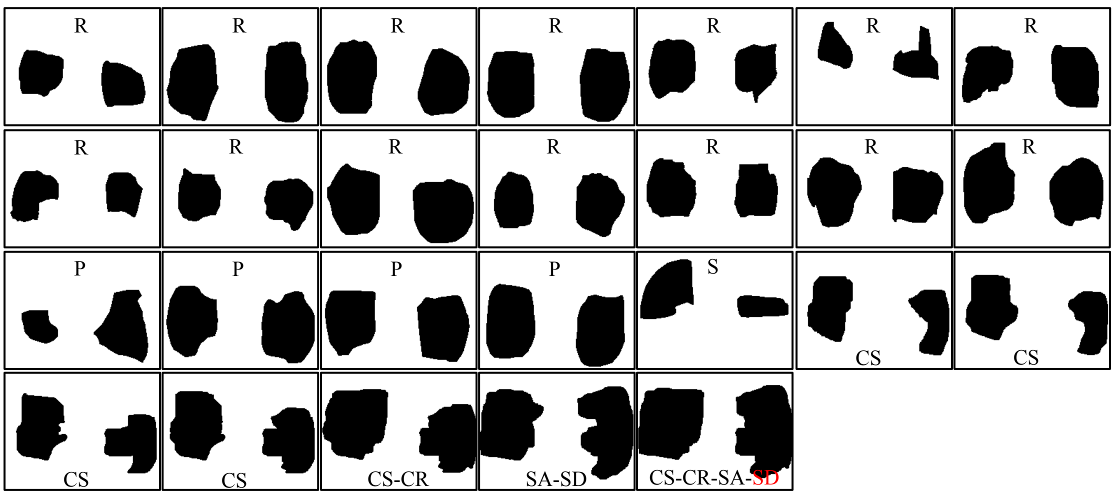

Figure 6-9: Cluster D contains wear scars from 14 revision (R), 4 postmortem (P), 1 ISO simulator (S), 4 chair sitting (CS), 1 combined chair sitting and rising (CS-CR), 1 combined stair ascent and descent (SA-SD) and 1 combined chair and stair (CS-CR-SA-SD) components.

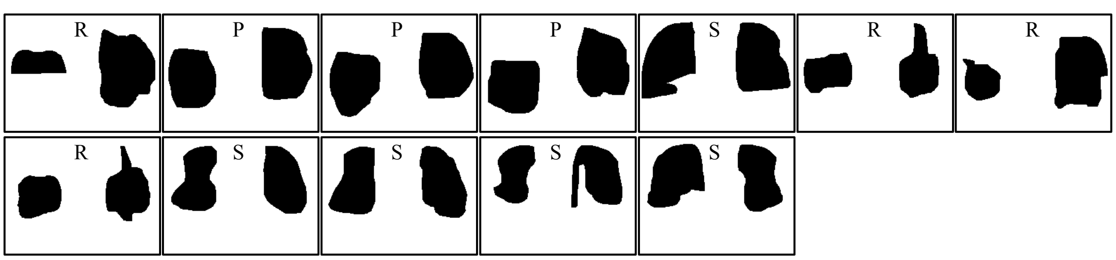

Figure 6-10: Cluster G contains 6 revision (R), 3 postmortem (P) and 5 simulator (s) components.

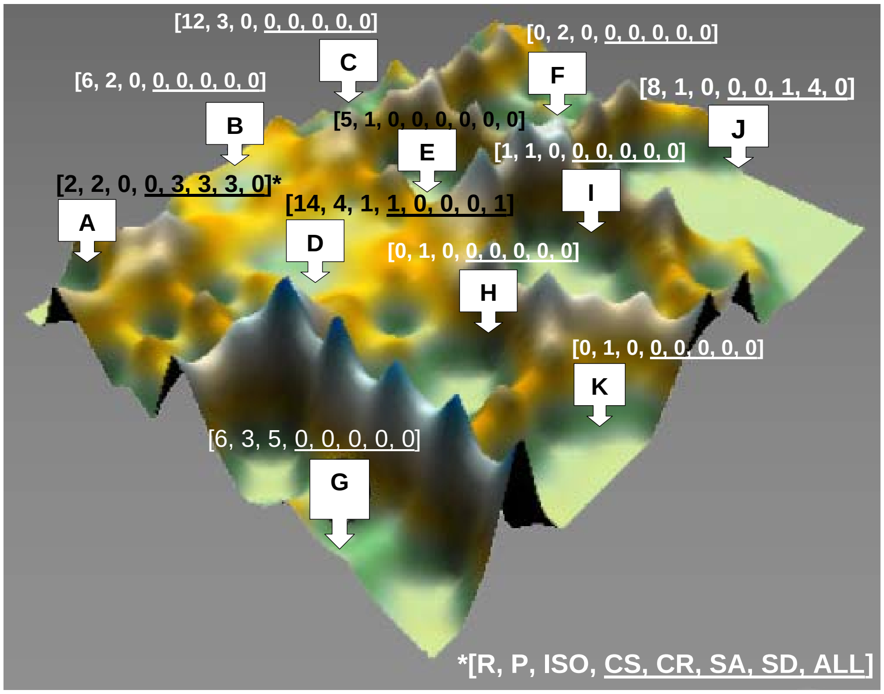

Figure 6-11: Topographic visualization of the SOFM containing eleven clusters generated by postmortem components. Wear scars generated chair and stair activities were assigned to either cluster A or cluster D.

6.2.4.3. Wear Scar Geometric Features

When compared with wear scars from revision, postmortem and ISO tested components (RPS), wear scars from chair rising appeared to be different than those generated by revision components but not different that those generated by postmortem or simulator components. Chair sitting wear scars were, almost across all geometric comparisons, not significantly different than the wear scars generated by RPS components. Stair ascent, similar to chair sitting, generated wear scars that, for the most part, were not significantly different than those generated by RPS components; however, the area of the lateral wear scars were significantly different from the area of the lateral wear scars generated by the postmortem and simulator components. Stair descent generated wear scars that tended to be not significantly different from the wear scars of RPS components; however, the perimeter of the medial wear scars was significantly different from the perimeter of the medial wear scars of the RPS components. Average geometric features for chair, stair, postmortem, revision and ISO tested components are provided in Table 6-5. Statistical comparison between chair and stair wear scars and wear scars from revision, postmortem and simulator components can be found in Table 6-6.

Table 6-5: Comparison of wear scar geometric features between chair and stair vs. revision, postmortem and ISO simulator tested components.

Component	Stats	Lateral Area (mm^2)	Lateral Perim. (mm)	Lateral M-L (mm)	Lateral A-P (mm)	Medial Area (mm^2)	Medial Perim. (mm)	Medial M-L (mm)	Medial A-P (mm)
Revision	Average	383.6	73.6	22.2	23.5	438.7	78.1	21.8	21.8
	StDev	239.2	21.8	6.8	8.8	250.9	23.5	5.9	8.5
Postmortem	Average	459.5	79.8	24.9	24.0	480.9	81.4	23.9	24.2
	StDev	135.7	12.4	3.1	5.0	133.5	11.2	3.5	5.2
ISO	Average	398.8	85.2	20.7	21.4	325.3	73.2	22.2	24.7
	StDev	39.3	12.2	1.9	6.6	104.0	10.3	2.0	2.2
Chair Rising	Average	541.3	98.7	27.2	25.2	314.2	76.2	18.3	23.6
	StDev	37.5	6.5	0.6	1.3	15.6	2.8	3.0	1.5
Chair Sitting	Average	444.0	87.4	21.4	27.8	349.8	85.5	19.1	26.4
	StDev	62.2	9.6	1.7	2.6	61.1	7.8	3.0	1.7
Stair Ascent	Average	306.2	73.4	25.2	16.7	431.6	97.0	21.5	30.0
	StDev	40.4	5.5	2.3	0.5	81.4	14.5	4.1	2.0
Stair Descent	Average	367.1	74.4	22.3	20.3	419.9	90.6	20.2	30.1
	StDev	2.5	0.9	1.1	0.2	2.3	4.3	2.4	0.2

Table 6-6: Chair and stair vs. postmortem, revision and ISO tested TKR components.

p-value	Lateral		Medial	
Comparison	**Area** (mm^2)	**Perim.** (mm)	**Area** (mm^2)	**Perim.** (mm)
Chair Rising vs. Revision	0.009	0.040	0.002	0.636
Chair Rising vs. Postmortem	0.098	0.083	0.000	0.156
Chair Rising vs. Simulator	0.053	0.123	0.809	0.536
Chair Sitting vs. Revision	0.264	0.104	0.116	0.248
Chair Sitting vs. Postmortem	0.750	0.302	0.032	0.475
Chair Sitting vs. Simulator	0.338	0.777	0.672	0.097
Stair Ascent vs. Revision	0.081	0.967	0.909	0.138
Stair Ascent vs. Postmortem	0.002	0.179	0.426	0.197
Stair Ascent vs. Simulator	0.031	0.085	0.152	0.083
Stair Descent vs. Revision	0.636	0.785	0.606	0.010
Stair Descent vs. Postmortem	0.005	0.065	0.050	0.034
Stair Descent vs. Simulator	0.106	0.083	0.076	0.009

p-values < 0.05 were considered significant (red)

6.2.5. DISCUSSION

6.2.5.1. Chair and Stair vs. ISO Generated Wear Scars

In this study, wear scars from chair and stair activities were generated *in vitro* using a mechanical wear simulator which was modified to accommodate the larger than walking ranges of motion generated by chair and stair maneuvers. The wear scars from chair sitting and rising and stair ascent and descent varied in shape and location. The SOFM assigned all the wear scars (individual and combined) to two different clusters, A and D. None of the wear scars were assigned to the cluster containing the majority of ISO simulator components, cluster G; thus indicating that wear scars from chair and stair activities contain features that made them less similar to wear scars generated by ISO walking testing protocols. While these results support our second hypothesis, which stated that wear scars from chair and stair were not going to be assigned to the same cluster group as the ISO tested components, our first hypothesis is not supported. The wear scar geometric features generated by chair and stair activities had, for the most part, characteristics (area and perimeter) that were not significantly different from ISO simulator wear scars. It appears that the SOFM classification of chair and stair wear scars was not dominated by the area or perimeter of the wear scar features. This was, to some degree, expected given the results from section 4, which indicated that even a greater variety of wear scar geometric descriptors could not conclusively explain the clustering results. The SOFM clustering may be, regarded as a better wear scar comparison tool given that clustering was based off a whole medial and lateral wear scar image, and was therefore not limited to single discrete geometric features. Furthermore, the SOFM clustering was non linear, which may explain the reason why statistical comparisons based of linear models are not able to explain the full complexity of the clustering results.

6.2.5.2. Chair and Stair vs. Revision and Postmortem Wear Scars

Wear scars from chair and stair activities were assigned to two clusters. Chair rising, stair ascent and stair descent were assigned to cluster A, which contains 3.7% and 9.5% of revision and postmortem components, respectively. Chair sitting as well as the combined wear scars from chair sitting and rising, stair ascent and descent and chair and stair were assigned to cluster D, which contains 25.9% and 19.0% of revision and postmortem components, respectively. These results seem to indicate that wear scars from chair and stair activities have features which make them more similar to wear scar from revision and retrieved components. Cluster A and D are next to each other and together contain close to one third of the revision and postmortem components. This makes the wear scars from chair and stair activities highly representative of the wear scar patterning observed *in vivo*. Chair and stair activities should therefore be considered for preclinical wear evaluation of TKR prosthesis.

6.2.5.3. Knee Simulator Modifications

Modifications to the knee simulator were successful at increasing the flexion-extension (F-E) range of motion from 60 degrees to 105 degrees. Such modifications were essential in the generation of wear scars from chair and stair activities given that both activities exercise F-E motions of up to 95 degrees. Special attention to testing fixtures and simulator components needs to be given when running a full multi-activity wear test lasting several million activity cycles. The higher loads and motions generated by chair and stair activities will impose higher stresses on the fixtures and simulator components which may fail during testing. Wear testing knee simulators will therefore need to be designed to accommodate more demanding activities of daily living, such as chair and stair.

6.2.6. LIMITATIONS

In this study, only the wear scars from chair and stair activities were investigated. Other activities of relevance to TKR wear, such as deep squatting, cycling and kneeling should be considered as well. The kinematics used to generate the wear testing profiles came from a purposely selected active TKR population and can therefore not be considered representative of the overall TKR population.

The assumption that a multi-activity wear scar can be created simply by overlapping the wear scar of one activity over another is debatable. This study showed that when wear scars from different activities were combined, a concatenated wear scar resulted which was always larger in size. This may not be the case *in vivo,* were the motions generated are not fixed to a specific distance or rotational range, but are rather the resultant of a complex balance of loading between the muscles, soft tissues and the prosthesis geometric features.

6.2.7. CONCLUDING REMARKS

Wear scars from chair and stair activities were successfully generated and analyzed in this investigation. Either on their own or when combined, chair and stair activities generated wear scar features that were different from those generated by standardized ISO testing (based on SOFM clustering). The clustering results of this investigation suggest that chair and stair activities need to be considered when performing preclinical wear evaluation of TKR components. These results however, only cover the contact damage pattern generated by each activity. In order to determine the wear impact each activity has, the loads and motions each activity generates needs to be considered as well. The following section will analyze the wear impact that chair and stair activities have on the TKR tibial component by considering not only the motions and loading the TKR joint undergoes for a given activity, but also the frequency with which each activity is performed by a sampled TKR patient population.

6.3. SPECIFIC AIM 3.3 - *To determine the wear impact of chair and stair activities by means of a wear model*

6.3.1. INTRODUCTION

Explanted total knee replacement (TKR) polyethylene liners have shown wear discrepancies when compared to liners tested *in vitro*, using standardized knee wear testing protocols [37, 83]. Similar findings were obtained with the artificial neural network model (SOFM) developed in section 4, where simulator tested components were clustered isolated from about 90% of retrieved revision and postmortem components [84]. Since current standardized knee wear testing protocols apply motion and load profiles of walking only, the wear scaring differences observed may be the result of omitting other activities of daily living (ADL) of relevance to the TKR joint.

Although walking has been regarded as the most frequent activity throughout the day [8], typically a greater and more complex variety of ADL are performed [75, 85]. Findings from section 5.2 indicated that while walking was the most prevalent activity performed throughout the day, the ratios of walking to other activities, such as chair, stair and stop-and-go motions, were considerably higher than previously reported [12, 14, 75]. Furthermore, the wear scar analysis performed in section 6.2 indicated that chair and stair activities generated wear scars that were different from those generated by standardized ISO testing, and similar to the wear scars found in revision- and postmortem-retrieved components (based on SOFM clustering results). While these findings suggest the need to consider chair and stair activities for preclinical wear testing evaluation, the wear impact of these activities, which is a factor of load, sliding distance and cross-shear motion, remains to be investigated.

6.3.2. PURPOSE

In this study, the potential wear impact from chair and stair activities was investigated and compared with standardized ISO walking. To do this, the axial joint load, sliding distance and cross-shear motion were calculated for each activity. The wear impact comparison was done using two cumulative wear models. The first model incorporated the activity frequency, axial load and sliding distance; while the second model was based on the activity frequency, axial load and cross-shear motion. It was hypothesized that when loading, sliding distance and cross-shear motion are taken into account, a higher proportional daily impact of chair and stair activities to walking will be achieved, than when considering cycle frequency alone.

6.3.3. MATERIALS and METHODS

6.3.3.1. Cumulative Wear Model Parameters

The wear impact generated by chair, stair and ISO walking was investigated using two cumulative wear models. These analytical models were based on the daily frequency, axial load and either the sliding distance (model 1) or the cross-shear motion (model 2) generated by each activity. The TKR activity frequency data collected in section 5.2 (Table 6-7) were readily available, however, the activity sliding distance and cross-shear motion needed to be calculated. This was done using the kinematic (Table 6-8) and kinetic (Table 6-9) data generated in section 5.3. All data came from the same twenty-three TKR patients (9M/14F, 60.8±7.1 years old, 41.8±29.7 months post-op) used in section 5.2. No additional patients were included in this IRB approved study.

Table 6-7: Test day activity frequency for the investigated TKR patient population

Activity counts/occurrences	**Average**	**StDev**	**Min.**	**Max.**	**Walking : ADL**
Normal Walking	2599	1220	222	4888	1:1
Stair Ascent	66	63	0	244	39:1
Stair Descent	139	138	4	554	19:1
Chair Sitting	90	59	6	336	29:1
Chair Rising	90	59	6	336	29:1

Table 6-8: External moments of the TKR joint during chair stair activities.

Activity	**Statistic**	**Ext**	**Flex**	**Add**	**Abd**	**IR**	**ER**
Chair Sitting	Average	-1.17	3.30	-0.64	0.24	-0.27	0.05
	StDev	0.58	0.81	0.45	0.24	0.14	0.05
Chair Rising	Average	-1.24	3.47	-0.80	0.48	-0.20	0.14
	StDev	0.63	1.04	0.46	0.33	0.12	0.11
Stair Ascent	Average	-1.95	3.45	-1.88	1.05	-0.48	0.30
	StDev	0.96	0.88	0.81	0.46	0.26	0.15
Stair Descent	Average	-2.32	3.72	-2.25	0.77	-0.67	0.16
	StDev	1.01	0.91	1.17	0.63	0.27	0.14

Table 6-9: Average A-P, I-E and F-E range of motion for chair sitting and rising, stair ascent and descent and ISO walking [47]

Activity	Range		Average	StDev
Chair Sitting	A-P	(mm)	28.3	14.8
	I-E	(deg)	17.7	9.8
	F-E	(deg)	84.6	11.3
Chair Rising	A-P	(mm)	33.5	19.6
	I-E	(deg)	21.3	13.9
	F-E	(deg)	95.4	13.9
Stair Descent	A-P	(mm)	34.8	21.8
	I-E	(deg)	17.0	8.4
	F-E	(deg)	95.4	13.9
Stair Ascent	A-P	(mm)	35.1	23.4
	I-E	(deg)	15.5	10.1
	F-E	(deg)	71.1	12.6
ISO Walking	A-P	(mm)	4.2	N/A
	I-E	(deg)	7.6	N/A
	F-E	(deg)	58.0	N/A

6.3.3.2. TKR Joint Load

Axial joint loads for the TKR population investigated in this study were calculated by Lundenberg et al. [86]. Axial joint forces were calculated for chair and stair activities using a parametric knee model, which generated a space of possible loading solutions. The method used and the analysis details are provided below.

An in-house developed [87] and validated [88] parametric knee model was used to estimate the amount of internal knee axial load generated during chair sitting and rising and stair ascent and descent. The model employed equilibrium equations to account for unknown muscle activation levels and three-dimensional medial and lateral knee joint contact forces. For equilibrium, external forces and moments acquired during motion analysis were equal to internal forces and moments from muscles, passive structures, and knee joint contact forces. Inputs to the model included the kinematics and kinetics acquired during motion analysis in section 5.3, the path of contact between the tibial and femoral TKR components, and, as a threshold, the maximum possible physiological muscle forces during the activity. For each activity trial (three per patient per activity), the contact paths of the medial and lateral femoral condyles on the tibial insert surface were computed using the knee kinematics and previously developed software [89]. Maximum muscle force magnitudes were calculated in OpenSim 2.26 (NCSSR, Stanford, California) by applying the measured leg kinematics to a modified lower limb musculoskeletal model [90]. The model calculated a solution space of the three dimensional knee reaction forces for each activity trial. The solution space of possible forces resulted from the parametric variation of the activation levels of individual muscles that scaled the maximum physiological muscle forces.

The mean total axial force (F_a, body weight, BW) of the solution space was compared for each activity trial. The average and standard deviation between trials of all subjects was calculated for each activity. Speeds of chair activities were normalized by matching the slope of knee flexion angle profiles for comparison between subjects. Stance phases of stair activities were defined from load-acceptance to load-removal (i.e. load-bearing phase) as measured by the force plate. Axial knee forces from chair and stair activities were compared with axial load suggested by standardized ISO wear testing protocols [47].

6.3.3.3. Sliding Distance

For each activity, the total average sliding distance (d_s) generated by the femur on the tibial prosthetic component as a function of flexion-extension (F-E) motion was calculated using Equation 7-1. Sliding distance was calculated only during the loading phase of the limb. A normalized femoral component size with a radius of 55mm was used for all TKR patients [72].

The sliding distance values generated by chair and stair activities were compared with the sliding distance generated by ISO walking.

$$d_{s,i} = \sum_j \frac{2\pi\, \mathrm{r} \left| \mathrm{F\text{-}E}_{i,j} - \mathrm{F\text{-}E}_{i,j+1} \right|}{360} \qquad \text{[mm]} \qquad \text{Equation 7-1}$$

where d_s= sliding distance (in m), j=percent of load-bearing phase (1 to 100%), i=activity (chair sitting, chair rising, stair ascent, stair descent and ISO walking), r=radius of femoral component (in m) and F-E=flexion-extension value (in deg) at the jth cycle point.

6.3.3.4. Linear Wear Index Model

Wear has been characterized as a function of the applied axial force and sliding distance of the articulating components [91]. In this study, the wear impact of each activity was calculated using a linear wear index model (LWI) previously introduced by Johnson et al. [92]. For each activity, a LWI was estimated for each load-bearing time point (Equation 7-2). This allowed for analysis and comparison of load-bearing regions with high potential for wear. A cumulative linear wear index for the complete activity cycle (CLWI , Equation 7-3) and a daily cumulative linear wear index (DCLWI, Equation 7-4), which took into account the frequency the activity was performed throughout the day, were also calculated. All the linear wear index models implemented in this study were used to assess the relative wear impact of chair and stair activities in comparison to ISO walking.

$$LWI = F_a \cdot d_s \qquad \text{[BW · m, joules, J]} \qquad \text{Equation 7-2}$$

$$CLWI = \int_{load-bearing} F_a \, d_s \qquad \text{[BW · m, J]} \qquad \text{Equation 7-3}$$

$$DCLWI = CLWI \times cycles_{day} \qquad \text{[BW · m, J]} \qquad \text{Equation 7-4}$$

where *LWI* is linear wear index, *CLWI* is the cumulative linear wear index and *DCLWI* is the daily cumulative wear index (in joules, J), F_a=axial force (in BW), d_s = sliding distance (in m). The *CLWI* integral is over the load-bearing phase (1 to 100%).

6.3.3.5. Directional Wear Index Factor

Polyethylene wear has also being characterized as a function of load and cross-shear motion. This is due to the unique structure of conventional polyethylene, where its molecules tend to align in the predominant sliding direction. This preferential molecular alignment results in anisotropic mechanical properties, which strengthens the material in sliding direction and weakens it perpendicular to it. In this study, a directional wear index factor (DWIF), introduced by Laurent et al. [11, 92], was implemented to assess the wear impact of chair and stair activities in comparison to ISO walking. The DWIF was used to assess the wear impact of each activity throughout the load-bearing cycle (Equation 7-5), in order to identify load-bearing regions which may be detrimental to polyethylene wear. A cumulative directional wear index factor for the complete activity cycle (CLWI, Equation 7-6) and a daily cumulative directional wear index factor (DCDWIF, Equation 7-7), which took the frequency of the activity into account, were also calculated. All the directional wear index models implemented in this study were used to assess the relative wear impact of chair and stair activities in comparison to ISO walking.

$$DWIF = F_a \cdot |v_s| \cdot \sin(\alpha)$$ [BW · mm] Equation 7-5

$$CDWIF = \int_{load-bearing} DWIF\,dt$$ [BW · mm] Equation 7-6

$$DCDWIF = CDWIF \times cycles$$ [BW · mm] Equation 7-7

where *DWIF* is directional wear index factor, *CDWIF* is the cumulative directional wear index factor and *DCDWIF* is the daily cumulative wear index factor (in BW · mm/s), F_a=axial force (in BW), $|v_s|$ = sliding velocity magnitude (m/s). The CDWIF integral is over the load-bearing time.

6.3.4. RESULTS

6.3.4.1. TKR Joint Load

The average and standard deviation of the peak axial load from the twenty-three TKR patients evaluated in this study are provided in Figure 6-12 and Table 6-10. In comparison to ISO walking, chair sitting, chair rising and stair ascent generated peak axial loads that were significantly different (p<0.05).

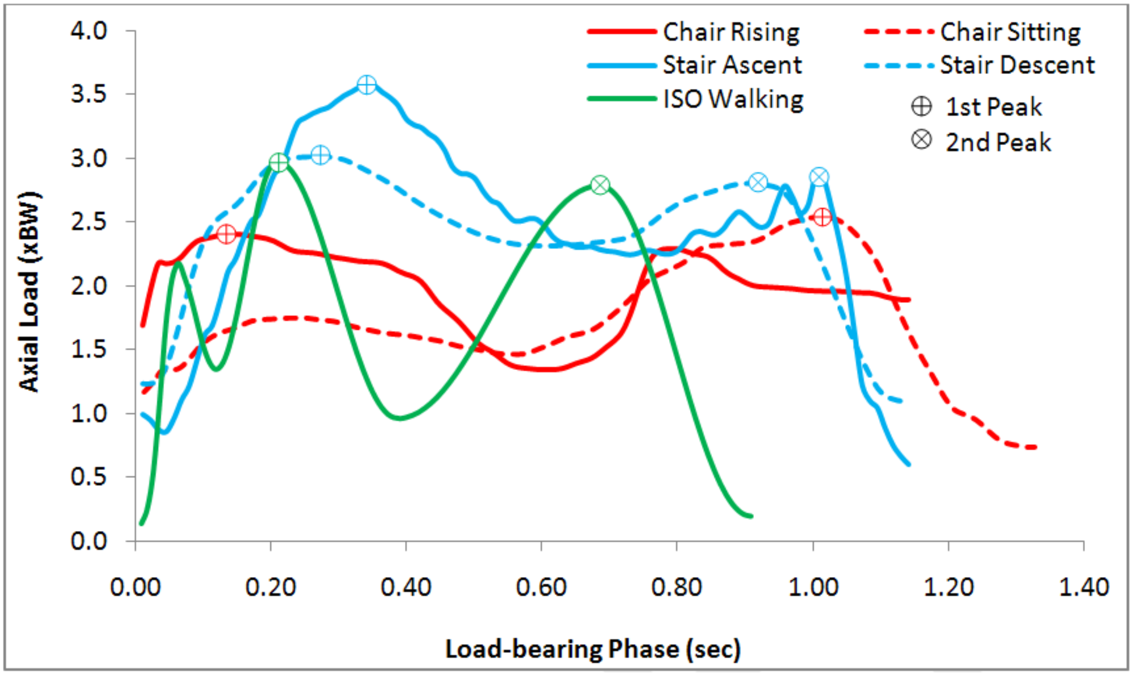

Figure 6-12: Axial load (xBW) for chair, stair and ISO walking activities throughout the activity load-bearing duration (sec).

Table 6-10: Peak axial loads from chair and stair activities (n=23 TKR patients).

Activity	**Peak**	**Load (BW)**		**Duration (s/Hz)**		**Chair and Stair vs. Walking**
		Average	StDev	Average	StDev	*p*-value
Chair Sitting	Main	2.54	0.67	1.3/0.8	0.3/0.01	0.0047
Chair Rising	Main	2.40	0.57	1.1/0.9	0.2/0.1	0.0001
Stair Ascent	1st 2nd	3.58 2.86	0.99 1.14	1.1/0.9	0.2/0.1	0.0082 0.6187
Stair Descent	1st 2nd	3.01 2.80	0.82 0.72	1.1/0.9	0.2/0.1	0.8623 0.2433
ISO Walking	1st 2nd	2.98 2.79	N/A N/A	1.0/1.0	0.1/0.1	N/A N/A

6.3.4.2. Sliding Distance

Chair and stair activities generated sliding distance values that were 1.5 to 1.9 times larger than the sliding distance generated during ISO walking (Table 6-11 and Figure 6-13).

Table 6-11: Max load and sliding distance of chair and stair vs. ISO walking.

Activity	Axial Load (F_a)		Sliding Distance (d_s)		Daily Sliding Distance (d_s)	
	(BW)	%	(m)	%	(m/day)	%
Chair Rising	2.54	85.2%	0.1	169.0%	9.3	5%
Chair Sitting	2.40	80.5%	0.12	190.7%	10.5	6%
Stair Ascent	3.58	120.1%	0.1	164.6%	6.6	4%
Stair Descent	3.01	101.0%	0.09	146.9%	12.5	7%
ISO Walking	2.98	100%	0.06	100%	182.3	100%

Percentages are based on comparison to ISO walking

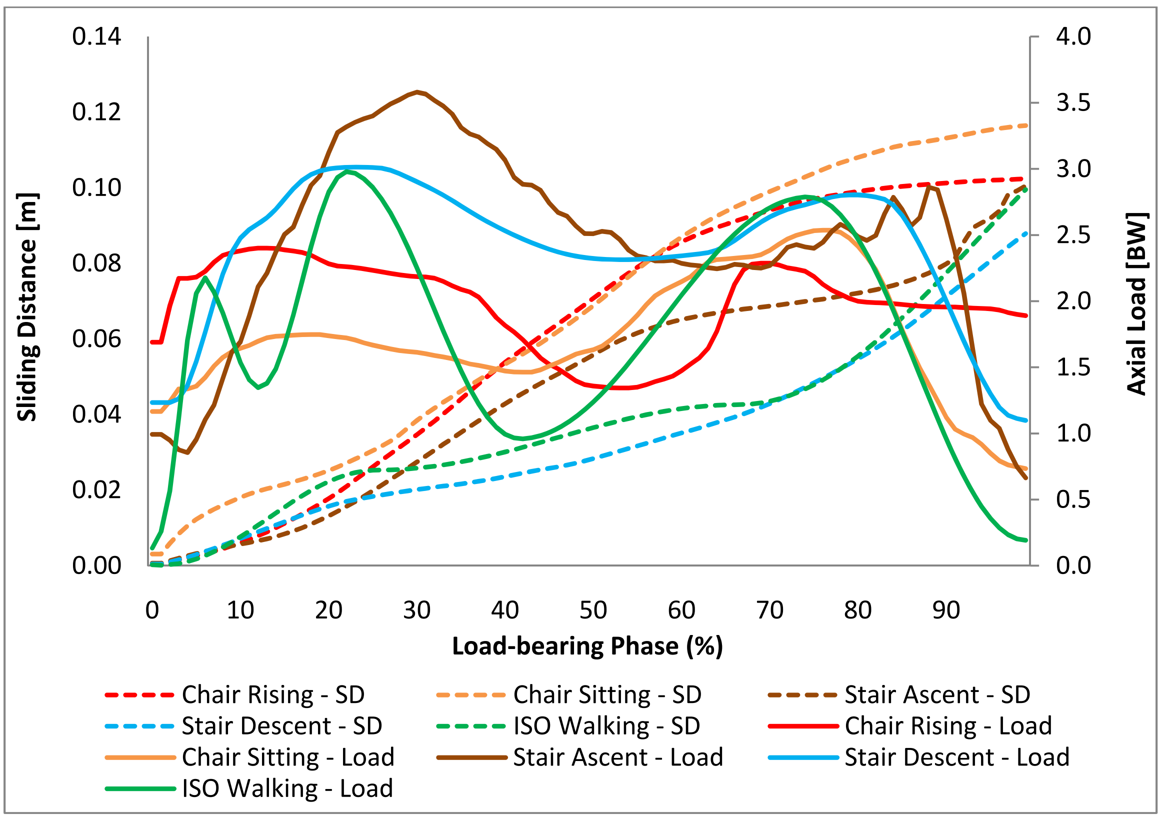

Figure 6-13: Sliding distance (SD) and Axial Load over the load-bearing cycle.

6.3.4.3. Linear Wear Index

Stair ascent was the only activity that generated higher LWI values than ISO walking. Stair descent, chair sitting and rising generated LWI values which were slightly lower than the LWI values generated by ISO walking (Table 6-12 and Figure 6-14). When looking at the cumulative linear wear index (CLWI) of the activity cycle, it was found that both chair and stair activities had a higher wear impact than ISO walking (Table 6-12). When comparing the daily cumulative factors of load and sliding distance vs. cycle frequency alone, the daily contribution from chair and stair activities increased from 13% (frequency only) to 17% (DCLWI) (Figure 6-15).

Table 6-12: Sliding distance and total linear wear index of chair and stair vs. ISO walking.

Activity	**Max LWI**		**CLWI**		**DCLWI**	
	(J)	%	(J)	%	(J)	%
Chair Rising	3.5	97%	167	130%	15,012	5%
Chair Sitting	3.2	89%	173	135%	15,588	5%
Stair Ascent	4.7	131%	202	157%	13,310	4%
Stair Descent	3.6	100%	170	132%	23,574	7%
ISO Walking	3.6	100%	128	100%	404.66	100%

Percentages are based on comparison to ISO walking

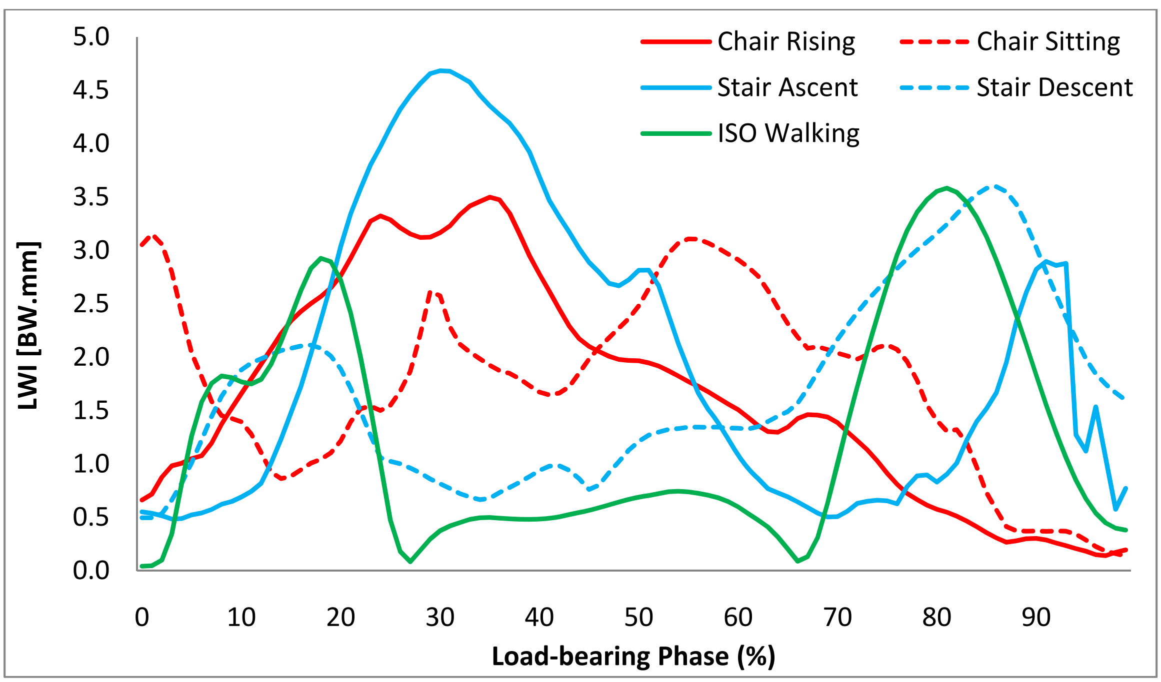

Figure 6-14: Linear wear index (LWI) throughout the load-bearing phase of a chair, stair and ISO walking activities.

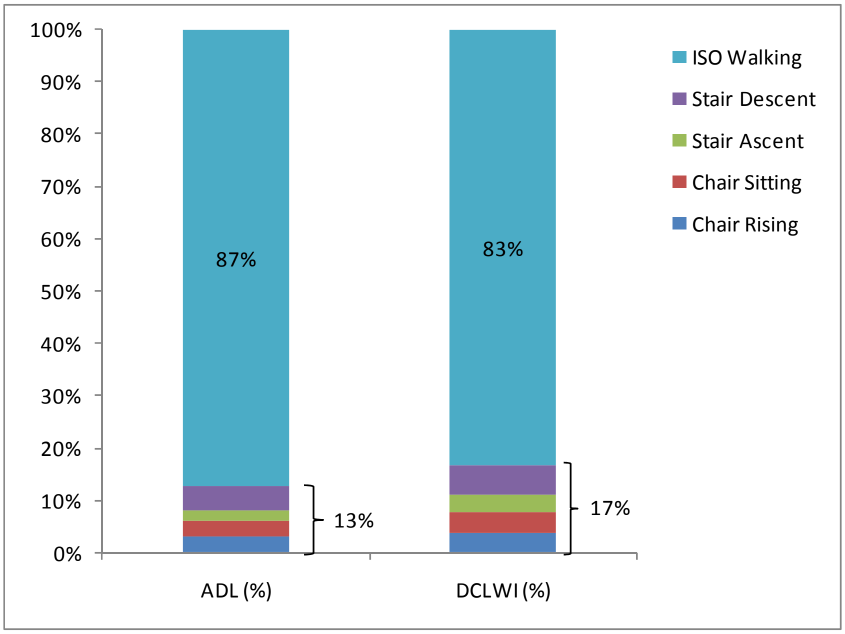

Figure 6-15: Daily proportion of chair, stair and walking maneuvers based on daily activity frequency and DCLWI.

6.3.4.4. Directional Wear Index Factor

Chair and stair activities generated DWIF that were 0.5 to 4.6 times larger than ISO walking; stair ascent generated the largest DWIF Table 6-13 and Figure 6-16). With regards to the cumulative directional wear factor, it was found that the wear impact chair and stair generated was 1.2 to 4.0 times larger than ISO walking (Table 6-13). When comparing the daily cumulative factors of load and cross-shear motion vs. cycle frequency alone, the daily contribution from chair and stair activities increased from 13% (frequency only) to 29% (DCDWIF, Figure 6-17).

Table 6-13: Directional wear index factor for chair and stair vs. ISO walking.

Activity	Max DWIF		CDWIF		DCDWIF	
	(BW·mm)	%	(BW·mm)	%	(BW·mm)	%
Chair Rising	1.8	129%	57.02	343%	5,132	12%
Chair Sitting	1.8	129%	60.76	365%	5,468	13%
Stair Ascent	6.4	457%	66.17	398%	4,367	10%
Stair Descent	0.7	50%	19.94	120%	2,772	6%
ISO Walking	1.4	100%	16.64	100%	43,243	100%

Percentages are based on comparison to ISO walking

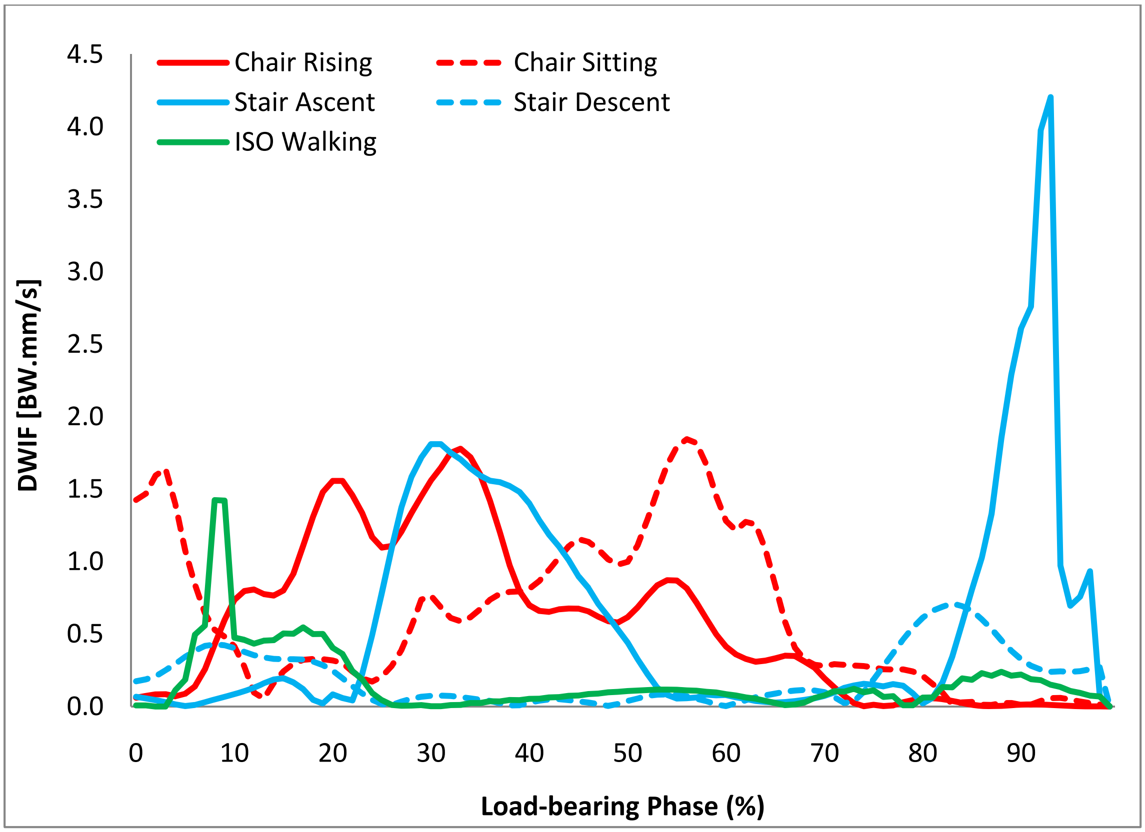

Figure 6-16: Directional wear index factor for chair, stair and ISO walking throughout the load-bearing cycle. The spike exhibited by stair ascent at about 90% of the load-bearing cycle, was cause by the coincidence of the peak load and a high rotational value generated during stair ascent.

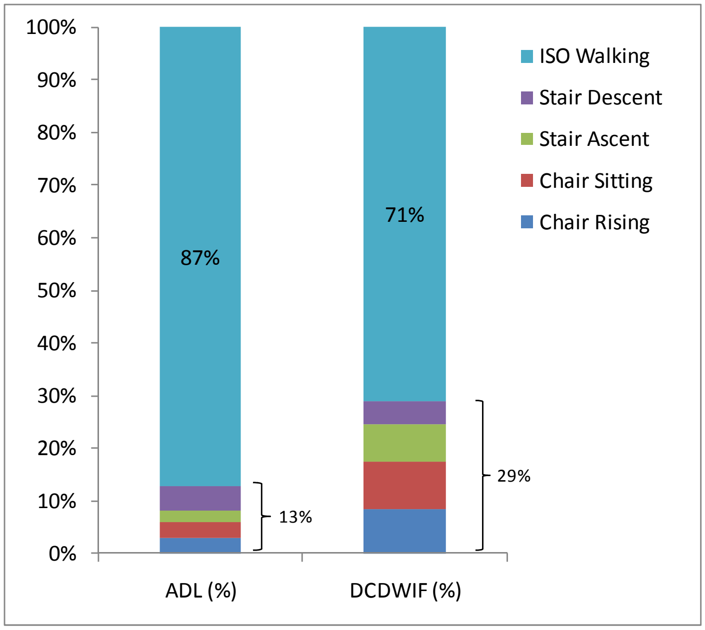

Figure 6-17: Daily proportion of chair, stair and walking maneuvers based on daily activity frequency and DCDWIF.

6.3.5. DISCUSSION

6.3.5.1. The Wear Impact of Load and Motion in TKR Wear

Daily activities other than walking are often overlooked due to their low frequency compared with walking [75]. Indeed, as seen in section 5.2, the relative contribution of chair and stair maneuvers to total ADL is low (13% combined) when only cycle frequency is considered. However, in agreement with our hypothesis, which stated that a higher proportional impact of chair and stair activities to walking will be reached, sliding distance and cross-shear motion are taken into account; it was found that the relevance of chair and stair maneuvers increased from 13% (frequency only) to 17% when load and sliding distance were considered (based on the DCLWI model), and to 29% when load and cross-shear motion were considered (based on DCDWIF model). These results suggest that chair and stair activities could potentially generate up to a third of the wear during the day. When considering the wear effect of load, sliding distance and cross-shear motion, it appears that current standardized wear testing protocols only account for about 70% of the wear that may be generated *in vivo*. Since these results are based on the average load, sliding distance and activity occurrence, there will be TKR patients for which standardized wear testing will account for even less than 70%. Perhaps, a worst case standardized wear testing protocol, which includes not only walking but also other ADL such as chair and stair, will be more clinically relevant as it will make sure TKR patients, which are highly active and engage in a variety of activities, are also covered.

6.3.5.2. Wear Testing Through Mechanical Wear Simulation

Given the great variety of TKR component materials and designs, understanding how the kinematics and kinetics of the TKR joint impact the prosthesis wear, will greatly help discern whether specific TKR components need to be tested or whether a specific wear testing protocol is needed to accommodate the design and needs of the prosthesis. Finite element models (FEA) could be designed to incorporate both liner and directional wear models. FEA wear modeling could considerably speed up and reduce the cost of preclinical wear testing.

Chair and stair activities have been previously evaluated through *in vitro* wear testing [12, 14, 77]. The loads and motions used by these studies, however, were obtained from different independent studies on healthy or TKR individuals with different prosthetic designs; the loads and motions used were not measured on the same TKR population, which is one of the advantages and values this thesis offers. Furthermore, previous studies only considered either stair ascent [12] or stair descent [14] and disregarded chair maneuvers; or included only stair ascent and chair rising, but omitted stair descent and chair sitting [77], pre-clinical wear evaluation should considered all activities with the potential to detrimentally affect the wear performance of the TKR components. Other limitations of the aforementioned studies are that the ratios of chair and stair maneuvers to walking cycles used did not reflect the higher frequency proportion of chair and stair activities that found in section 5.2. A comprehensive *in vitro* wear testing protocol that includes the most relevant activities to the TKR population and that reflects the activity level of the increasingly younger and more active TKR patient population [21] remains to be performed.

6.3.6. LIMITATIONS

This study only investigated the wear impact of chair and stair maneuvers. There are other activities of relevance to TKR, such as gardening (and thus squatting), bicycling, and unclassified stepping maneuvers, with noticeable frequencies that may challenge the wear performance of knee prosthetic devices [73]. All activities of relevance to TKR wear should be considered when creating a multi-activity wear testing protocol. Another limitation of this study is that it was assumed that the implant design did not constraint the imparted motion. Furthermore, the wear models used in this study did not considered the effect of tractive rolling (tangential forces) on wear, which are generated due to slip (creepage) on the contact, or the sliding distance generated by the anterior-posterior motion of the joint.

6.3.7. CONCLUDING REMARKS

In conclusion, the findings from this study suggest that ADL, such as chair and stair, should be included for pre-clinical wear evaluation of TKR polyethylene prosthesis. In addition to chair and stair activities, other ADL of relevant to the TKR joint should also be considered, especially if these activities generate kinematics and kinetics which may result in a significant wear increase, even if their frequency of occurrence is low. While a standardized wear testing protocol cannot cover all possible outcomes, it is important that a pre-clinical wear test is designed so that the worst-case conditions are taken into account. Not all patients will be putting their TKR joint prosthesis through a marathon race, but it should be expected that the contemporary TKR joint allows their hosts to engage in activities that are similar to healthy individuals without joint replacement implants.

7. SUMMARY AND CONCLUSIONS

Total knee replacement (TKR) is a surgical procedure that patients with joint disease or trauma undergo to alleviate pain and increase functional mobility. While there have been several improvements in the materials and designs of TKR [1, 2], wear of the polyethylene tibial insert has remained as one of the leading causes of TKR long-term failure [3-7].

The purpose of this study was to investigate the wear impact from daily physical activities on TKR tibial components. Patient factors such as joint loading, motion and frequency of daily activities and their transitions were investigated with the goal to develop wear testing protocols that are more physiologically relevant and better recreate *in vivo* wear conditions.

Representativeness of Current ISO Standards

In order to compare the contact damage patterns (wear scars) of *in vivo* and *in vitro* worn components, a non-traditional modeling approach was developed for the comparison of wears scar images of simulator-tested and retrieved TKR tibial liners. This model, which has been based on the Self-Organizing Feature Map network (SOFM), was useful in grouping tibial components with similar wear scar features. The clustering results generated by the SOFM network suggested that the wear scars generated by ISO tests, which are based on the application of level walking only, do not fully represent the greater and more variable wear scar characteristics of *in vivo* worn components. Since the wear scar characteristics of the TKR tibial component are substantially influenced by the kinetics and kinematics of the knee joint, the findings of this study suggest that the wear scar variability observed in retrieved components may be the result of the loads and motions of several physical activities.

Identification and Measurement of Physical Activities of Relevance to TKR Wear

Two activity monitoring devices were validated and used to gain more knowledge about frequencies and durations of daily physical activities and their transitions. To do this, TKR patients were recruited and followed throughout the day. Patient activity level (based on step counts) was also investigated for a seven-day time period. Activity monitoring results indicated that, as expected, walking was the dominant activity throughout the day. However, contributions from other activities such as chair sitting/rising, stair ascent/descent and stop-and-go motions were also found. In order to evaluate the significance of the loads and motions generated by chair and stair activities (i.e. the most frequent physical activities other than walking), the external knee moments and internal knee motions of the TKR joint were obtained. The knee moments and motions were then used to calculate knee contact forces using a parametric modeling approach. While their frequencies are lower than walking, chair and stair activities generated knee join motions and loads that were considerable larger and comprised longer period of time. Since polyethylene wear is a factor of sliding distance and cross-shear motion, the potential for wear generated by chair and stair activities appeared to be significant.

The Wear Impact of Chair and Stair Activities

Two previously proposed wear models, based on sliding distance or cross-shear motion, were used to assess the wear impact of different physical activities. These models, in addition to the motion and loading parameters, included also the frequency of the activity that was performed during the day. An *in vitro* methodology to accelerate the creation and assessment of wear scars generated by different physical activities was developed and validated to compare the wear scar characteristics of each physical activity with wear scars on retrieved components generated *in vivo*. Results from the sliding distance and cross-shear wear models indicated that the wear impact of chair and stair activities increased considerably; from 13% to 29%, thus indicating that standardized preclinical wear evaluation currently only accounts for about 70% of the wear generated *in vivo*. Implementing chair ascending/descending and chair rising/sitting into the simulator protocol generated wear scars that were placed more centrally on the feature map when feeding the wear scar images into the neural network. Hence they share similarities with all the components, not just those from a fringe group. The wear scar features produced by chair and stair activities were found to share more similarities with *in vivo* worn components than with those components tested according to ISO.

In conclusion, wear of the TKR tibial component is a multi-factorial and complex process where the implant, the patient and the surgeon all play an important role. The results of this study suggest that patient factors, such as frequency, load and motion from chair and stair activities, need to be considered in standardized wear testing protocols for the pre-clinical wear evaluation of TKR prostheses. Such a multi-activity wear testing protocol may generate wear conditions that better recreate those occurring *in vivo*. In addition to developing a more physiological and demanding pre-clinical wear test, the results of this thesis also speak of the use of crosslinked polyethylene tibial components, as this material has been shown to reduce the amount cross-shear wear.

8. CITED LITERATURE

1. Crowninshield RD, Muratoglu OK, Implant Wear Symposium 2007 Engineering Work Group. How have new sterilization techniques and new forms of polyethylene influenced wear in total joint replacement? J Am Acad Orthop Surg. 2008;16 Suppl 1:S80-5.

2. Kurtz SM, Walker PS, Implant Wear Symposium 2007 Engineering Work Group. How have new designs and new types of joint replacement influenced wear behavior? J Am Acad Orthop Surg. 2008;16 Suppl 1:S107-10.

3. Mulhall KJ, Ghomrawi HM, Scully S, Callaghan JJ, Saleh KJ. Current etiologies and modes of failure in total knee arthroplasty revision. Clin Orthop Relat Res. 2006 May;446:45-50.

4. Naudie DD, Ammeen DJ, Engh GA, Rorabeck CH. Wear and osteolysis around total knee arthroplasty. J Am Acad Orthop Surg. 2007 Jan;15(1):53-64.

5. Sharkey PF, Hozack WJ, Rothman RH, Shastri S, Jacoby SM. Insall award paper. why are total knee arthroplasties failing today? Clin Orthop Relat Res. 2002 Nov;(404)(404):7-13.

6. Swedish knee arthroplasty register. Annual report 2006 - part 2. 2006.

7. Robertsson O, Dunbar MJ, Knutson K, Lewold S, Lidgren L. The swedish knee arthroplasty register. 25 years experience. Bull Hosp Jt Dis. 1999; 58(3):133-8.

8. Seedhom BB, Wallbridge NC. Walking activities and wear of prostheses. Ann Rheum Dis. 1985 Dec;44(12):838-43.

9. Schwenke T, Orozco DA, Schneider E, Wimmer MA. Differences in wear between load and displacement control tested total knee replacements. Wear. 2008.

10. Turell M, Wang A, Bellare A. In: Quantification of the effect of cross-path motion on the wear rate of ultra-high molecular weight polyethylene. International conference on wear of materials No14; 2003;1034-6.

11. Laurent MP, Johnson TS, Yao JQ, Blanchard CR, Crowninshield RD. In vitro lateral versus medial wear of a knee prosthesis. Wear. 2003 0;255(7–12):1101-6.

12. Cottrell JM, Babalola O, Furman BS, Wright TM. Stair ascent kinematics affect UHMWPE wear and damage in total knee replacements. J Biomed Mater Res B Appl Biomater. 2006 Jul;78(1):15-9.

13. Harman MK, Markovich GD, Banks SA, Hodge WA. Wear patterns on tibial plateaus from varus and valgus osteoarthritic knees. Clin Orthop Relat Res. 1998 Jul;(352)(352):149-58.

14. Benson LC, DesJardins JD, Harman MK, LaBerge M. Effect of stair descent loading on ultra-high molecular weight polyethylene wear in a force-controlled knee simulator. Proc Inst Mech Eng [H]. 2002;216(6):409-18.

15. Muratoglu OK, Bragdon CR, O'Connor DO, Perinchief RS, Jasty M, Harris WH. Aggressive wear testing of a cross-linked polyethylene in total knee arthroplasty. Clin Orthop Relat Res. 2002 Nov;(404)(404):89-95.

16. ISO 14243-3:2004. Implants for surgery -- wear of total knee-joint prostheses -- part 3: Loading and displacement parameters for wear-testing machines with displacement control and corresponding environmental conditions for test. ISO G, Switzerland.

17. ISO 14243-1:2009. Implants for surgery -- wear of total knee-joint prostheses -- part 1: Loading and displacement parameters for wear-testing machines with load control and corresponding environmental conditions for test. ISO G, Switzerland.

18. Andriacchi TP, Alexander EJ, Toney MK, Dyrby C, Sum J. A point cluster method for in vivo motion analysis: Applied to a study of knee kinematics. J Biomech Eng. 1998 Dec;120(6):743-9.

19. Lundberg HJ, Foucher KC, Wimmer MA. A parametric approach to numerical modeling of TKR contact forces. Journal of Biomechanics. 2008.

20. Kurtz S, Ong K, Lau E, Mowat F, Halpern M. Projections of primary and revision hip and knee arthroplasty in the united states from 2005 to 2030. J Bone Joint Surg Am. 2007 Apr;89(4):780-5.

21. Crowninshield RD, Rosenberg AG, Sporer SM. Changing demographics of patients with total joint replacement. Clin Orthop Relat Res. 2006 Feb;443:266-72.

22. Harris WH. Wear and periprosthetic osteolysis: The problem. Clin Orthop Relat Res. 2001 Dec;(393)(393):66-70.

23. Gill HS, Waite JC, Short A, Kellett CF, Price AJ, Murray DW. In vivo measurement of volumetric wear of a total knee replacement. Knee. 2006 Aug;13(4):312-7.

24. Beaule PE, Campbell PA, Walker PS, Schmalzried TP, Dorey FJ, Blunn GW, et al. Polyethylene wear characteristics in vivo and in a knee stimulator. J Biomed Mater Res. 2002 Jun 5;60(3):411-9.

25. Kellett CF, Short A, Price A, Gill HS, Murray DW. In vivo measurement of total knee replacement wear. Knee. 2004 Jun;11(3):183-7.

26. Short A, Gill HS, Marks B, Waite JC, Kellett CF, Price AJ, et al. A novel method for in vivo knee prosthesis wear measurement. J Biomech. 2005 Feb;38(2):315-22.

27. Hood RW, Wright TM, Burstein AH. Retrieval analysis of total knee prostheses: A method and its application to 48 total condylar prostheses. J Biomed Mater Res. 1983 Sep;17(5):829-42.

28. Wimmer MA, Kunze J, Orozco DA, Ngai V, Laurent MP, Jacobs JJ. Rare earth tracers to determine backside wear of TKA polyethylene inserts. 54th Annual Meeting of the Orthopaedic Research Society, San Francisco, CA, USA, 2008.

29. Knowlton CB, Hanson G, Orozco DA, Laurent MP, Wimmer MA. Geometric measurement of wear in tibial inserts through an autonomous reconstruction of the original surface. Proceedings of the ASME 2011 Summer Bioengineering Conference (SBC2011) June 2011.

30. Andriacchi TP, Dyrby CO. Interactions between kinematics and loading during walking for the normal and ACL deficient knee. J Biomech. 2005 Feb;38(2):293-8.

31. Wimmer MA, Paul P, Haman J, Schwenke T, Rosenberg AG, Jacobs JJ. In: Differences in damage between revision and postmortem retrieved TKR implant. 51st annual meeting of the orthopaedic research society; 2005; Washington, DC.

32. Harman MK, Banks SA, Hodge WA. Polyethylene damage and knee kinematics after total knee arthroplasty. Clin Orthop Relat Res. 2001 Nov;(392)(392):383-93.

33. Fregly BJ, Sawyer WG, Harman MK, Banks SA. Computational wear prediction of a total knee replacement from in vivo kinematics. J Biomech. 2005 Feb;38(2):305-14.

34. Wimmer MA, Andriacchi TP. Tractive forces during rolling motion of the knee: Implications for wear in total knee replacement. J Biomech. 1997 Feb;30(2):131-7.

35. Wimmer MA, Andriacchi TP, Natarajan RN, Loos J, Karlhuber M, Petermann J, et al. A striated pattern of wear in ultrahigh-molecular-weight polyethylene components of miller-galante total knee arthroplasty. J Arthroplasty. 1998 Jan;13(1):8-16.

36. Benson LC, DesJardins JD, LaBerge M. Effects of in vitro wear of machined and molded UHMWPE tibial inserts on TKR kinematics. J Biomed Mater Res. 2001;58(5):496-504.

37. Harman M, DesJardins J, Banks S, Benson L, LaBerge M, Hodge W. In: Damage patterns on polyethylene inserts after retrieval and after wear simulation. ORS transactions; 2001; San Francisco, California.

38. Bertis E. Mining pixels: The extraction and classification of astronomical sources. ESO Symposia: Mining the Sky. 2001:353-71.

39. Castellani B, Castellani J. Data mining: Qualitative analysis with health informatics data. Qual Health Res. 2003 Sep;13(7):1005-18.

40. Fornells A, Martorell JM, Golobardes E, Garrell JM, Vilasis X. Patterns out of cases using kohonen maps in breast cancer diagnosis. Int J Neural Syst. 2008 Feb;18(1):33-43.

41. Huang J, Shimizu H, Shioya S. Clustering gene expression pattern and extracting relationship in gene network based on artificial neural networks. J Biosci Bioeng. 2003;96(5):421-8.

42. Silver H, Shmoish M. Analysis of cognitive performance in schizophrenia patients and healthy individuals with unsupervised clustering models. Psychiatry Res. 2008 May 30;159(1-2):167-79.

43. Yang ZR, Chou KC. Mining biological data using self-organizing map. J Chem Inf Comput Sci. 2003 Nov-Dec;43(6):1748-53.

44. Glover CJ, Rabow AA, Isgor YG, Shoemaker RH, Covell DG. Data mining of NCI's anticancer screening database reveals mitochondrial complex I inhibitors cytotoxic to leukemia cell lines. Biochem Pharmacol. 2007 Feb 1;73(3):331-40.

45. Yan S, Abidi SS, Artes PH. Analyzing sub-classifications of glaucoma via SOM based clustering of optic nerve images. Stud Health Technol Inform. 2005;116:483-8.

46. Endo M, Ueno M, Tanabe T. A clustering method using hierarchical self-organizing maps. J.VLSI Signal Process.Syst. 2002;32(1/2):105-18.

47. ISO 14243-2:2000. Implants for surgery -- wear of total knee-joint prostheses -- part 2: Methods of measurement. ISO G, Switzerland, editor.

48. Kohonen T. Self-organizing maps. 3rd ed. Berlin ; New York: Springer; 2001.

49. Vesanto J, Alhoniemi E. Clustering of the self-organizing map. Neural Networks, IEEE Transactions on. 2000;11(3):586-600.

50. Haese K. Self-organizing feature maps with self-adjusting learning parameters. IEEE Trans Neural Netw. 1998;9(6):1270-8.

51. Ultsch A, Siemon HP. In: Kohonen’s self organizing feature maps for exploratory data analysis. Proc. of the intl. neural networks conference; Dordrecht. Kluwer Academic Press; 1990. p. 305-8.

52. Ngai V, Wimmer MA. Kinematic evaluation of cruciate-retaining total knee replacement patients during level walking: A comparison with the displacement-controlled ISO standard. J Biomech. 2009.

53. Maffiuletti NA, Gorelick M, Kramers-de Quervain I, Bizzini M, Munzinger JP, Tomasetti S, et al. Concurrent validity and intrasession reliability of the IDEEA accelerometry system for the quantification of spatiotemporal gait parameters. Gait Posture. 2008 Jan;27(1):160-3.

54. Zhang K, Werner P, Sun M, Pi-Sunyer FX, Boozer CN. Measurement of human daily physical activity. Obes Res. 2003 Jan;11(1):33-40.

55. Broglio SP, Ferrara MS, Macciocchi SN, Baumgartner TA, Elliott R. Test-retest reliability of computerized concussion assessment programs. J Athl Train. 2007 Oct-Dec;42(4):509-14.

56. McGraw KO, Wong SP. Forming inferences about some intraclass correlation coefficients. Psychol Methods. 1996;1:30-46.

57. Brazdzionyte J, Macas A. Bland-altman analysis as an alternative approach for statistical evaluation of agreement between two methods for measuring hemodynamics during acute myocardial infarction. Medicina (Kaunas). 2007;43(3):208-14.

58. Hamilton C, Stamey J. Using bland-altman to assess agreement between two medical devices--don't forget the confidence intervals! J Clin Monit Comput. 2007 Dec;21(6):331-3.

59. Myles PS, Cui J. Using the bland-altman method to measure agreement with repeated measures. Br J Anaesth. 2007 Sep;99(3):309-11.

60. Marsh AP, Vance RM, Frederick TL, Hesselmann SA, Rejeski WJ. Objective assessment of activity in older adults at risk for mobility disability. Med Sci Sports Exerc. 2007 Jun;39(6):1020-6.

61. Saremi K, Marehbian J, Yan X, Regnaux JP, Elashoff R, Bussel B, et al. Reliability and validity of bilateral thigh and foot accelerometry measures of walking in healthy and hemiparetic subjects. Neurorehabil Neural Repair. 2006 Jun;20(2):297-305.

62. Mackey AH, Stott NS, Walt SE. Reliability and validity of an activity monitor (IDEEA) in the determination of temporal-spatial gait parameters in individuals with cerebral palsy. Gait Posture. 2008 Nov;28(4):634-9.

63. Karabulut M, Crouter SE, Bassett DR,Jr. Comparison of two waist-mounted and two ankle-mounted electronic pedometers. Eur J Appl Physiol. 2005 Oct;95(4):335-43.

64. Heil DP, Bennett GG, Bond KS, Webster MD, Wolin KY. Influence of activity monitor location and bout duration on free-living physical activity. Res Q Exerc Sport. 2009 Sep;80(3):424-33.

65. Bennett D, Humphreys L, O'Brien S, Kelly C, Orr J, Beverland DE. Activity levels and polyethylene wear of patients 10 years post hip replacement. Clin Biomech (Bristol, Avon). 2008 Jun;23(5):571-6.

66. Thorp LE, Orozco DA, Block JA, Sumner DR, Wimmer MA. Activity levels in healthy older adults: Implications for joint arthroplasty. ISRN Orthopedics. 2012 2012(Article ID 727950).

67. Powell R, Allan JL, Johnston DW, Gao C, Johnston M, Kenardy J, et al. Activity and affect: Repeated within-participant assessment in people after joint replacement surgery. Rehabil Psychol. 2009 Feb;54(1):83-90.

68. Tudor-Locke C, Hatano Y, Pangrazi RP, Kang M. Revisiting "how many steps are enough?". Med Sci Sports Exerc. 2008 Jul;40(7 Suppl):S537-43.

69. Barink M, De Waal Malefijt M, Celada P, Vena P, Van Kampen A, Verdonschot N. A mechanical comparison of high-flexion and conventional total knee arthroplasty. Proc Inst Mech Eng [H]. 2008 Apr;222(3):297-307.

70. Mundermann A, Dyrby CO, D'Lima DD, Colwell CW,Jr, Andriacchi TP. In vivo knee loading characteristics during activities of daily living as measured by an instrumented total knee replacement. J Orthop Res. 2008 Sep;26(9):1167-72.

71. D'Lima DD, Steklov N, Patil S, Colwell CW,Jr. The mark coventry award: In vivo knee forces during recreation and exercise after knee arthroplasty. Clin Orthop Relat Res. 2008 Jun 19.

72. Wimmer MA, Haenni M, DeWilde P, Kehl T, Murlock MM. Joint motion and daily activity profile of the knee patients in comparison with the ISO knee wear simulator. ORS, 48th Annual Meeting, Dallas, TX, USA. 2002.

73. Weiss JM, Noble PC, Conditt MA, Kohl HW, Roberts S, Cook KF, et al. What functional activities are important to patients with knee replacements? Clin Orthop Relat Res. 2002 Nov;(404)(404):172-88.

74. Nechtow W. A daily activity profile of american total knee replacement patients [dissertation]. Chicago, IL, USA: University of Illinois at Chicago; 2004.

75. Morlock M, Schneider E, Bluhm A, Vollmer M, Bergmann G, Muller V, et al. Duration and frequency of every day activities in total hip patients. J Biomech. 2001 Jul;34(7):873-81.

76. Lonner JH, Lotke PA. Aseptic complications after total knee arthroplasty. J Am Acad Orthop Surg. 1999 Sep-Oct;7(5):311-24.

77. Popoola OO, Yao JQ, Johnson TS, Blanchard CR. Wear, delamination, and fatigue resistance of melt-annealed highly crosslinked UHMWPE cruciate-retaining knee inserts under activities of daily living. J Orthop Res. 2010 Sep;28(9):1120-6.

78. Sehatzadeh S, Kaulback K, Levin L. Metal-on-metal hip resurfacing arthroplasty: An analysis of safety and revision rates. Ont Health Technol Assess Ser. 2012;12(19):1-63.

79. Liao Y, Hoffman E, Wimmer M, Fischer A, Jacobs J, Marks L. CoCrMo metal-on-metal hip replacements. Phys Chem Chem Phys. 2012 Nov 30.

80. Klous M, Muller E, Schwameder H. Three-dimensional knee joint loading in alpine skiing: A comparison between a carved and a skidded turn. J Appl Biomech. 2012 May 10.

81. Mont MA, Marker DR, Seyler TM, Jones LC, Kolisek FR, Hungerford DS. High-impact sports after total knee arthroplasty. J Arthroplasty. 2008 Sep;23(6 Suppl 1):80-4.

82. Kuster MS. Exercise recommendations after total joint replacement: A review of the current literature and proposal of scientifically based guidelines. Sports Med. 2002;32(7):433-45.

83. Harman MK, DesJardins J, Benson L, Banks SA, LaBerge M, Hodge WA. Comparison of polyethylene tibial insert damage from in vivo function and in vitro wear simulation. J Orthop Res. 2009 Apr;27(4):540-8.

84. Orozco DA, Schwenke T, Wimmer MA. In: Wear scar similarities of retrieved and simulator tested tibial plateaus - an artificial neural network approach. 30th annual meeting and exposition, society for biomaterials; 2005; Memphis, Tennessee, USA. ; 2005.

85. Orozco DA, Briggs AL, Ngai V, Wimmer MA. In: Occurrence of daily activity transitions in an active TKR population. Transactions vol.33, san francisco, CA, 2008.

86. Lundberg HJ, Knowlton CB, Orozco DA, Wimmer MA. Calculated axial forces at the knee in total knee replacement patients during chair and stair activities. Proceedings of the ASME Summer Bioengineering Conference. 2012.

87. Lundberg HJ, Foucher KC, Wimmer MA. A parametric approach to numerical modeling of TKR contact forces. J Biomech. 2009 Mar 11;42(4):541-5.

88. Lundberg HJ, Foucher KC, Andriacchi TP, Wimmer MA. Direct comparison of measured and calculated total knee replacement force envelopes during walking in the presence of normal and abnormal gait patterns. J Biomech. 2012 Apr 5;45(6):990-6.

89. Swanson AJ, Wimmer MA. In vivo methods for locating the tibio-femoral contact pathway in total knee replacements during gait. Proc ASME Summer Bioengineering Conference. 2007.

90. Delp SL, Loan JP, Hoy MG, Zajac FE, Topp EL, Rosen JM. An interactive graphics-based model of the lower extremity to study orthopaedic surgical procedures. IEEE Trans Biomed Eng. 1990 Aug;37(8):757-67.

91. Hutchings IM. Tribology: Friction and wear of engineering materials. London: Edward Arnold; 1992.

92. Johnson TS, Laurent MP, Yao JQ, Gilbertson LN. The effect of displacement control input parameters on tibiofemoral prosthetic knee wear. Wear. 2001 10;250(1–12):222-6.

9. APPENDICES

Appendix 1-I
Wear scar images assigned to all clusters. ‘R’ is for revision retrieved components, ‘P’ for postmortem and ‘S’ for simulator components.

Cluster ‘A’: 2 revision and 2 postmortem components

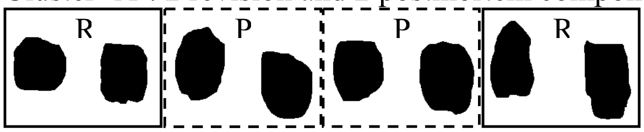

Cluster ‘B’: 6 revision and 2 postmortem components

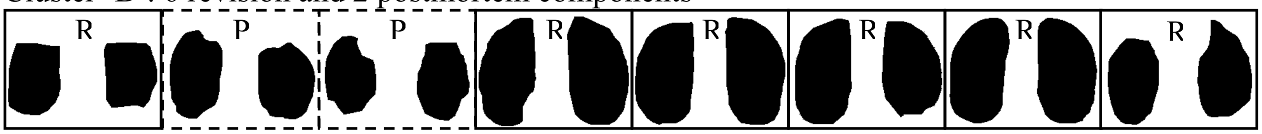

Cluster ‘C’: 12 revision and 3 postmortem components

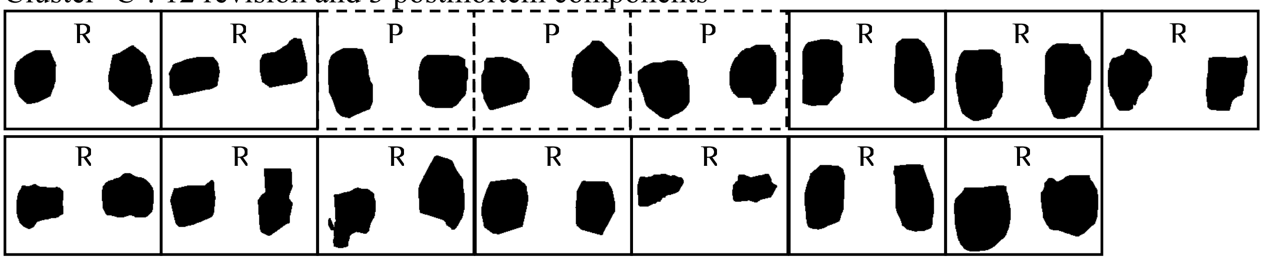

Cluster ‘D’: 14 revisions and 4 postmortem components

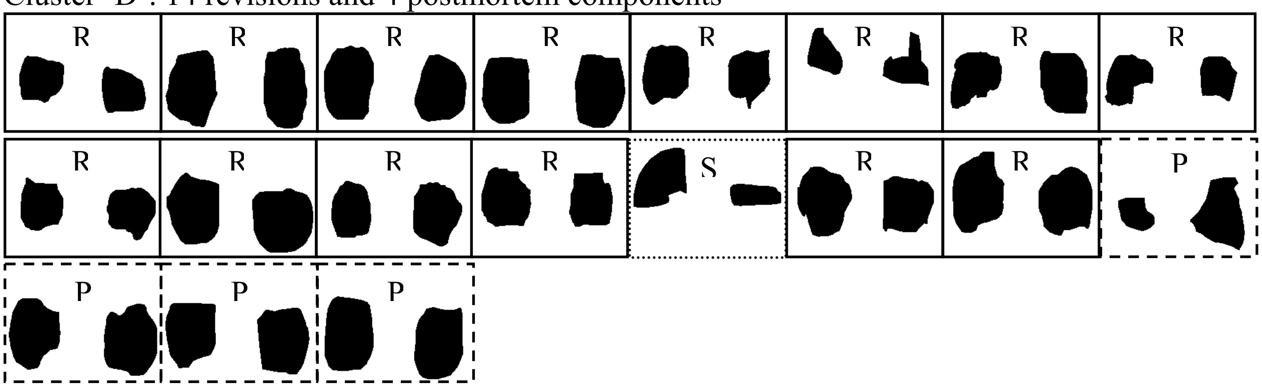

Cluster ‘E’: 8 revision and 2 postmortem components

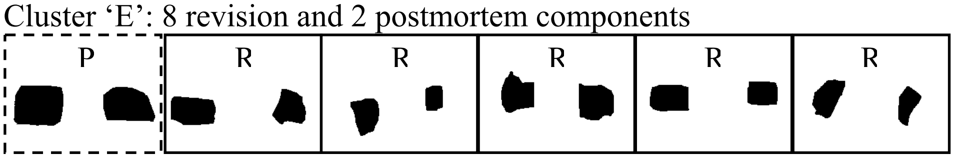

Cluster ‘F’: 0 revision and 2 postmortem components

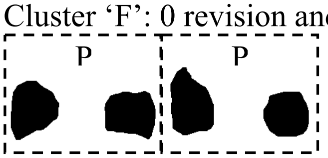

Cluster ‘G’: 6 revision, 3 postmortem and 5 simulator components

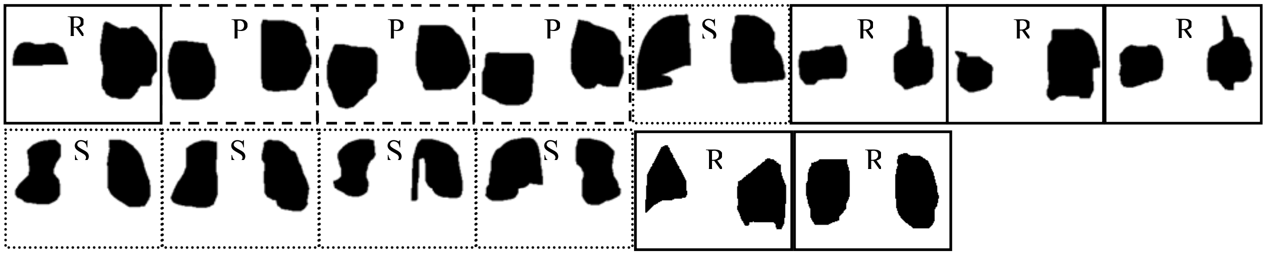

Cluster ‘H’: 0 revision and 1 postmortem component

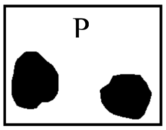

Cluster ‘I’: 1 revision and 1 postmortem components

Cluster ‘J’: 8 revision and 1 postmortem component

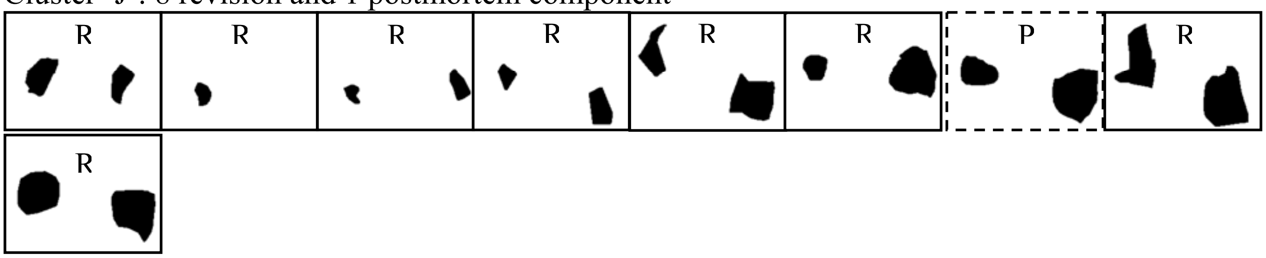

Cluster ‘K’: 1 postmortem component

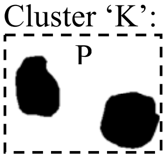

Appendix 1-II

Summary of geometric parameters for retrieved and simulator component

	Parameter	Revision (N=54) Average	St-Dev	COV	Postmortem (N=21) Average	St-Dev	COV	Simulator (N=6) Average	St-Dev	COV
LATERAL	AP Stretch (mm)	23.5	8.8	0.4	24.0	5.0	0.2	21.4	6.6	0.3
	Area (mm^2)	438.7	250.9	0.6	480.9	133.5	0.3	325.3	104.0	0.3
	Centroid X (mm)	21.7	4.0	0.2	22.3	1.4	0.1	18.7	1.5	0.1
	Centroid Y (mm)	18.8	5.2	0.3	18.1	3.9	0.2	27.4	1.4	0.1
	M Inertia X (mm^4)	191885.6	145536.7	0.8	178309.6	105400.7	0.6	245767.1	87422.7	0.4
	M Inertia Y (mm^4)	236159.5	155929.9	0.7	261875.3	100905.4	0.4	122882.7	38609.8	0.3
	ML Stretch (mm)	23.1	6.6	0.3	24.9	3.1	0.1	20.7	1.9	0.1
	Perimeter (mm)	78.1	23.5	0.3	81.4	11.2	0.1	73.2	10.3	0.1
	Roundness $^+$	1.2	0.3	0.2	1.1	0.1	0.1	1.4	0.1	0.1
	Roundness factor $^+$	3.4	0.6	0.2	3.3	0.1	0.0	3.7	0.2	0.0
	Shape Factor $^+$	0.8	0.2	0.2	0.9	0.0	0.1	0.7	0.1	0.1
MEDIAL	AP Stretch (mm)	21.8	8.5	0.4	24.2	5.2	0.2	24.7	2.2	0.1
	Area (mm^2)	383.6	239.2	0.6	459.5	135.7	0.3	398.8	39.3	0.1
	Centroid X (mm)	-22.3	2.4	-0.1	-22.1	2.0	-0.1	-18.9	1.1	-0.1
	Centroid Y (mm)	19.8	3.6	0.2	18.0	4.1	0.2	26.4	2.3	0.1
	M Inertia X (mm^4)	174903.2	121809.6	0.7	194929.9	102667.4	0.5	315654.5	30448.0	0.1
	M Inertia Y (mm^4)	215727.0	148446.4	0.7	254901.5	99129.2	0.4	154635.0	35637.4	0.2
	ML Stretch (mm)	21.8	5.9	0.3	23.9	3.5	0.1	22.2	2.0	0.1
	Perimeter (mm)	73.6	21.8	0.3	79.8	12.4	0.2	85.2	12.2	0.1
	Roundness $^+$	1.3	0.2	0.2	1.1	0.1	0.0	1.5	0.5	0.3
	Roundness factor $^+$	3.5	0.3	0.1	3.3	0.1	0.0	3.8	0.5	0.1
	Shape Factor $^+$	0.8	0.1	0.1	0.9	0.0	0.0	0.7	0.2	0.2

Appendix 2-I

Full wave forms for chair sitting, chair rising, stair ascent, stair descent and squatting. Values are average and standard errors of the mean (SE).

Chair Sitting						
Load Bearing %	**F-E**	**F-E SE**	**A-P**	**A-P SE**	**I-E**	**I-E SE**
1	16.80	2.63	-9.74	2.03	-2.71	1.07
3	10.77	2.32	-12.06	2.25	-3.23	1.16
5	6.25	2.07	-13.44	2.38	-3.85	1.27
7	3.37	1.96	-14.00	2.46	-4.47	1.36
9	1.54	1.94	-14.27	2.53	-4.97	1.38
11	0.37	1.99	-14.36	2.54	-5.36	1.34
13	0.00	2.13	-14.13	2.51	-5.64	1.28
15	0.40	2.26	-13.81	2.45	-5.66	1.21
19	2.35	2.48	-13.59	2.45	-5.06	1.16
21	3.59	2.63	-13.45	2.50	-4.72	1.16
23	4.96	2.83	-13.15	2.53	-4.46	1.19
25	6.52	3.02	-12.60	2.52	-4.30	1.21
27	8.36	3.21	-11.82	2.48	-4.17	1.22
29	10.52	3.40	-10.84	2.44	-3.96	1.23
31	12.95	3.60	-9.76	2.35	-3.67	1.23
33	15.59	3.79	-8.67	2.20	-3.34	1.23
35	18.34	3.99	-7.60	1.99	-3.02	1.21
37	21.16	4.19	-6.68	1.83	-2.66	1.15
39	24.09	4.38	-5.87	1.76	-2.21	1.07
41	27.18	4.53	-5.00	1.72	-1.72	1.03
43	30.41	4.65	-3.96	1.69	-1.16	1.01
45	33.77	4.73	-2.99	1.66	-0.52	0.99
47	37.22	4.78	-2.12	1.57	0.14	1.00
49	40.71	4.80	-1.29	1.44	0.72	1.02
51	44.20	4.78	-0.52	1.40	1.19	1.06
55	50.98	4.62	0.43	1.33	2.19	1.19
57	54.12	4.51	0.36	1.26	2.82	1.28
59	57.11	4.39	-0.01	1.34	3.48	1.36
61	60.03	4.27	-0.43	1.54	4.06	1.46
63	62.89	4.15	-0.72	1.76	4.54	1.57
65	65.61	4.07	-1.06	1.93	5.07	1.67
67	68.09	3.99	-1.54	2.04	5.51	1.75
69	70.31	3.87	-2.02	2.15	5.76	1.81
71	72.32	3.72	-2.50	2.28	5.93	1.88
73	74.23	3.58	-3.03	2.42	6.09	1.95
75	76.11	3.47	-3.58	2.56	6.24	2.01
77	77.90	3.38	-4.28	2.70	6.39	2.05
79	79.55	3.30	-5.25	2.85	6.53	2.09
81	81.00	3.23	-6.48	3.02	6.69	2.13
83	82.20	3.18	-7.70	3.18	6.84	2.18
85	83.13	3.13	-8.66	3.29	6.88	2.21
87	83.83	3.07	-9.41	3.36	6.84	2.23
89	84.31	3.01	-10.10	3.45	6.85	2.24
91	84.58	2.96	-10.74	3.56	6.92	2.25
93	84.55	2.92	-11.20	3.63	6.91	2.24
95	84.25	2.88	-11.47	3.63	6.77	2.21
97	83.93	2.85	-11.74	3.61	6.59	2.16
99	83.75	2.83	-12.13	3.61	6.44	2.12

Chair Rising						
Load Bearing %	**F-E**	**F-E SE**	**A-P**	**A-P SE**	**I-E**	**I-E SE**
1	96.00	2.92	-14.33	6.95	9.23	2.59
3	96.11	3.01	-14.40	6.98	9.12	2.54
5	95.87	3.09	-14.15	6.99	9.02	2.48
7	95.16	3.14	-13.60	6.98	8.93	2.44
9	94.01	3.15	-12.79	6.95	8.74	2.45
11	92.49	3.15	-11.77	6.92	8.35	2.48
13	90.59	3.20	-10.59	6.88	7.86	2.51
15	88.33	3.31	-9.40	6.83	7.43	2.48
17	85.76	3.52	-8.30	6.78	7.05	2.41
19	82.96	3.79	-7.40	6.75	6.60	2.35
21	79.95	4.11	-6.64	6.73	6.01	2.31
23	76.73	4.43	-5.98	6.74	5.41	2.28
25	73.31	4.75	-5.51	6.74	4.93	2.22
27	69.72	5.05	-5.33	6.74	4.55	2.15
29	66.04	5.31	-5.36	6.75	4.15	2.08
31	62.31	5.50	-5.47	6.74	3.66	2.03
33	58.55	5.61	-5.70	6.70	3.11	1.96
35	54.77	5.66	-6.13	6.64	2.53	1.85
37	50.98	5.68	-6.85	6.58	2.01	1.74
39	47.24	5.68	-7.93	6.54	1.59	1.63
41	43.62	5.66	-9.29	6.50	1.28	1.55
43	40.16	5.60	-10.73	6.44	1.00	1.48
45	36.86	5.51	-12.12	6.38	0.70	1.42
47	33.68	5.39	-13.40	6.31	0.36	1.35
49	30.60	5.26	-14.67	6.25	0.02	1.27
51	27.63	5.14	-15.91	6.19	-0.31	1.23
53	24.80	5.01	-17.14	6.13	-0.67	1.24
55	22.15	4.89	-18.31	6.07	-1.14	1.27
57	19.70	4.75	-19.33	6.04	-1.68	1.28
59	17.49	4.59	-20.15	6.02	-2.18	1.26
61	15.57	4.42	-20.75	6.00	-2.56	1.23
63	13.92	4.24	-21.12	5.98	-2.86	1.20
65	12.51	4.05	-21.37	5.96	-3.13	1.20
67	11.28	3.86	-21.63	5.93	-3.41	1.22
69	10.21	3.68	-21.91	5.91	-3.69	1.25
71	9.31	3.52	-22.17	5.89	-3.91	1.28
73	8.57	3.37	-22.31	5.87	-4.04	1.29
75	7.95	3.23	-22.37	5.86	-4.08	1.28
77	7.38	3.08	-22.43	5.85	-4.08	1.29
79	6.83	2.93	-22.55	5.83	-4.08	1.30
81	6.33	2.80	-22.72	5.81	-4.14	1.32
83	5.89	2.67	-22.82	5.80	-4.25	1.33
85	5.52	2.57	-22.89	5.80	-4.36	1.35
87	5.21	2.47	-22.91	5.80	-4.41	1.36
89	4.95	2.39	-22.92	5.80	-4.42	1.36
91	4.72	2.31	-22.91	5.80	-4.45	1.36
93	4.52	2.24	-22.87	5.81	-4.50	1.36
95	4.36	2.17	-22.79	5.81	-4.55	1.36
97	4.25	2.10	-22.80	5.81	-4.59	1.35
99	4.17	2.04	-22.83	5.81	-4.59	1.35

Stair Ascent						
Load Bearing %	F-E	F-E SE	A-P	A-P SE	I-E	I-E SE
1	66.33	2.20	25.07	2.95	9.41	1.68
3	67.46	2.33	24.16	3.04	9.54	1.73
5	68.58	2.47	23.21	3.11	9.61	1.78
7	69.47	2.58	22.44	3.13	9.64	1.82
9	69.99	2.69	21.87	3.10	9.59	1.83
11	70.09	2.81	21.49	3.04	9.49	1.83
13	69.73	2.94	21.21	2.96	9.33	1.81
15	68.87	3.05	20.96	2.88	9.15	1.77
17	67.50	3.11	20.72	2.78	8.99	1.71
19	65.70	3.12	20.44	2.68	8.90	1.64
21	63.56	3.10	20.18	2.57	8.90	1.55
23	61.17	3.07	19.97	2.47	8.92	1.45
25	58.58	3.02	19.91	2.39	8.88	1.34
27	55.83	2.96	19.94	2.31	8.71	1.24
29	52.95	2.87	20.08	2.22	8.40	1.15
31	50.01	2.77	20.31	2.14	8.00	1.08
33	47.05	2.65	20.50	2.07	7.58	1.02
35	44.11	2.52	20.58	2.02	7.16	0.96
37	41.18	2.38	20.51	1.98	6.76	0.89
39	38.29	2.23	20.27	1.91	6.36	0.82
41	35.46	2.06	19.95	1.83	5.95	0.74
43	32.74	1.91	19.62	1.74	5.54	0.67
45	30.16	1.79	19.30	1.68	5.15	0.62
47	27.71	1.69	19.03	1.63	4.80	0.59
49	25.39	1.60	18.69	1.61	4.50	0.56
51	23.15	1.48	18.25	1.60	4.27	0.54
53	21.00	1.35	17.69	1.59	4.12	0.52
55	19.00	1.23	16.97	1.58	4.04	0.51
57	17.21	1.12	16.16	1.52	4.00	0.49
59	15.66	1.02	15.36	1.42	3.96	0.47
61	14.37	0.93	14.64	1.33	3.89	0.46
63	13.34	0.86	14.08	1.28	3.82	0.47
65	12.61	0.82	13.77	1.28	3.75	0.49
67	12.18	0.82	13.61	1.35	3.71	0.52
69	11.99	0.85	13.58	1.44	3.65	0.56
71	11.95	0.90	13.59	1.52	3.54	0.58
73	11.94	0.97	13.56	1.56	3.36	0.58
75	11.90	1.03	13.39	1.56	3.12	0.58
77	11.79	1.09	13.13	1.54	2.86	0.59
79	11.60	1.14	12.76	1.52	2.63	0.62
81	11.31	1.19	12.36	1.54	2.49	0.66
83	10.88	1.22	11.90	1.59	2.51	0.70
85	10.24	1.23	11.32	1.67	2.76	0.74
87	9.29	1.22	10.55	1.73	3.27	0.77
89	7.91	1.16	9.51	1.76	4.01	0.79
91	6.05	1.01	8.18	1.76	4.91	0.81
93	3.88	0.74	6.70	1.76	5.88	0.82
95	1.86	0.40	5.38	1.77	6.82	0.85
97	0.65	0.13	4.60	1.80	7.55	0.92
99	0.95	0.31	4.72	1.81	7.96	1.01

Stair Descent						
Load Bearing %	**F-E**	**F-E SE**	**A-P**	**A-P SE**	**I-E**	**I-E SE**
1	0.01	0.03	4.73	1.60	6.42	0.93
3	0.75	0.19	4.80	1.60	6.02	0.88
5	1.76	0.41	5.19	1.59	5.58	0.83
7	3.00	0.65	5.83	1.60	5.17	0.77
9	4.40	0.88	6.66	1.64	4.82	0.71
11	5.86	1.07	7.61	1.68	4.54	0.65
13	7.32	1.21	8.57	1.70	4.31	0.60
15	8.70	1.30	9.49	1.68	4.11	0.56
17	9.95	1.35	10.36	1.62	3.94	0.53
19	11.02	1.37	11.17	1.53	3.77	0.51
21	11.90	1.39	11.86	1.44	3.61	0.50
23	12.58	1.40	12.46	1.36	3.47	0.49
25	13.09	1.42	12.93	1.31	3.38	0.50
27	13.44	1.45	13.28	1.30	3.35	0.50
29	13.66	1.48	13.42	1.29	3.37	0.51
31	13.80	1.51	13.42	1.29	3.45	0.53
33	13.90	1.53	13.29	1.31	3.55	0.54
35	13.99	1.56	13.06	1.33	3.66	0.56
37	14.10	1.58	12.77	1.38	3.74	0.57
39	14.26	1.61	12.51	1.44	3.79	0.58
41	14.49	1.64	12.29	1.49	3.79	0.59
43	14.80	1.67	12.19	1.52	3.75	0.59
45	15.20	1.70	12.21	1.55	3.69	0.57
47	15.72	1.73	12.36	1.60	3.64	0.56
49	16.34	1.77	12.63	1.68	3.61	0.54
51	17.06	1.82	12.93	1.79	3.61	0.52
53	17.89	1.88	13.23	1.94	3.66	0.51
55	18.81	1.94	13.48	2.10	3.72	0.51
57	19.80	2.00	13.65	2.27	3.79	0.50
59	20.86	2.06	13.77	2.42	3.84	0.50
61	21.98	2.12	13.85	2.54	3.86	0.48
63	23.15	2.16	13.90	2.62	3.85	0.47
65	24.36	2.20	13.92	2.68	3.81	0.46
67	25.63	2.23	13.98	2.72	3.74	0.46
69	26.94	2.27	14.03	2.76	3.67	0.47
71	28.29	2.31	14.07	2.81	3.61	0.48
73	29.70	2.36	14.07	2.89	3.56	0.51
75	31.17	2.42	14.03	2.99	3.57	0.54
77	32.71	2.49	13.92	3.11	3.63	0.59
79	34.35	2.56	13.75	3.21	3.75	0.63
81	36.12	2.62	13.52	3.28	3.93	0.67
83	38.04	2.67	13.33	3.30	4.15	0.71
85	40.18	2.70	13.27	3.30	4.38	0.76
87	42.57	2.73	13.47	3.29	4.59	0.81
89	45.24	2.73	14.03	3.34	4.76	0.86
91	48.20	2.73	14.98	3.46	4.89	0.92
93	51.39	2.72	16.26	3.66	5.00	0.98
95	54.72	2.71	17.68	3.90	5.11	1.05
97	58.06	2.70	19.03	4.13	5.23	1.12
99	61.23	2.66	20.12	4.31	5.38	1.20

Squatting						
Load Bearing %	**F-E**	**F-E SE**	**A-P**	**A-P SE**	**I-E**	**I-E SE**
1	18.58	1.93	9.52	2.20	1.20	1.00
3	12.43	0.37	7.05	2.26	1.50	0.96
5	8.96	0.59	6.70	3.04	1.62	0.87
7	6.47	0.65	6.22	2.29	1.65	0.81
9	4.22	0.17	5.06	0.30	1.71	0.79
11	2.71	0.15	4.74	1.00	1.80	0.72
13	2.03	0.16	5.10	1.14	1.86	0.65
15	1.53	0.22	5.04	1.48	1.90	0.63
17	1.03	0.32	4.49	2.42	1.93	0.60
19	0.84	0.25	4.58	2.84	1.96	0.54
21	0.86	0.15	5.03	2.22	2.01	0.51
23	0.83	0.17	4.86	1.68	2.08	0.51
25	0.91	0.15	4.33	1.81	2.12	0.51
27	1.31	0.10	4.04	2.19	2.12	0.49
29	1.68	0.55	3.70	2.07	2.13	0.51
31	1.80	1.13	3.09	1.58	2.15	0.54
33	2.16	1.88	2.91	0.97	2.15	0.55
35	3.09	2.82	3.59	0.24	2.09	0.58
37	4.24	3.78	4.36	0.65	2.00	0.65
39	5.27	4.64	4.62	1.50	2.00	0.68
41	6.30	5.36	4.76	1.90	2.07	0.61
43	7.46	5.87	4.87	2.29	2.09	0.60
45	8.77	6.15	4.50	2.59	2.06	0.63
47	10.42	6.19	4.43	2.48	2.05	0.68
49	12.72	6.01	5.27	2.17	2.07	0.71
51	15.74	5.59	6.22	1.91	2.11	0.75
53	19.48	4.84	6.87	1.84	2.12	0.83
55	24.15	3.71	8.51	1.26	2.14	0.90
57	29.88	2.33	11.67	0.13	2.15	0.91
59	36.27	1.02	14.64	1.32	2.08	0.88
61	42.85	0.02	16.69	2.74	1.92	0.84
63	49.35	0.75	19.08	3.17	1.78	0.73
65	55.58	1.24	22.03	2.83	1.72	0.49
67	61.27	1.66	24.17	2.90	1.67	0.24
69	66.30	2.15	25.08	3.66	1.49	0.15
71	70.73	2.79	25.34	4.37	1.27	0.15
73	74.62	3.47	25.57	4.24	1.14	0.03
75	77.91	4.03	25.55	3.58	1.07	0.22
77	80.55	4.36	25.01	3.28	0.97	0.40
79	82.54	4.50	24.22	3.39	0.82	0.44
81	84.02	4.53	23.63	3.23	0.71	0.48
83	85.11	4.41	23.16	3.03	0.67	0.55
85	85.80	4.14	22.91	3.23	0.64	0.58
87	86.10	3.87	23.08	3.47	0.60	0.53
89	86.18	3.69	23.63	3.34	0.59	0.47
91	86.24	3.52	23.92	3.17	0.61	0.45
93	86.29	3.30	23.87	3.45	0.64	0.44
95	86.25	3.13	23.89	3.87	0.64	0.45
97	86.14	3.04	24.11	3.84	0.62	0.46
99	85.99	2.87	24.17	3.88	0.63	0.44

10. VITA

NAME: Diego Alejandro Orozco Villaseñor

EDUCATION: B.S., Computer Science, University of Colima, Colima, Mexico, 2002
M.S. Bioengineering, University of Illinois at Chicago, Chicago Illinois, 2006

HONORS:
- FMC Fellowship, University of Illinois at Chicago, Chicago, Illinois, 08/2008 – 05/2009
- Fulbright – Garcia Robles Scholarship, 03/2003 – 08/2005
- Academic Excellence Recognition, University of Colima, Colima Mexico, 08/2002
- Honor's Scholarship, University of Colima, Colima, Mexico, 1997-2001
- "Premio Peña Colorada" Award for academic merits Consorcio Minero Benito Juarez, Colima, Col. Mexico, 12/2001
- "El Mejor Estudiante de México" (Mexico's Best Students) Award, Diario de México y el Ateneo de las Ciencias, México DF, 10/2001
- Exchange Student Award and Stipend, University of Alicante, - Spain, 01-09/2001
- Summer of Science Award and Stipend, CITEDI IPN, Mexico, 1998

INVITED LECTURES:
1. *Wear of Total Joint Prosthesis: Biomechanics and materials*. XX Anniversary of the Electro mechanical Engineering School (FIE), University of Colima, Col. Mexico, 03/2005
2. *The Impact of Daily Physical Activities on TKR Wear*. 12th International and Interdisciplinary NRW Symposium, Universität Duisburg Essen, Essen, Germany, 03/2010
3. *Introduction to Bioengineering*. Seminar at the College of Engineering, Valparaiso University, Valparaiso, Indiana, 12/2012

ABSTRACTS:
1. Orozco DA, Mimnaugh KD, Hertzler JS, Rufner AS. *Significant Wear Reduction Maintained after 44 Mc with a Grafted-Vitamin E Polyethylene*. Accepted at the ORS meeting, 2013
2. Orozco DA, Mimnaugh KD, Hertzler JS, Rufner AS. *Steady State Head Penetration Rates of Grafted-Vitamin E Hip Components*. Accepted at the ORS meeting, 2013
3. Orozco DA, Mimnaugh KD, Hertzler JS, Rufner AS. *Six-week Accelerated Aging Effect on the Wear Performance of Grafted-Vitamin E Hip Components*. Accepted at the ORS meeting, 2013
4. Rufner AS, Peiserich MS, Guo M, Orozco DA, Popoola OO, Freiberg AA. *Crosslinked Vitamin E (VE)-Grafted UHMWPE*

Acetabular Cups Have Ultra Low Wear and Do Not Oxidize. Accepted at the AAOS meeting, 2013

5. Hannah JL, Christopher BK, Orozco DA, Wimmer MA. *Calculated Axial Forces at the Knee in Total Knee Replacement Patients During Chair and Stair Activities*. Proceedings of the ASME 2012 Summer Bioengineering Conference. June 20-23, Fajardo, Puerto Rico, USA
6. Knowlton C, Hanson G, Orozco DA, Laurent MP, Wimmer MA. *Geometric Measurement of Wear in Tibial Inserts through an Autonomous Reconstruction of the Original Surface*. Proceedings of the ASME 2011 Summer Bioengineering Conference (SBC2011), June 2011
7. Orozco DA, Ngai V, Wimmer MA. *Development of a Multi-Activity Protocol for TKR Wear Assessment*. ORS Transactions Vol. 36, Long Beach, CA, 2011
8. Orozco DA, Wimmer MA. *The Impact of Daily Physical Activities on TKR Wear.* BIOmaterialien: Interdisciplinary Journal of Functional Materials, Biomechanics, and Tissue Engineering. 11. Jahr, Heft S1, März 2010
9. Orozco DA, Wimmer MA. *Cumulative loading of TKR during Activities of Daily Living: The contribution of chair and stair maneuvers*. ORS Transactions Vol. 35, New Orleans, LA, 2010
10. Foucher K, Orozco DA, Berger R, Wimmer MA. *Relationships Between Habitual and Laboratory Walking Speeds and Clinical Function after Total Hip Replacement*. ORS Transactions Vol.34, Las Vegas, NV, 2009
11. Orozco DA, Briggs AL, Ngai V, Wimmer MA. Occurrence *of Daily Activity Transitions in an Active TKR Population*. ORS Transactions Vol.33, San Francisco, CA, 2008
12. Orozco DA, Wimmer MA. *Análisis del Patrón de Desgaste del Componente Tibial de Polietileno Utilizado en Artroplastía Total de Rodilla*. CNIB (National Congress of Biomedical Engineering), Guadalajara, Jal. Mexico, 2008
13. Wimmer MA, Kunze J, Orozco DA et al. Rare Earth Tracers to Determine Backside Wear of TKA Polyethylene Inserts. ORS Transactions Vol.33, San Francisco, CA, 2008
14. Orozco DA, Schwenke T, Wimmer MA. *Wear Scar Similarities of Retrieved and Simulator Tested Tibial Plateaus - An Artificial Neural Network Approach*. SFB 2005
15. Orozco DA, Wimmer MA. *Differences in the Wear Scar Formation of Retrieved and Simulator Tested Tibial Polyethylene Plateaus - An Artificial Neural Network Approach. Biomechanica Congress*, Hamburg Germany, 2005

PUBLICATIONS:

1. Thorp LE, Orozco DA, Block JA, Sumner DR, Wimmer MA. *Activity Levels in Healthy Older Adults: Implications for Joint Arthroplasty*. ISRN Orthopedics. September 15, 2012

2. Foucher K, Thorp LE, Orozco DA, Hildebrand M, Wimmer MA. *Differences in preferred walking speeds in a gait lab compared to the "real world" after total hip replacement*. Archives of Physical Medicine and Rehabilitation, Archives of Physical Medicine and Rehabilitation, 2010
3. Schwenke T, Orozco DA, Schneider E, Wimmer MA. *Differences in wear between load and displacement control tested total knee replacements*. Wear, 2009
4. Orozco DA, Schwenke T, Wimmer MA. *Wear Scar Prediction Based on Wear Simulator Input Data—A Preliminary Artificial Neural Network Approach*. J ASTM International 3(9) - JAI100249, 2006